

The Role of Immune Regulation In Host and Parasite Fitness

By

Justin Thomas Critchlow

Dissertation

Submitted to the Faculty of the
Graduate School of Vanderbilt University

in partial fulfillment of the requirements

for the degree of

DOCTOR OF PHILOSOPHY

in

Biological Sciences

December, 16, 2023

Nashville, Tennessee

Approved:

Julián F. Hillyer, Ph.D.

Patrick Abbot, Ph.D.

Megan Behringer, Ph.D.

Eric Skaar, Ph.D.

Ann Tate, Ph.D.

DEDICATION

This dissertation is dedicated to my parents, for their unconditional love and encouragement. To my brother, for being the best role model I could ask for. To my wife, Jeanette, for your limitless capacity to love, listen, and encourage me. To my son, Kai, sitting here with you next to me I realize that every hardship I overcame was for you. I love you all now and always.

ACKNOWLEDGMENTS

I would like to express my deepest gratitude to my fellow Tate lab members. Over the past six years, you have been my constant companions through every challenge and triumph. Your collaborative spirit, countless laughs, willingness to help, and shared passion for our work have made even the most daunting problems surmountable.

To Dr. Ann Tate, my advisor, thank you for your endless patience and unwavering belief in me. I will miss our weekly chats about our dogs (and science) and how excited you get when I tell you a tornado might be nearby. Over the past six years, I've not only benefited from your academic guidance but have also learned invaluable lessons in how to be a leader. You treated every person that came through your door with the same level of respect, no matter if they are a freshman at office hours or a visiting professor. I hope to do the same.

I want to thank Dr. Kurt Vandegrift, as my first scientific advisor, without your mentorship I would never have had the courage to pursue this path. Cheers.

Lastly, I extend my sincere thanks to my committee members. The opportunity to learn from and work alongside each of you has been a privilege, and your guidance has been instrumental in molding me into the scientist I am today.

To all of you, thank you for being such a positive part of this incredible journey.

TABLE OF CONTENTS

	Page
DEDICATION	ii
ACKNOWLEDGEMENTS	iii
LIST OF TABLES.....	ix
LIST OF FIGURES	x
CHAPTER 1	
Introduction.....	1
Navigating the costs and benefits of immunity when facing infectious diseases	1
Natural variation in immune systems vary among life stages in infection history .	4
Parasite trade-offs and evolution to host immunity.....	5
Research aims and thesis structure	6
CHAPTER 2	
The legacy of larval infection on immunological dynamics over metamorphosis.....	10
Preface	10
Abstract.....	11
Introduction.....	12
Methods.....	19
Gregarine infections.....	19
Flour beetle rearing and sample collection.....	20
Quantification of immune gene expression via RT-qpcr.....	21
Statistical analyses of gene expression.....	23

Results	24
The impact of gregarine infection on pupal development	24
Immune gene expression differs by tissue.....	24
The effect of developmental stage and parasite exposure on immune gene expression	27
Discussion	28
 CHAPTER 3	
Exploration of immune regulators in the <i>Tribolium castaneum</i> Toll and IMD pathways	33
Preface	33
Abstract.....	34
Introduction.....	35
Materials and Methods.....	40
Beetle sources, rearing, and experimental grouping	40
Primer sequences	40
DsRNA synthesis	41
RNAi injections.....	41
Microbial challenge.....	42
Immune gene expression via RT-qpcr.....	43
Statistical analyses	43
Results	44
Combinatorial knockdowns of tollip with either dnr1 or pgrp-sc2 do not significantly alter constitutive AMP transcription	44
RNAi knockdown of dnr1 does not significantly alter AMP transcription in response to microbial challenge	46
DsRNA-mediated knockdown of pgrp-sc2 and tollip does not	

alter humoral immune dynamics in beetle guts	48
10-day RNAi-mediated knockdown of <i>skpA</i> decouples <i>T. castaneum</i> Toll and IMD signaling	49
Discussion	52
<i>SkpA</i> functions as a pathway-dependent regulator in <i>T. castaneum</i> humoral immune signaling	53
<i>Pgrp-sc2</i> silencing may influence the peak expression of IMD signaling	54
<i>Pgrp-sc2</i> silencing does not alter gut-specific IMD signaling	55
<i>Dnr1</i> silencing does not alter humoral immune signaling.....	55
 CHAPTER 4	
Mapping the functional form of the trade-off between infection resistance and reproductive fitness under dysregulated immune signaling	57
Preface	57
Abstract.....	58
Introduction.....	59
Results	63
Cactus RNAi increases constitutive and total transcriptional activation and delays decay of Toll signaling	63
Amplification of Toll Signaling via cactus RNAi increases total circulating hemocytes	66
Uninhibited Toll signaling enhances antibacterial activity	68
The magnitude of Toll pathway activation depends on the dose of cactus dsRNA	68
Elevated Toll pathway signaling increases survival to septic bacterial infection	70
Increased Toll pathway signaling has severe fitness related costs	71

Discussion	74
Small increases in Toll signaling have massive costs to reproductive potential	74
Dose dependent Cactus depletion regulates Toll signaling	76
Toll signaling increases circulating hemocytes after microbe challenge	77
Increasing Toll signaling amplifies damage to host health.....	77
Conclusion	79
Materials and Methods	80
Beetle rearing and experimental groups	80
DsRNA synthesis	80
RNAi treatments	81
Microbial infections	82
Immune gene expression and Bt load quantification via RT-qpcr	83
Hemocyte proliferation quantification.....	84
Antibacterial activity.....	85
Host survival experiments.....	86
Resistance to live Bt infection	87
Female reproductive output	87
Body mass and fat body dissections	88
Gut/intestinal integrity quantification (Smurf assay).....	88

CHAPTER 5

Efficient methods for experimental evolution of bacillus thuringiensis isolated against variable immune defenses in flour beetles	90
---	----

Preface	90
Abstract.....	91
Introduction.....	92
Methods	94
Representative Results	96
Serial passaged strains evolve lower virulence to their passaged population	97
Serial passaging in a low-susceptibility host increases in vitro lag time.....	100
Discussion	102
FUTURE DIRECTIONS.....	104
REFERENCES	106
APPENDIX	121

LIST OF TABLES

Table		Page
2.1	The interaction of metamorphosis and immune function across holometabolous insect orders.....	15
2.2	Primers used to assay immune gene expression in <i>T. castaneum</i>	22
2.3	Summary of statistical results for the impact of stage, larval parasite exposure, or their interaction on immune gene expression in the gut and whole body. ...	27

LIST OF FIGURES

Figure		Page
2.1	The proposed functional roles of <i>T. castaneum</i> immune genes quantified in chapter II.	19
2.2	The influence of tissue type and gregarine parasite exposure on immune gene expression across developmental stages of the flour beetle <i>T. castaneum</i>	25
2.3	Gene expression correlations suggest partial decoupling of immune genes between tissues and among life stages.	26
3.1	Simplified view of Toll and IMD signaling parameters.	37
3.2	DsRNA-mediated knockdown of <i>dnr1</i> , <i>pgrp-sc2</i> , and <i>tollip</i> in combination does not constitutively increase <i>cec-2</i> nor <i>def-2</i> expression.	46
3.3	DsRNA-mediated knockdown of <i>dnr1</i> results no change in Toll nor IMD signaling.	47
3.4	DsRNA-mediated knockdown of <i>tollip</i> and <i>pgrp-sc2</i> results no change in Toll nor IMD signaling in beetle guts.	49
3.5	10-day incubation after dsRNA injection significantly silences gene expression for <i>dnr1</i> , <i>skpA</i> , and <i>pgrp-sc2</i>	51
3.6	DsRNA-mediated knockdown of <i>skpA</i> significantly increases IMD signaling while decreasing Toll signaling.	52
4.1	Simplified overview of the flour beetle Toll signaling pathway.	61
4.2	DsRNA-mediated knockdown of <i>cactus</i> results in increased Toll signaling	65
4.3	Toll signaling increases functional metrics of cellular immunity and antibacterial activity	67
4.4	Quantitative knockdown of <i>cactus</i> transcripts benefits resistance and survival during infection.	69
4.5	The costs of immune over-activation to fitness-associated traits.	72
5.1	<i>Bt</i> killing rate after serial passaging.	99
5.2	Shifts in <i>Bt</i> growth parameters after serial passaging.	101

CHAPTER 1

Introduction

Navigating the costs and benefits of immunity under the threat of infectious diseases

Infectious diseases are a pervasive threat to the well-being and survival of human, animal, and plant populations. In humans, diseases such as tuberculosis (TB) continue to be a major driver of morbidity and mortality worldwide (Chakaya et al., 2021). Emergence of infectious diseases to new susceptible populations can even endanger and destabilize entire species, such as white-nose syndrome, which is responsible for killing over 5 million bats in Eastern USA and Canada (C. L. Frank et al., 2014). Similarly, Rust fungi represent one of the most serious threats to agriculture and wood production, causing extensive damage to plants and threatening food security (Lorrain et al., 2019). Given these widespread threats, the heavy burden of infectious diseases necessitates substantial efforts in hosts to control infections.

In response to these pervasive threats, hosts have fortunately evolved immune systems to recognize and expel foreign invaders. Site-specific defenses, such as barriers, act as the first line of defense by preventing colonization, which is complemented by wound healing mechanisms like blood clotting and resistance mechanisms triggered by the recognition of foreign invaders. Subsequently, these early defenses signal for immune cells and signaling cascades that induce the expression of infection-specific immune factors (Hamilton et al., 2008). In the context of TB, for example, cilia and mucus in the lung help trap TB to prevent colonization, apoptosis mechanisms help eliminate infected cells, and the activation of macrophages contain the bacteria by initiating the production of cytokines and chemokines that draw other additional immune cells to the site of infection (de Martino et al., 2019; Guirado et al., 2013). While indispensable for eliminating parasites and protecting host health, immune

defenses require substantial resources and can themselves inflict significant damage to self, leading to immunopathology and autoimmunity (Graham et al., 2021).

Allocating resources to immunity inherently requires the diversion of energy from other vital processes like development or reproduction (Schwenke et al., 2016). In flax plants with the *L6* resistance mutations against Rust fungi, for example, energy is diverted away from growth and reproduction before there is even an infection (Howles et al., 2005). Constitutive defenses like these prevent infections from colonizing and replicating, reducing the impacts of parasite-induced pathology and curbing parasite transmission (Boots & Best, 2018). Even in the absence of infections, however, constitutive defenses require the allocation of precious resources. In contrast, inducible defenses limit immunological costs absent infection but risk being overwhelmed by fast-growing parasites if the response is not fast and strong enough (Hamilton et al., 2008). Yet, failure to dampen an induced immune response can have similar dire consequences that threaten the health and lifespan of a host (Duneau et al., 2017). For example, it is crucial for macrophages to recognize and respond to TB infection, but their increased sensitivity also increases the risk of chronic inflammation leading to rheumatoid arthritis (Buscher et al., 2017). To prevent such runaway immunological costs, hosts utilize multiple layers of control (S. A. Frank & Schmid-Hempel, 2019; Luecke et al., 2021).

The layers of regulation on inducible immune signaling through the insect Toll and IMD pathways provide particularly well documented case studies of the costs and benefits of controlling the flux of immune signaling after infection.(Mitchell et al., 2016). For the Toll pathway, circulating immune cells recognize a microbial invasion by identifying microbe-associated molecular patterns (MAMPs) like Lys-type peptidoglycan. This recognition initiates peptidase cascades to activate the Toll receptor ligand SPZ to move the signal through the cell membrane (Arnot et al., 2010). SPZ-ligand binding recruits intracellular adaptors to form the Myddosome signaling complex (Balka & De Nardo,

2019). Signaling kinases then act as regulatory hubs that manage the initiation, amplification, and termination of downstream effectors through phosphorylation (Luecke et al., 2021). This phosphorylation unlocks the transcription factors Dif and Dorsal (Engström, 1999; Whalen & Steward, 1993), which facilitates their translocation into the nucleus for transcription. To regulate this pathway, some insects use extracellular serine protease inhibitors (serpins) to inhibit peptidase cascades (Gulley et al., 2013; Ligoxygakis et al., 2002). As the signal passes through the cell membrane, intracellular negative regulators, like Tollip in mammals, dampen the signal by inhibiting signaling complexes (P. H. Wang et al., 2013). As the signal continues, the protein Cactus binds to the transcription factors (TFs) Dif and Dorsal to prevent them from moving to the nucleus to induce AMP transcription (AMPs) (Roth et al., 1991; Whalen & Steward, 1993).

To respond to the vast diversity of parasitic threats while mitigating fitness costs, immune systems can modify their regulatory elements at each level of the signal transduction cascade to create unique immune phenotypes tailored to specific threats (Luecke et al., 2021). By altering the localization and abundance of receptors, hosts can finely tune the rate of transmembrane signaling (Chen et al., 2017; Roberts et al., 2017). Additionally, variations in the characteristics of signaling complexes, such as the speed of Myddosome scaffolding and the half-life of the complex, offer another layer of modulation (Luecke et al., 2021). The signaling process is further refined through the addition or removal of ubiquitin chains to adaptors, which controls the speed of scaffolding and the proteasomal degradation of various immune proteins, significantly impacting signal propagation (F. Wang & Xia, 2018). Altering the activity of phosphorylation allows hosts to adjust the speed and strength of the signal (Witzel et al., 2012). The culmination of these modifications then dictate the activation dynamics of transcription factors and post-transcriptional modifiers (Hayden & Ghosh, 2004). This malleable approach enables immune responses to produce a response appropriate for the specific parasitic attack while

balancing the costs of other fitness traits. While the field has made significant strides in identifying these regulatory levers that modulate components of immune responses, there remains a substantial gap in understanding how these components naturally vary across individuals, populations, and species. Furthermore, the exploration of how shifts in fitness landscapes exert selective pressures on these immune mechanisms, and the identification of the evolutionary constraints that govern their adaptation, are areas ripe for further investigation.

Natural variation in immune systems vary among life stages in infection history

Constraints from life history trade-offs and early life exposure to parasites can give rise to a wide variety of phenotypes. As organisms age, their interactions with microbes shape the maturation and specialization of their immune systems. For instance, children recovering from severe Respiratory Syncytial Virus (RSV) infection undergo long-term alterations in microbiome composition, metabolism, and dendritic cell transcription and epigenetics, priming the immune system for secondary infections and increasing the risk of pulmonary diseases like asthma (Malinczak et al., 2020). Alternatively, early life exposure to microbes can train the immune system, allowing it to tolerate subsequent infections and thereby reduce the risk of destructive immunopathology (Metcalf et al., 2022). As the organism matures, life history traits like growth, development, and reproduction impose new energetic and physiological demands, leading to age-specific limitations on immune system investments (Tate & Graham, 2015a). In the case of field crickets (*Gryllus campestris*), an induced immune response can lead to a reduction in body condition and a decrease in sexual signaling, affecting mate choice and reducing male cricket fitness (Jacot et al., 2004). Given this trade-off, crickets that are too sensitive to avirulent, ubiquitous infections could be less reproductively successful. Recognizing why and how immune systems evolve and adapt over an organism's life course will enable more accurate predictions and interventions, especially in populations with a diverse age structure.

Parasite trade-offs and adaptation to host immunity

In 2016, 8.5 million people died from parasitic infections (Ritchie & Roser, 2018). While microbial harm to hosts might seem counterproductive, the consensus of evolutionary theory connects the harm a parasite inflicts to its ability to transmit to a new host (Anderson & May, 1986). Since parasites need host resources to replicate and transmit, evolving quicker growth rates requires increased host exploitation resulting in higher virulence (α), represented as host mortality from infection in the following virulence-transmission trade-off model: $R_0 = \frac{\beta(\alpha)N}{\mu + \alpha + v(\alpha)}$ (Anderson & May, n.d.; Day, 2003). Increasing host exploitation leads to increased transmission potential (β) and, consequently, increased fitness (R_0), or the number of new infections from a single infection (Alizon et al., 2009; Anderson & May, 1986). The term virulence can also describe the infectiousness of a parasite (Jaenike, 1996) or the presence of specific factors that cause pathology (Dussurget et al., 2004), but neither of these definitions capture the effect of host damage on parasite fitness. An increase in exploitation is also theorized to increase the host's immune response to clear infection (v) and the mortality from infection (α) both of which shorten the infection transmission period. This produces a trade-off where increasing host exploitation increases parasite density, but it also decreases the time allowed for transmission, thus an intermediate level of virulence is predicted to maximize parasite fitness.

Trade-offs between parasite traits can also manifest from energetic constraints like overproduction of costly virulence factors. For example, *Salmonella typhimurium* expresses its type III secretion system, ttss-1, to induce host inflammation to outcompete resident microbiota and prevent clearance from the immune response so it can successfully infect epithelial cells and achieve transmission (Sturm et al., 2011); however, this mechanism is costly and reduces its growth rate allowing for competition from faster growing strains. *S. typhimurium* clones overcome this trade-off by

dividing labor among genetically identical cells; a subset of bacteria express *ttss-1* while a different subset focus exclusively on growth, preventing the establishment of coinfecting strains (Diard et al., 2013). Task specialization is only one of many strategies (e.g. quorum-sensing, nutrient sensing-dependent modules, or virulence factor production) that parasites take to maximize their fitness (Diard & Hardt, 2017; Rumbaugh et al., 2009), and different strategies could have different payoffs at each step of the infection cycle, from colonization to replication and through transmission.

The host immune response is a key contributor to variation in the microenvironments that the parasite experiences over its life cycle, contributing to variation in selection pressures at each stage of the infection process (Hawley & Altizer, 2011; Long & Boots, 2011). Immune mechanisms that clear infection before the parasite can reach its transmission phase will disproportionately influence parasite fitness, which is predicted to select for increased virulence (S. A. Frank & Schmid-Hempel, 2008; Grenfell et al., 2004). However, constraints on parasite evolution can create trade-offs between traits. For example, when *Staphylococcus aureus* is experimentally evolved against two AMPs, it mutates in either the *pmt* or *nsa* operons to resist the AMPs (Makarova et al., 2018). This resistance is costly though, resulting in longer *in vitro* lag phases. Despite the many examples of parasites evolving to overcome immune responses, our understanding of the influence of individual immune mechanisms and strategies on parasite fitness and evolution remains scarce (Armitage et al., 2022). When researchers infected *Tenebrio molitor* with the evolved *S. aureus* strains, they observed no fitness benefit for *S. aureus*, even though the AMPs are essential for *T. molitor* to survive *S. aureus* infection. An ideal system to study how parasites overcome immune responses would allow researchers to control individual mechanisms of the host immune response and evolve the parasites in these different immune environments *in vivo*.

Research aims and thesis structure

In our ever-changing world, the landscape of natural infections is continually shifting, with varying selection pressures on both hosts and parasites. Given that climate change is likely to systematically alter ecological conditions and the resulting selection pressures on extant species as their range expands and changes, integrating context into the mechanistic study of immune systems becomes imperative to enhance our understanding and prediction of the factors influencing infectious disease outcomes. My dissertation adds to our understanding of how life-stage and infection life-history can influence immune phenotypes. Additionally, it uncovers examples of regulators of immune signaling in the model system *T. castaneum*. The dissertation then dives into a key *T. castaneum* negative regulator to reveal the fitness-related benefits and costs of failing to properly regulate an immune signaling pathway. Finally, my work outlines an *in vivo* serial passaging protocol that isolates the interaction between a pathogenic bacterium and inducible immune defenses to understand how varying immune environments influence parasite evolution and disease outcomes.

In **chapter 2**, we investigate the long-term impact on the *T. castaneum* immune system from parasite exposure as larva. We expose beetles to a protozoan parasite that inhabits the midgut of the larval and adult life stages, despite clearance during metamorphosis. The study then measures changes in immune gene expression across larval, pupal, and adult life-stages in the gut and whole body. Our study finds that larval exposure to the benign parasite casts a shadow over immune gene expression in the larval gut and whole body that continues through metamorphosis and into adulthood. This study indicates that early life infection experiences can have long-lasting impacts on the maturation of immune systems, providing a source of natural immunological variation and revealing the variation in parasite selection pressures over ontogeny.

In **chapter 3** I aim to uncover the mechanisms that negatively regulate the flour beetle immune response. Regulatory immune genes are known to heavily influence basal, max expression, and the

decay of an immune response, which can influence host-parasite disease outcomes. Yet, the regulatory architecture and the costs and benefits of having layered regulators is not well described despite its importance for understanding immune system evolution. Here we lay the groundwork for revealing those costs and benefits in the model organism *T. castaneum* while also prodding the extent to which these regulators are conserved across taxa, thus revealing more about the potential selection pressures acting on immunity. In this study I target the orthologous *Drosophila* negative regulators *pgrp-sc2* (Guo et al., 2014), *dnr1* (Guntermann et al., 2009), and *skpA* (Khush et al., 2002) as well as the mammalian and weevil negative regulator *tollip* (Anselme et al., 2008; Zhang & Ghosh, 2002a). My study found potential changes in peak AMP expression when silencing *pgrp-sc2* for 10 days. The chapter also indicates that *skpA* may play a dual role as a negative regulator of the IMD pathway but a positive regulator of the Toll pathway. This highlights the imperative for broader investigations into non-model insects, as it can reveal diverse mechanisms and tactics employed to balance the costs associated with immune responses.

In **chapter 4** we take advantage of the unique RNAi system characteristics in flour beetles to alter the expression of *cactus*, a key negative regulator of Toll pathway signaling, thereby modulating the activation level of the Toll pathway in the red flour beetle. Our research reveals that while intensifying immune pathway activation bolsters immune responses and survival against bacterial infections, it imposes a notably severe penalty on female egg production, gut health, body mass, and lifespan. This insight highlights the substantial health and reproductive implications that can arise from even minor alterations in negative regulation and immune pathway activation.

Finally in **Chapter 5**, I introduce and implement a serial passaging protocol designed to focus on the interplay between immunity and the microbial parasite, *Bacillus thuringiensis* (Bt), in *T. castaneum*. Our results indicate that passaging Bt through populations with varying susceptibility to infection can

alter Bt's ability to kill its host. This protocol provides a framework that distinguishes early resistance mechanisms from downstream inducible immunity, paving the way for studies to explore how immune responses shape the evolutionary trajectories of parasites.

Altogether, my dissertation delves into the consequences that parasite exposure history and variation in regulatory immune genes have on host fitness and disease outcomes. The methodologies and insights presented pave the way for a deeper understanding of immune system evolution, bridging crucial gaps in our knowledge of immune signaling network dynamics and host-parasite interactions. The dissertation then details potential avenues for expanding upon the current work, emphasizing its implications for refining intervention strategies, improving theoretical models, and ultimately charting the nuanced relationship between immune investment and fitness.

CHAPTER 2

The legacy of larval infection on immunological dynamics over metamorphosis

Preface

This chapter establishes that metamorphosis partially decouples immune gene expression covariance among tissues and life stages. It also demonstrates that early-life exposure to a benign gut protozoan parasite affects host immune gene expression during the larval stage, which continues to influence immune phenotypes through metamorphosis. This finding is significant since it reveals that while metamorphosis can decouple immune gene coregulation, a seemingly harmless protozoan infection can overcome this decoupling to leave a lasting imprint on the insect's immune response. My advisor, Dr. Ann Thomas Tate, conceptualized and obtained funding for this study. Adriana Norris and I conducted the experiments and processed the samples. All authors analyzed the data and wrote the manuscript. All authors approved the final version of this manuscript. This work was supported by the National Institute of General Medical Sciences at the National Institutes of Health (grant number R35GM138007). This chapter is adapted from “*The legacy of larval infection on immunological dynamics over metamorphosis*”, published in 2019 in the journal *Philosophical Transactions of the Royal Society B* (374) and has been reproduced with the permission of the publisher and my co-authors, Adriana Norris and Dr. Ann Thomas Tate.

Abstract

Insect metamorphosis promotes the exploration of different ecological niches, as well as exposure to different parasites, across life stages. Adaptation should favor immune responses that are tailored to specific microbial threats, with the potential for metamorphosis to decouple the underlying genetic or physiological basis of immune responses in each stage. However, we do not have a good understanding of how early-life exposure to parasites influences immune responses in subsequent life stages. Is there an developmental legacy of larval infection in holometabolous insect hosts? To address this question, we exposed flour beetle (*Tribolium castaneum*) larvae to a protozoan parasite that inhabits the midgut of larvae and adults despite clearance during metamorphosis. We quantified the expression of relevant immune genes in the gut and whole body of exposed and unexposed individuals during the larval, pupal, and adult stages. Our results suggest that parasite exposure induces the differential expression of several immune genes in the larval stage that continues into adulthood. We also demonstrate that immune gene expression covariance is partially decoupled among tissues and life stages. These results suggest that larval infection can leave a lasting imprint on immune phenotypes, with implications for the evolution of metamorphosis and immune systems.

Introduction

Few factors have a greater impact on the outcome of an interaction between host and parasite, or the spread of disease in a host population, than the age and stage of the host. As hosts age, cumulative exposure to microbes shapes the maturation and polarization of their immune systems. Life history priorities shift from growth to reproduction, inducing alterations in behavior, food source, and even ecological niche (Urban et al., 2013). As a result, hosts experience dynamic changes over their ontogeny in both exposure to parasites and susceptibility to infection once exposed (Tate & Graham, 2015b). The consequences of these ontogenetic dynamics can be observed across broad swaths of the tree of life. In plants, for example, gibberellin hormones that promote plant growth also inhibit signals related to defense against predators and parasites. At the same time, signaling from the salicylic acid pathway, which is involved in the response to biotrophic pathogens, inhibits the action of the growth hormones (Karasov et al., 2017). As a result, growing plants are susceptible to different pathogens than mature stages, and infection can influence the growth trajectories of their plant hosts (Navarro et al., 2008). In humans, lack of early-life exposure to beneficial microbes and other environmental antigen can set the stage for chronic inflammation, allergy, and other forms of immunopathology (Simon et al., 2015; Yassour et al., 2016). From an evolutionary perspective, the risk of immunopathology in early life is predicted to favor decreased immunological sensitivity to infection later in life (Metcalf et al., 2017). In all of these examples host ontogeny is a fairly continuous process, punctuated by hormonal signals that encourage flowering or the onset of puberty but otherwise keep major organs and physiological structures intact. In animals that undergo metamorphosis, however, developmental continuity is swapped for discrete stages characterized by transition periods of dramatic physiological restructuring that alter the calculus of host-parasite interactions.

During metamorphosis, tadpoles become frogs and caterpillars become butterflies, allowing

hosts to exploit disparate resources and environments that individually maximize particular, stage-associated traits like growth or reproduction (Haldane, 1932). Metamorphosis is not a requirement for stage-specific niche differentiation; even within insects, dragonflies and mosquitoes both have an aquatic juvenile stage and a terrestrial adult stage, but dragonflies undergo relatively continuous maturation from instar to instar while the holometabolous mosquitoes undergo pupation prior to adulthood. Why bother with metamorphosis, then? After all, the pupal stage can be a liability as it is generally sessile, poorly defended, and unable to acquire resources to fuel its energetic needs. The adaptive decoupling hypothesis suggests that the pupal stage might be the price paid for immature and mature developmental modules that can respond relatively independently to evolutionary pressures (Moran, 1994), allowing organisms to simultaneously maximize performance in multiple life stages. The re-invention of the midgut during complete metamorphosis is a particularly potent example of adaptive flexibility achieved by decoupling one life stage from another. In most insects, the midgut comprises epithelial cells, goblet cells, and stem cells (Hakim et al., 2010; Parthasarathy & Palli, 2008; Royet, 2011). The ratio and renewal rates of these cell types differ extensively from one life stage to another, and vary dynamically even within life stages. For example, as larvae grow larger and molt, the stem cells of the midgut undergo proliferation and differentiate into new, polyploid epithelial cells and goblet cells (Parthasarathy & Palli, 2008). This renewal process is also crucial in the host response to bacterial toxins and viruses that rely on the invasion of epithelial cells to colonize the host (Loeb et al., 2001). As insects transition to the pupal stage, however, the old somatic cells are excised into the lumen to form the yellow body, which undergoes apoptosis and autophagy to recycle the nutrients before being evacuated during eclosion of the new adult (Hakim et al., 2010). In the midgut of a new pupa only the intestinal stem cells remain, imaginal structures that proliferate and differentiate into the epithelial cells that will eventually compose the adult gut (Parthasarathy & Palli, 2008). Consistent with the adaptive

decoupling hypothesis, the relative morphologies of larval and adult epithelial cells reflect the relative feeding ecologies of each life stage. For example, in fruit flies, the polyploid epithelial cells of larvae facilitate the rapid acquisition and processing of nutrients from complex food media, while the smaller, diploid nuclei of adult midgut epithelial cells reflect the narrower breadth of adult food sources (Royet, 2011). On the other hand, the larval and adult stages of the flour beetle *Tribolium castaneum* both feed on the same resource (Parthasarathy & Palli, 2008), and both contain midgut epithelial cells that share a common, polyploid morphology.

Midgut remodeling during insect metamorphosis can exert complex effects on the persistence of parasites and other microbes. Protozoan trophozoites that remain embedded in the flour beetle (*T. confusum*) gut when a larva enters metamorphosis, for example, are evacuated with the yellow body (THOMAS & RUDOLF, 2010), allowing the adult to eclose without a parasite burden. On the other hand, the elimination of the gut epithelia could also eliminate beneficial microiota, allowing any remaining opportunistic pathogens to exploit the pupa or colonize the new adult gut. Indeed *Galleria mellonella* moth pupae cooperate with a beneficial microbe (*Enterococcus mundtii*) to exclude pathogenic *Serratia* strains during metamorphosis (Johnston & Rolff, 2015). Knocking down host immune gene expression or preventing the *E. mundtii* strain from producing bacteriocins allowed *Serratia* to dominate, at a cost to pupal survival. Furthermore, the cessation of resource acquisition during pupal gut remodeling can render larvally-acquired infections hazardous during metamorphosis. The microsporidian parasite *Nosema whiteii* kills its flour beetle host during the pupal stage after manipulating the host into an extended larval stage during which the parasite converts acquired resources into spores (Blaser & Schmid-Hempel, 2005). Conversely, a protozoan parasite (*Ophryocystis elektroscirrha*) of the Monarch butterfly (*Danaus plexippus*) can lethally deform its host during the pupal stage if it reaches excessive spore densities in the larval stage, prematurely curtailing transmission (de Roode et al., 2008). Thus,

metamorphosis can shape parasite life history evolution while also influencing host phenotypes and fitness.

The impact of metamorphosis on the adaptive decoupling of gene expression is hypothesized to extend to the immune system (FELLOUS & LAZZARO, 2011; League et al., 2017), since life stages that use different resources or display disparate behaviors are also likely to encounter different types of parasites that requires alternate forms of immunological defense. Empirical evidence from multiple holometabolous insect species support this hypothesis, as summarized in **Table 1**. For example, the larvae and adults of *Drosophila melanogaster* fruit flies express the antimicrobial peptide *diptericin* at similar levels, but fundamentally differ in their expression of the antimicrobial peptide *drosomycin* (FELLOUS & LAZZARO, 2011). In a similar vein, the larvae of the *Anopheles gambiae* mosquito, which lives in a microbe-rich aquatic environment, exhibits higher numbers of hemocytes that phagocytose bacteria and higher levels of immune gene expression than adults (League et al., 2017). These examples suggest that expression of an immune phenotype in the larval stage does not indelibly predict adult phenotypes, allowing plasticity in immunological investment over ontogeny.

Table 1. The interaction of metamorphosis and immune function across holometabolous insect orders. Notes: AMP = antimicrobial peptides, PO = Phenoloxidase.

Host	Immune challenge	Tissues	Stages	Immunological Dynamics	Host Phenotype	References
<i>Manduca sexta</i> (Lepidoptera)	none	Gut	Ecdysis at the larval to pupal transition	AMPs are prophylactically excreted into gut lumen during early metamorphosis		[46, 50]
<i>Manduca sexta</i> (Lepidoptera)	<i>Photorhabdus luminescens</i>	Fat body, hemocytes, cell-free hemolymph	Pre-wandering and newly ecdysed larvae	Cellular and humoral defenses reduced upon entering metamorphosis	Older larvae succumb faster to infection	[51]

<i>Manduca sexta</i> (Lepidoptera)	peptidoglycan	Hemolymph	Wandering larvae, pupae, and new adults	PO and AMP activity peak in larval stage, nadir in pupal stage		[52]
<i>Galleria mellonella</i> (Lepidoptera)	Bacteria (<i>E. coli</i> , <i>M. luteus</i>) and fungi (<i>S. cerevisiae</i>)	Hemolymph	Larvae, pupae, adults	Antimicrobial properties highest in pupae	Imm. challenge shortens development time, decreases pupal mass	[53]
<i>Galleria mellonella</i> (Lepidoptera)	none	Hemolymph and cuticle	Every day from last instar larva to new adult	PO activity lowest during late pupal stage		[54]
<i>Galleria mellonella</i> (Lepidoptera)	Symbiotic (<i>E. mundii</i>) and pathogenic (<i>Serratia</i> , <i>Staphylococcus</i>) bacteria	Gut	Multiple stages of larval to pupal molt; adults	Lysozyme and symbiont interaction important for excluding pathogens as pupae	Pathogenic bacteria in pupal microbiota increased mortality hazard	[14, 63]
<i>Bombyx mori</i> (Lepidoptera)	<i>S. aureus</i> , <i>E. coli</i> bacteria	Gut	Multiple stages of the larval to pupal molt Feeding and wandering stage larvae; pupae	Toll pathway AMPs highly expressed during ecdysis		[25]
<i>Bombyx mori</i> (Lepidoptera)	none	Gut	Multiple stages of the larval to pupal molt Feeding and wandering stage larvae; pupae	AMP expression increased just prior to pupation; changes in midgut morphology		[55]
<i>Danaus plexippus</i> (Lepidoptera)	<i>Ophyrocystis elektroscirrha</i> (protozoan)	Hemolymph	Larvae, adults	Hemocyte count higher in larvae but PO activity higher in adults	Individuals infected as larvae had shorter lifespans as adults	[56]
<i>Arctia plantaginis</i> (Lepidoptera)	none	Whole body	Multiple larval and pupal stages; adult	Cold larval rearing temperatures increased larval and adult body melanization	Larval body melanization trades off with antipredator coloration	[64]

<i>Drosophila melanogaster</i> (Diptera)	none	Whole body	Larvae, Adults	AMPs differed in the strength of correlation between larval and adult expression	Larval expression of the AMP <i>drosomycin</i> correlated with male offspring weight	[18]
<i>Drosophila melanogaster</i> (Diptera)	<i>Erwinia carotovora</i> (Ecc15)	Gut, whole body	Multiple larval and pupal stages; adult	Duox-controlled gene expression highly expressed in late larval and late pupal stages but declines during adulthood		[43]
<i>Anopheles gambiae</i> (Diptera)	<i>Enterobacter</i> or <i>E. coli</i>	Hemolymph, whole body	Larva and adult	Hemocyte metrics differed between larvae and adults; generally higher in larvae	Larval immune challenge increases adult susceptibility to <i>Plasmodium</i>	[17, 62]
<i>Apis mellifera</i> (Hymenoptera)	Lipopolysaccharide (LPS)	Hemolymph	Multiple larval, pupal, and adult stages	PO activity increased over development from larva to adult		[42]
<i>Apis mellifera</i> (Hymenoptera)	<i>E. coli</i>	Hemolymph	Larva, pupa, adult	AMP induction after bacterial exposure in pupae is much lower than other stages	Pupae fail to clear bacteria and succumb to infection	[57]
<i>Carabus lefebvrei</i> (Coleoptera)	none	Hemolymph	Larvae, pupae, adult	Hemocyte counts are much higher in pupae than in adults or larvae		[44]
<i>Nicrophorus vespilloides</i> (Coleoptera)	none	Hemolymph	Multiple larval stages, pupa, adult	Hemocyte count lower but PO activity higher in pupae than in other stages		[58]

Despite the importance of complete metamorphosis for the outcome of host-parasite interactions, we know little about the legacy of larval infection on the immunological state of pupal and adult stages,

particularly upon remodeling of the midgut. Most of what we do know (**Table 1**) focuses on the response to immune challenge with bacteria. As both beneficial endosymbionts and virulent entomopathogens, bacteria are undoubtedly important selective factors on the adaptive decoupling of immune responses across life stages. Horizontally-transmitted, relatively avirulent parasites like eugregarine protozoa are also ubiquitous among insect populations (Clopton, 2009; Detwiler & Janovy, 2008; Rodriguez et al., 2007), and yet we know almost nothing about host immune responses to these parasites or their interaction with host metamorphosis. In this paper, we compare the expression of immune genes in the guts and whole bodies of larval, pupal, and adult flour beetles (*T. castaneum*) that were infected as larvae with a naturally occurring and common gregarine parasite that gets expelled with the gut epithelia during metamorphosis. We chose to assay the expression of antimicrobial peptides, recognition proteins, and other immune effectors previously associated with the insect gut, metamorphosis, and/or protozoan infection (**Fig. 1**). Because larval and adult flour beetles live in the same flour medium, we predicted that, in the absence of infection, immune gene expression would not differ substantially between life stages. However, we expected that larval infection would inform the expression of immune genes in pupae and adults even after the expulsion of larvally acquired parasites, in anticipation of re-exposure as adults. We discuss the implications of our results for our understanding of the evolution of metamorphosis and innate immune systems.

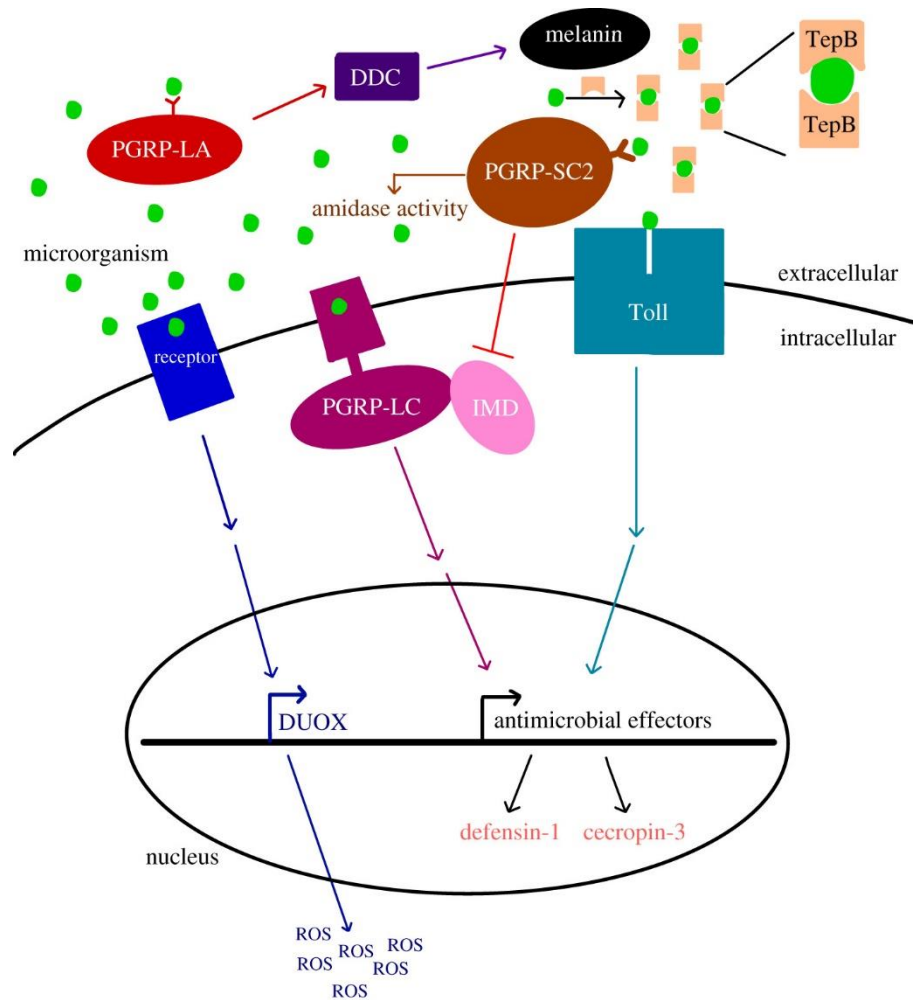


Figure 1. The proposed functional roles of *T. castaneum* immune genes quantified in chapter II. Peptidoglycan recognition proteins homologs (e.g. PGRP-LC and PGRP-LA) are thought to recognize parasites and stimulate signaling cascades that result in the production of antimicrobial effectors. The immune factors in this study are involved in the melanization pathway (DDC), production of reactive oxygen species (DUOX), opsonization by phagocytes (TepB), and degradation of microbial peptidoglycan via amidase activity (PGRP-SC2). The expression of antimicrobial peptides Defensin-1 and Cecropin-3 provide read-outs on the activation of Toll and IMD pathways.

Methods

Gregarine infections

Septate eugregarine protozoa are ubiquitous and generally avirulent inhabitants of insect midguts (Detwiler & Janovy, 2008; Janovy et al., 2007; Tate & Graham, 2015c; THOMAS & RUDOLF, 2010). The strain of *Gregarina* parasites used in this study was originally derived from infected *T. castaneum*

beetles collected at a feed store in Kentucky in June 2017 and subsequently maintained in a continuously infected colony. We have not observed any obvious disease-induced mortality or other symptoms of virulent infection with this parasite. This parasite is transmitted via the secretion of gametocysts from the infected insect gut. The gametocyst produces oocysts in the flour environment that are then ingested by the new host. Thus, the addition of beetle eggs to flour derived from a heavily infected colony is sufficient to reliably expose newly hatched larvae to the parasites (Detwiler & Janovy, 2008; Janovy et al., 2007; Tate & Graham, 2015c; THOMAS & RUDOLF, 2010). Before the start of the experiment we confirmed infection in the source colony by dissecting the guts of 15 mature larvae and staining with a 60% iodine saline solution to visualize gregarine parasites via light microscopy (25x). We found that 7/15 larvae had visible trophozoites in the midgut, although the infection rate is likely higher as the trophozoites are hard to see until almost ready to enter syzygy. None of the 15 pupae that we dissected showed signs of infection, agreeing with previous observations (THOMAS & RUDOLF, 2010) that parasites are unlikely to survive in the pupal gut because the epithelia to which they are attached are destroyed.

Flour beetle rearing and sample collection

We set up 11 petri dishes containing all-purpose white flour, to which we added 40 *T. castaneum* adults from the “Snave” colony, originally collected from a Pennsylvania grain elevator in July 2013 and subsequently maintained in the lab (Tate & Graham, 2015c). Three days later we sieved approximately 300 eggs from the breeding groups and distributed them into new petri dishes, to which we added either 10 grams of gregarine-positive flour from the heavily infected *T. castaneum* colony or 10 grams of gregarine-free flour from a parasite-negative colony. Three weeks later we pulled 50 pupae as well as 50 larvae with an approximate length of 4mm from each treatment, and 25 newly eclosed, virgin adults from each treatment a week after that. For development assays, we collected 30 pre-pupae from each

treatment and placed them in individual wells of a 96 well plate, monitoring them daily first for pupation and then for eclosion as new adults. All beetles were kept at 29°C in the same incubator in the dark except when handled.

Individuals destined for gene expression studies were starved for approximately 24 hours prior to sample processing to eliminate non-colonized parasites and food in the guts, and then dipped in sterile water to remove excess flour immediately prior to sample collection. We dissected guts from all stages by making an incision in the abdomen and gently removing the gut with tweezers while the insect was immersed in 10uL insect saline. Guts were immediately placed in a 1.5 mL collection tube on dry ice. After collections were complete, guts were kept at -80°C. We originally treated a subset of guts with iodine as well to visualize parasites before freezing the guts, but after finding that iodine treatment severely affected gene expression, we eliminated these samples from subsequent analyses, leaving us with 5-7 gut samples per exposure treatment per life stage. Whole individuals (8-10 per treatment/life stage) were placed in individual tubes, frozen, and kept at -80°C.

Quantification of immune gene expression via RT-qPCR

We isolated gut RNA using the Qiagen All Prep Micro Kit, and isolated whole body RNA with Qiagen All Prep and RNeasy kits. We synthesized cDNA with 0.5uL RNA (whole body) or 4uL RNA (gut) in a 5uL or 10uL reaction using the manufacturer-recommended protocol with SuperScript IV VILO master mix (ThermoFisher Scientific), and diluted the cDNA with 30-40 µL nuclease free water. We conducted RT-qPCR on the Biosystems Quantstudio 6 Flex machine using sybr green chemistry (PowerUp SYBR green master mix from Applied Biosystems, 500nM primers, 10-50ng cDNA). Thermal cycling conditions were 95 °C for 2 minutes, followed by 40 cycles of 95 °C (15 sec), 55 °C (10 sec), and 60 °C (1min). All samples were run in duplicate or triplicate and the average ct value was

used for subsequent analyses as long as technical replicates were within 1ct.

We used RT-qPCR to quantify the expression of immune response-associated genes (**Fig. 1**) including *defensin-1*, *cecropin-3*, *dopa decarboxylase* (DDC), thioester containing protein-B (*TepB*), dual oxidase (*duox*), and the peptidoglycan recognition proteins *pgrp-LA*, *pgrp-LC*, and *pgrp-SC2* (**Table 2**). *Defensin-1* and *cecropin-3* are anti-microbial peptides (AMPs) that are thought to be activated by both the IMD and Toll pathways in *T. castaneum* and have orthologs that are upregulated during bacterial oral challenge in *Bombyx mori* and *D. melanogaster* (Tzou et al., 2000; Yokoi, Koyama, Minakuchi, et al., 2012a). *Pgrp-LA* and *pgrp-LC* are transmembrane receptor proteins for the IMD pathway in *T. castaneum* and essential for its production of AMPs (Koyama et al., 2015a). *PGRP-SC2* is the *T. castaneum* homolog of *pgrp-LB* in *D. melanogaster*, which downregulates the IMD pathway (Paredes et al., 2011a). DDC is a precursor in the melanization pathway which kills malaria parasites in the midgut of *Anopheles* mosquitoes (WHITTEN et al., 2006; Wu et al., 2010). TEPs are highly expressed in the crop and proventriculus in *D. melanogaster* (Bou Aoun et al., 2011). Finally, Duox synthesizes reactive oxygen species (ROS) in gut epithelial cells, and RNAi knockdown of Duox has been shown to increase susceptibility to oral bacterial infection in *D. melanogaster* (Ha et al., 2005). We used ribosomal protein S18 (*rps18*) as a reference gene for quantification of relative gene expression (Schmittgen & Livak, 2008a), as it has been shown to be stably expressed during infection (Lord et al., 2010a) in *T. castaneum*.

Table 2. Primers used to assay immune gene expression in *T. castaneum*.

Primer Set	Full Name	Function	Forward Oligo Sequence	Reverse Oligo Sequence	AT. (°C)
Def1	Defensin-1	Toll/IMD AMP	TTTRYCGTTGCARTAKCCTCC	TCAARSTGAATCATGCCGCW TG	55
Cec3	Cecropin-3	Toll AMP	AACATGARYACCAAACCTTTT	CCAAYTTATMGGCTKTGGW G	55
PGRP	Peptidoglyca	IMD	TGCCACCTTAAACTTCTCTAA	GACTGCACCCTTTGCGAACA	55

-LA	n recognition protein LA	recognition	AC	T	
PGRP-LC	Peptidoglycan recognition protein LC	IMD recognition	ACGAAGGCCGGGGATGGAAA	GTTGTTTGCAAGCCGTTATC TG	55
PGRP-SC2	Peptidoglycan recognition protein SC2	IMD recognition	ACAGTTGGATGCKTTGAAACA GT	AACTSGTYCTGCTCCCTTG	55
DDC	Dopa decarboxylase	Melanin synthesis	AGAAGTCGTGATGCTKGACT	CTTGRATCACGCCGCC	55
Duox	Dual oxidase	ROS synthesis	CGCAATTGATCGGCCACTTT	AGCTCCAAGGGATTTGGTTCG	55
TEP-B	Thioester containing protein B	Cellular recognition	AGGTTTCACCTCATCGCAGG	GTTGAAATTGTGGCGCTGGT	55
S18	Ribosomal Protein S18	Ribosomal Protein	CGAAGAGGTCGAGAAAATCG	CGTGGTCTTGGTGTGTTGAC	55

Statistical analyses of gene expression

We calculated the Δct values for each gene for each individual sample by subtracting the target gene mean ct value from the reference gene mean ct value. Thus, the Δct value represents the log₂-transformed relative expression value of the target gene (Schmittgen & Livak, 2008a). As our expression data were log-normally distributed, we retained the log₂-transformed value for subsequent analyses. All statistical analyses were conducted in R (v3.5.2) To analyze the main effect of tissue on overall host gene expression, we conducted a MANOVA with our eight genes as dependent variables and tissue as the independent variable. To analyze the impact of each life stage, parasite exposure, and their individual interactions within each tissue on gene expression, we used linear models (lm function) of the form (target relative expression ~ stage + exposure + stage*exposure). We adjusted the p values with the Benjamini-Hochberg method to control for the false discovery rate (Benjamini & Yekutieli, 2001). Finally, to analyze pairwise expression correlations between genes, we used the cor() function on gut, whole body, larva, pupa, and adult data. To get differences in covariance relationships among these datasets,

we subtracted the absolute value of one matrix from another and graphed the resulting differences using the `lowerUpper` (psych package) and `ggcorrplot` (ggcorrplot package) functions.

Results

The impact of gregarine infection on pupal development

The majority of individuals from both treatment groups took six days to develop from newly ecdysed pupae to newly eclosed adults and thus the distribution of development times was underdispersed (dispersion parameter = 0.05). Nevertheless, individuals exposed to gregarine parasites as larvae developed significantly faster than those who were not exposed (quasi-poisson GLM, $t = 2.05$, $p = 0.046$), although the effect size was less than one day among treatments.

Immune gene expression differs by tissue

The overall effect of tissue (gut vs. whole body) on gene expression was highly significant (MANOVA, $F_{1,89} = 31.34$, $p < 2e-16$). Models for individual genes revealed that the gene *ddc* had, on average, 5.7-fold higher expression in the whole body than in the gut ($F_{1,89} = 27.7$, $p < 1e-6$). Genes that showed significant upregulation in the gut relative to the whole body, on the other hand, include *pgrp-LC* (fold change = 2.6, $F_{1,89} = 21.4$, $p < 2e-5$), *duox* (fold change = 11.47, $F_{1,89} = 66.2$, $p < 1e-11$), and *cecropin-3* (fold change = 14.8, $F_{1,89} = 31.4$, $p < 1e-6$). There was no significant tissue-driven difference in expression for the genes *pgrp-LA*, *defensin-1*, *pgrp-SC2*, or *tepB* ($p > 0.05$). **Fig. 2** illustrates relative expression of four genes among tissues (top row in each panel = gut expression, bottom row = whole body expression).

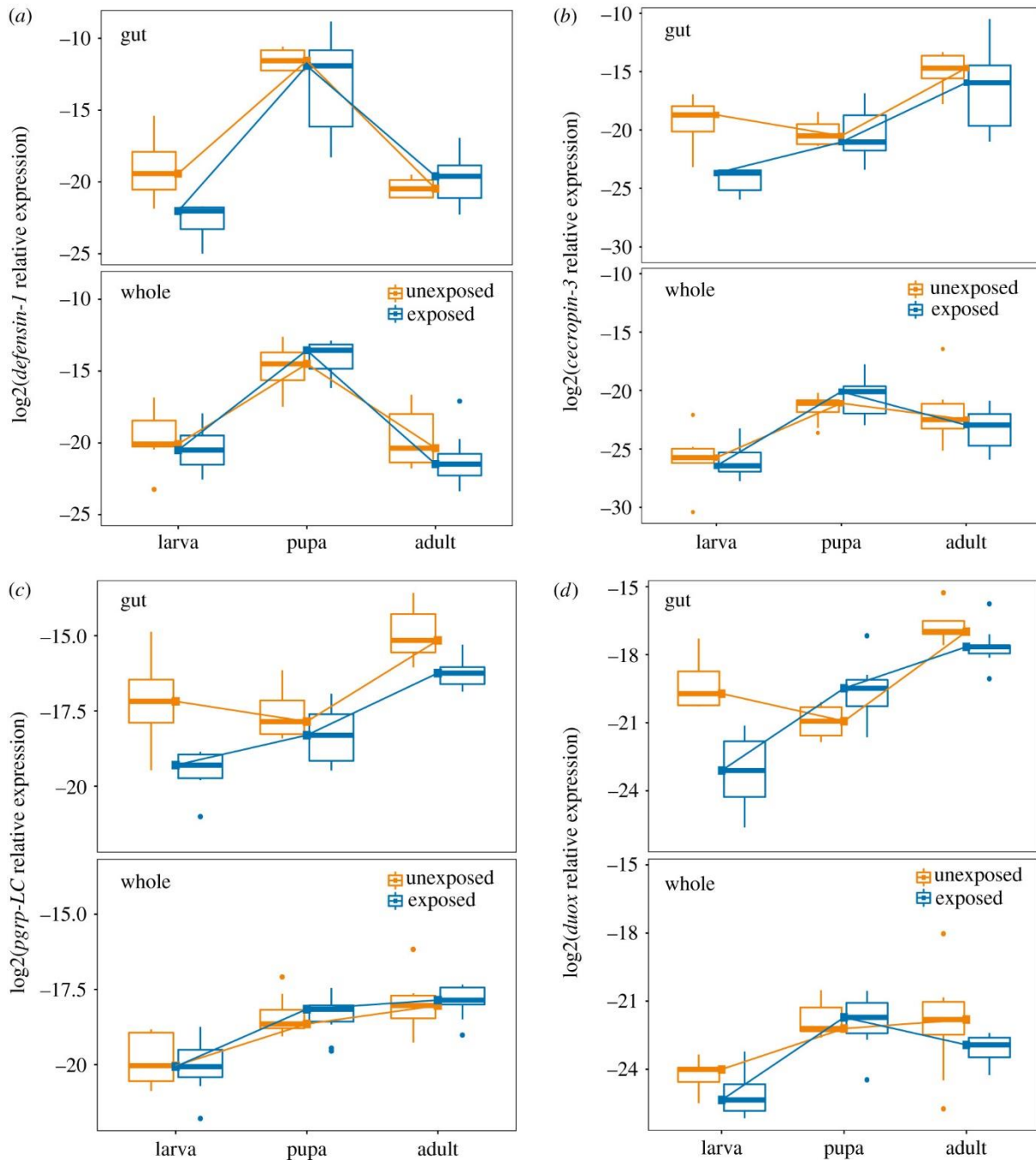
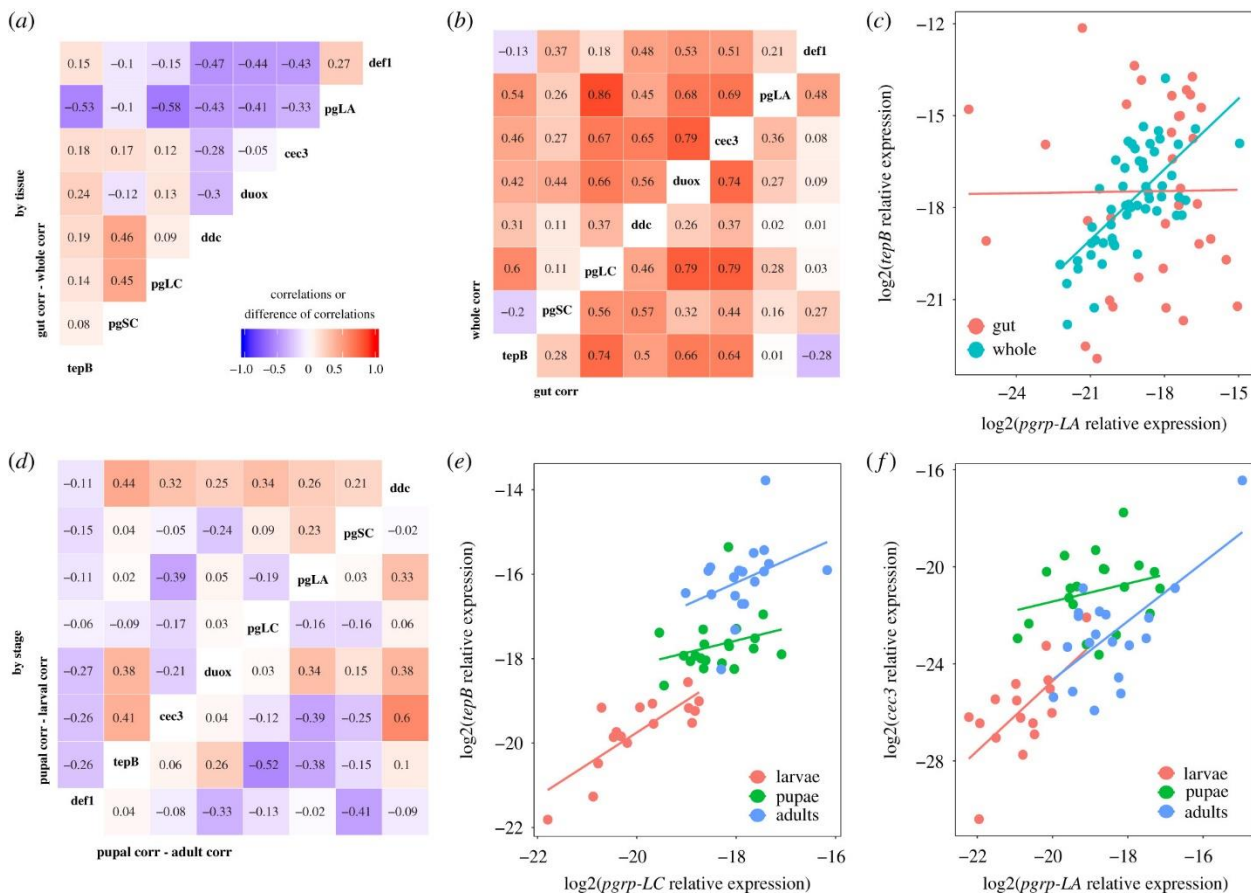


Figure 2. The influence of tissue type and gregarine parasite exposure on immune gene expression across developmental stages of the flour beetle *T. castaneum*. The expression of the antimicrobial peptides *defensin -1* (A), and *cecropin-3* (B), the recognition protein *pgrp-LC* (C), and the reactive oxygen species generator *duox* (D) were assayed in extracted guts (top row of each panel) or whole bodies (bottom row) from larvae, pupae, or adults that were either exposed to gregarine parasites as larvae (blue) or not (orange). The expression of each gene relative to the reference gene *RPI8s* is represented on a log₂ scale. Lines have been added to visualize the developmental trajectory of median

gene expression.

Does the modularity of immune gene expression differ between tissues? Previous work on *T. castaneum* and other model insects like *D. melanogaster* have proposed that several of our genes are likely to be under control of common pathways like IMD and Toll (e.g. (Yokoi, Koyama, Ito, et al., 2012a)), resulting in expression patterns that covary among co-regulated genes. In our data, all genes showed a moderate to high correlation of expression with at least one other assayed gene (**Fig. 3B**), but these relationships were not always consistent among tissues (**Fig. 3A**). For example, *pgrp-LA* and *tepB* were tightly correlated at the whole body level, but show no relationship in the gut (**Fig. 3C**).



3. Gene expression correlations suggest partial decoupling of immune genes between tissues and among life stages. The pairwise Pearson correlation values of whole body gene expression was subtracted from those of gut-only pairwise correlations to get the difference in correlation strength (A). Large positive values indicate a stronger relationship in the gut, while large negative values indicate

stronger correlations in the whole body. The underlying correlations are visualized in (B) for whole body (top left) or gut only (bottom right); colors and numbers indicate the Pearson correlation coefficient. The breakdown of the correlation of *pgrp-LA* and *tepB* expression (log2 scale, relative to reference gene) in the gut relative to the whole body (C) illustrates decoupling among tissues. There was also decoupling by life stage, as illustrated by the relative magnitudes of the correlation coefficients for pupae against larvae (D, top left) and pupae against adults (D, bottom right). Stage-specific pairwise comparisons of *pgrp-LC* vs. *tepB* expression (E.) and *pgrp-LA* vs. *cecropin-3* expression (F) illustrate different examples of differences in coefficients among stages.

The effect of developmental stage and parasite exposure on immune gene expression

To analyze the impact of developmental stage, larval gregarine exposure, and their interaction on immune gene expression (Fig. 2), we performed linear modeling on each gene. We analyzed gut and whole body datasets separately because of the complex tissue-specific genic interactions described above. In the whole body, there was no significant effect of gregarine exposure on gene expression (Table 3), but expression differed broadly by life stage. Most genes showed higher expression in pupae and adults relative to larvae (Appendix A “whole body”). *Pgrp-LC*, *pgrp-LA* and *tepB* increased in each subsequent life stage, while *defensin-1* (Fig. 2A) and to a lesser extent *cecropin-3*, *duox*, and *ddc* peaked in the pupal stage. Only *pgrp-SC2* expression showed no significant effect of stage.

Table 3. Summary of statistical results for the impact of stage, larval parasite exposure, or their interaction on immune gene expression in the gut and whole body. Full statistical tables for each gene are available in Appendix A. The expression of each gene was fit with the model: $\text{expression} \sim \text{stage} * \text{exposure}$ using the `lm()` function in R, where stage has three levels (larva, pupa, adult) and parasite exposure has two levels (exposed, unexposed). P values were adjusted for false discovery rate using the Benjamini-Hochberg method, and asterisks indicate the level of significance for at least one level of factor or interaction, relative to unexposed larvae: * $\text{padj} < 0.05$, ** $\text{padj} < 0.01$, *** $\text{padj} < 0.001$. '-' indicates lack of statistical significance.

Gene	Gut			Whole Body		
	Stage	Exposure	Stage*Exposure	Stage	Exposure	Stage*Exposure
<i>Defensin-1</i>	***	-	-	***	-	-
<i>Duox</i>	*	***	***	***	-	-
<i>TepB</i>	***	-	-	***	-	-

<i>Cecropin-3</i>	-	*	-	***	-	-
<i>Ddc</i>	-	-	-	**	-	-
<i>Pgrp-LC</i>	*	**	-	***	-	-
<i>Pgrp-LA</i>	-	-	-	***	-	-
<u><i>Pgrp-SC2</i></u>	-	-	-	-	-	-

The expression of immune genes in the gut was more diverse in their responses to stage and exposure (**Table 3**). Larval exposure to gregarines resulted in the overall down-regulation of *cecropin-3* (**Fig. 2B**), *pgrp-LC* (**Fig. 2C**), and *duox* (**Fig. 2D**). The expression of *duox* further depended on the interaction of exposure and life stage (**Appendix A**) as expression was suppressed in exposed larvae but upregulated in the guts of pupae that were previously exposed (**Fig. 2B**). Only *defensin-1* was more highly expressed in pupae than in larvae and adults (**Fig. 2A**), but *pgrp-LC*, *duox* and *tepB* were significantly more highly expressed in adults relative to larvae (e.g. **Fig. 2C,D**). No gene was most highly expressed in larvae than in other life stages.

In whole organisms, the strength of pairwise gene expression correlations differed among life stages (**Fig. 3D**). For example, *pgrp-LC* and *tepB* expression was tightly and steeply correlated in larvae but less so in pupae and adults (**Fig. 3E**), while the strong positive relationship observed between *pgrp-LA* and *cecropin-3* in larvae and adults broke down in pupae (**Fig. 3F**).

Discussion

Our data suggest that larval exposure to a relatively benign protozoan parasite can leave an imprint on gut immune system function that persists through metamorphosis. Our study also reflects a dynamic change in the immunological profile of the insects as they mature through metamorphosis into adulthood. As we know little about the insect immune response to eugregarines despite their ubiquity

and diversity, and moreover the immunological dynamics of metamorphosis are still poorly described for most insects, this study provides a unique window into the integration of parasites with the life history of holometabolous insects. Most urgently, the persistent downregulation of several important immune recognition and effector genes beginning in the gut of infected larvae raises the possibility of trade-offs with resistance to bacterial infection that could haunt the host in later life stages.

The downregulation of antimicrobial peptides observed in infected larvae in our study may reflect parasitic manipulation of IMD and Toll pathways, but it could also hint at the polarization of the immune response toward defenses aimed at eukaryotic parasites at the expense of antibacterial defenses. Evidence from the Egyptian cotton leafworm (*Spodoptera littoralis*), for example, suggests that antibacterial activity trades off with cellular immune function and cuticular melanization in larvae (Cotter et al., 2004). While the insect immune response to gregarines has not been well-described prior to this study, we do have evidence that gregarine infection can impact concurrent or subsequent infections. For example, larval *T. confusum* infection with the gregarine parasite *Gregarina minuta* primed the resulting adults to better resist re-infection (THOMAS & RUDOLF, 2010) although the impact of gregarines across generations was less beneficial to their flour beetle hosts; gregarine-infected *T. confusum* females produced offspring that were more susceptible to infection with the virulent bacterial entomopathogen *Bacillus thuringiensis* (Tate & Graham, 2015c). Gregarines do not always facilitate entomopathogens, however, as cockroaches (*Blattella germanica*) were less competent hosts for parasitic nematodes if they were first infected with gregarines (Randall et al., 2013). While the polarization of helper-T cell responses (FENTON et al., 2008), for example, is well-characterized in mammals, we still have not delineated analogous mechanisms that contribute to functional trade-offs among arms of the immune system in insects. Gregarine infection may represent an underappreciated route for exploring the costs of maintaining multiple immunological fronts in invertebrate immune

systems.

Given that both larval and adult flour beetles live in the same milled grain substrate and therefore experience similar environmental challenges (Van Allen & Rudolf, 2013) (including exposure to gregarine parasites), we may not expect dramatic evolutionary decoupling of the larval and adult immune systems. However, there are fine-scale spatial and behavioral differences among the life stages that could bias relative rates of parasite exposure. Larvae tend to burrow down into the flour column and are renowned for their tendency to cannibalize multiple life stages (Costantino et al., 1997), making the transmission of obligate killer parasites an occupational hazard. Adults, who generally only cannibalize eggs and then only under high-density conditions, tend to congregate at the top of the column where they can find mates or achieve dispersal. Mating is a well-known test of immunological competence in insect systems, as exposure to sexually-transmitted diseases and the resource-intensive costs of producing offspring can tax host defenses (Reaney & Knell, 2010).

Thus, we might still expect selection to favor adaptive decoupling of immunological architecture in this system. Our observation of monotonically increasing recognition and effector gene expression over ontogeny is consistent with a few examples from **Table 1** (e.g. PO activity in *Apis mellifera* (Laughton et al., 2011)), but at odds with others that demonstrate peak responses during larval (Ahn et al., 2012; League et al., 2017) or pupal (Giglio & Giulianini, 2013) stages. Only *defensin-1*, an antimicrobial peptide that tends to be highly expressed in both the presence and absence of infection in flour beetles (Tate et al., 2017), peaked in expression during the pupal stage (**Fig. 2A**), consistent with observations in lepidopteran hosts of high antimicrobial peptide expression against opportunistic infections by microbes escaping the gut lumen during metamorphosis (Johnston & Rolff, 2015; Russell & Dunn, 1996). In addition to dynamic changes in the magnitude of immune responses over ontogeny, we found that the same immune genes might be under different control mechanisms in different life stages

or even tissues within the same life stage, as illustrated by the pairwise covariance patterns among genes (**Fig. 3**). This agrees in part with previous work on the ontogenic (FELLOUS & LAZZARO, 2011) and tissue-specific (Tzou et al., 2000) decoupling of AMP expression in *D. melanogaster*, although our work suggests that there might be an interaction between the two variables as well. Our study also emphasizes the need to consider local, tissue-specific immune responses when assessing the legacy of early-life infection, as the signal of gregarine infection on immunity was largely lost at the whole-organism level. Future work using stage and tissue-specific functional genetics approaches could help to clarify the relative contributions of canonical and non-canonical immune pathways to the generation of antimicrobial effectors across tissues and life stages.

Moving forward, how can we assess the role of infection and immunity in the evolution of metamorphosis, and conversely the role of metamorphosis in immune system evolution? First, it would be interesting to leverage the overlap in stage-structured ecological niches among holometabolous and hemimetabolous insects such as mosquitoes and damselflies or milkweed bugs and milkweed beetles to characterize, for example, patterns of parasite prevalence or immune function as a function of environment, stage, and developmental mode. With the maturation of the i5k project (“The I5K Initiative: Advancing Arthropod Genomics for Knowledge, Human Health, Agriculture, and the Environment,” 2013) and related efforts to sequence and annotate insect genomes, comparative analyses of immune gene architecture or stage-structured transcriptional dynamics among species could help to disentangle the effects of phylogeny from ecology and ontogeny on immune system evolution. Finally, better characterization of the natural enemies of insects, including their relative exposure and susceptibility metrics for each life stage and their impact on host demography through mortality or impacts on development, could complement current descriptions of immunological dynamics in model insects against lab-amenable bacteria. Connecting empirical patterns of infection and immunity across

ontogeny with mathematical models of age- and stage-structured immune system evolution (Ashby & Bruns, 2018; Metcalf et al., 2017; Tate & Graham, 2015b) could provide a unifying framework for understanding patterns of immunological variation in nature.

CHAPTER 3

Exploration of Immune Regulators in the *Tribolium castaneum* Toll and IMD Pathways

Preface

This chapter characterized the role of putative *T. castaneum* immune regulators Pgrp-SC2, Dnr1, SkpA, and Tollip using RNAi in adults. Our results showed that, ten days after injecting *skpA* dsRNA, IMD signaling increased while Toll decreased. Additionally, silencing the extracellular amidase pgrp-SC2 resulted in heightened IMD signaling six hours after microbial exposure. Throughout this work, I had the honor of mentoring the exceptional recent Vanderbilt alumnus, Katherine Zhong. Katherine managed the gut-specific project, overseeing the process from dsRNA injections through RT-qPCR analysis. For the combinatorial project, I handled dsRNA injections, while our rotation student, Shabbir Ahmed, managed the RT-qPCR. In the ten-day incubation experiment, I administered the dsRNA injections, and Morgan Pfeffer took charge of the bacterial challenge and RT-qPCR. I conducted all statistical analyses and crafted the experimental figures for this chapter. Dr. Arun Prakash created the illustration of induction and decay signaling parameters. Dr. Tate and I wrote this chapter. Dr. Tate obtained funding and resources for this study. This chapter was included in this dissertation with the permission of my collaborators, Katherine Zhong, Shabbir Ahmed, Morgan Pfeffer, Dr. Arun Prakash, and Dr. Ann Tate.

Abstract

The energetic demands of immune activation can divert resources from other vital processes and, if left unchecked, may harm the host. To manage these costs, organisms have evolved intricate immune signaling networks with multiple layers of regulation. These regulatory layers ensure that immune responses are calibrated to the level of threat while acting as safeguards to minimize the marginal costs associated with the disruption or malfunction of any single regulatory element. Much of our current understanding of these regulatory mechanisms comes from studies on the model organism, *Drosophila melanogaster*. While invaluable, this focus on a single model provides a limited view of the myriad ways in which immune networks can be constructed and regulated. In this study, we characterize the impact of knocking down regulatory genes up and down the Toll and IMD pathways on inducible immune dynamics using RNAi in the flour beetle. We observed that RNAi knock down of the E3 ligase *skpA* increased IMD signaling and simultaneously decreased Toll signaling. Silencing the extracellular amidase gene *pgrp-sc2* resulted in a non-significant rise in peak IMD signaling after microbial challenge. Surprisingly, these phenotypes were only identified after an extended dsRNA treatment time of 10 days, indicating potential differences in protein turnover or network robustness between *T. castaneum* and *D. melanogaster*. This study indicates that while *D. melanogaster* and *T. castaneum* possess orthologous immune signaling proteins, their effects on the production of humoral defenses differ. This underscores the need for more extensive research into non-model insects to uncover the varied mechanisms and strategies that can be used to mitigate the costs of immune responses.

Introduction

Parasites are ubiquitous, and due to the significant costs of infection, they shape host reproductive strategies (Antonson et al., 2020), mediate competition among host populations (Park, 1948; Rovenolt & Tate, 2022), and drive the development of robust immune responses. Immune responses can mitigate the damage from infection (tolerance), or it can reduce or eliminate parasite numbers (resistance) (Roy & Kirchner, 2000). These strategies are essential for hosts to maintain their fitness in the face of parasitic threats. However, they can also be energetically taxing, diverting resources from growth and reproduction, and if misdirected or overactive, can result in immunopathology, potentially harming the host even in the absence of a parasite (Graham et al., 2005; Roy & Kirchner, 2000).

To defend against parasitic threats, hosts can deploy two immune defense strategies that vary in timing and their costs to the host. One strategy is to invest in immune defenses that are active even without infection; these constitutive defenses prevent the colonization and development of parasites, minimizing the cost from parasite-induced damage and preventing further transmission (Shudo & Iwasa, 2001; Westra et al., 2015). However, these defenses continuously draw on host resources even when no infection is present (Boots & Best, 2018). The second strategy is to activate immune cascades in response to a parasitic threat. While inducible immunity conserves energy in the absence of infections, a delayed or insufficient response can leave the host vulnerable to fast-growing parasites (Duneau et al., 2017). For example, the intracellular bacterial parasite *Legionella pneumophila* rapidly replicates within macrophages. In response, tumor necrosis factor (TNF) signaling enables infected macrophages to undergo rapid cell death before bacterial load becomes overwhelming (Pollock et al., 2023). Yet, an overzealous immune response can be just as detrimental. In rheumatoid arthritis, CD4⁺ T cell activation signals for the overproduction of TNF- α in the joints leading to chronic inflammation, joint damage, and pain (Farrugia & Baron, 2016). Balancing this trade-off requires immune networks to control the speed, magnitude, and duration of the response with each of these parameters playing a pivotal role in determining the cumulative costs of an

immune response (Lazzaro & Tate, 2022). To strike a balance and prevent excessive immunological costs, hosts have evolved negative feedback mechanisms to regulate these responses.

The IMD pathway in *Drosophila melanogaster* exemplifies the intricate regulatory mechanisms that can modulate the constitutive, rate of induction, total magnitude, decay rate, and final resolution state of immune pathways (**Figure 1**) (Kleino & Silverman, 2014; Lee & Ferrandon, 2011; Silverman*, 2008; Wang & Xia, 2018). The IMD pathway ignites when peptidoglycan recognition receptors (PGRPs) recognize *meso*-diaminopimelic acid-type peptidoglycan (DAP-type PGN), which is present on bacterial surfaces (Kaneko et al., 2004; Leulier et al., 2003; Stenbak et al., 2004; Werner et al., 2003). Once the transmembrane PGRP-LC binds to PGN, the protein oligomerize (Mellroth et al., 2005). PGRP-LC then signals to the adaptor protein IMD, which recruits dFADD (Leulier et al., 2002) and DREDD (Leulier et al., 2000) to form a signaling complex. This signaling complex then helps unbind the transcription factor (TF) Relish from the negative regulator Caspar to translocate into the nucleus for transcription of IMD target genes like AMPs.(Hedengren et al., 1999). To prevent overactivation of the IMD pathway, negative regulating proteins modulate the recognition, signaling, and output of the pathway (Lee & Ferrandon, 2011). Extracellular circulating amidases like PGRP-SC2 degrade PGN into non-stimulatory fragments (cite). The intracellular regulator PIRK then interrupts adaptor scaffolding by interrupting the IMD-PGRP-LC interaction (Aggarwal et al., 2008; Basbous et al., 2011; Kleino et al., 2008; Vincent & Dionne, 2021). The addition or subtraction of ubiquitin chains then modulate protein stability of the complex and TFs like when the E3 ligase Dnr1 mediates the degradation of Dredd (Guntermann et al., 2009). Finally, once in the nucleus, Relish can be outcompeted by other transcription factors like Caudal (cite).

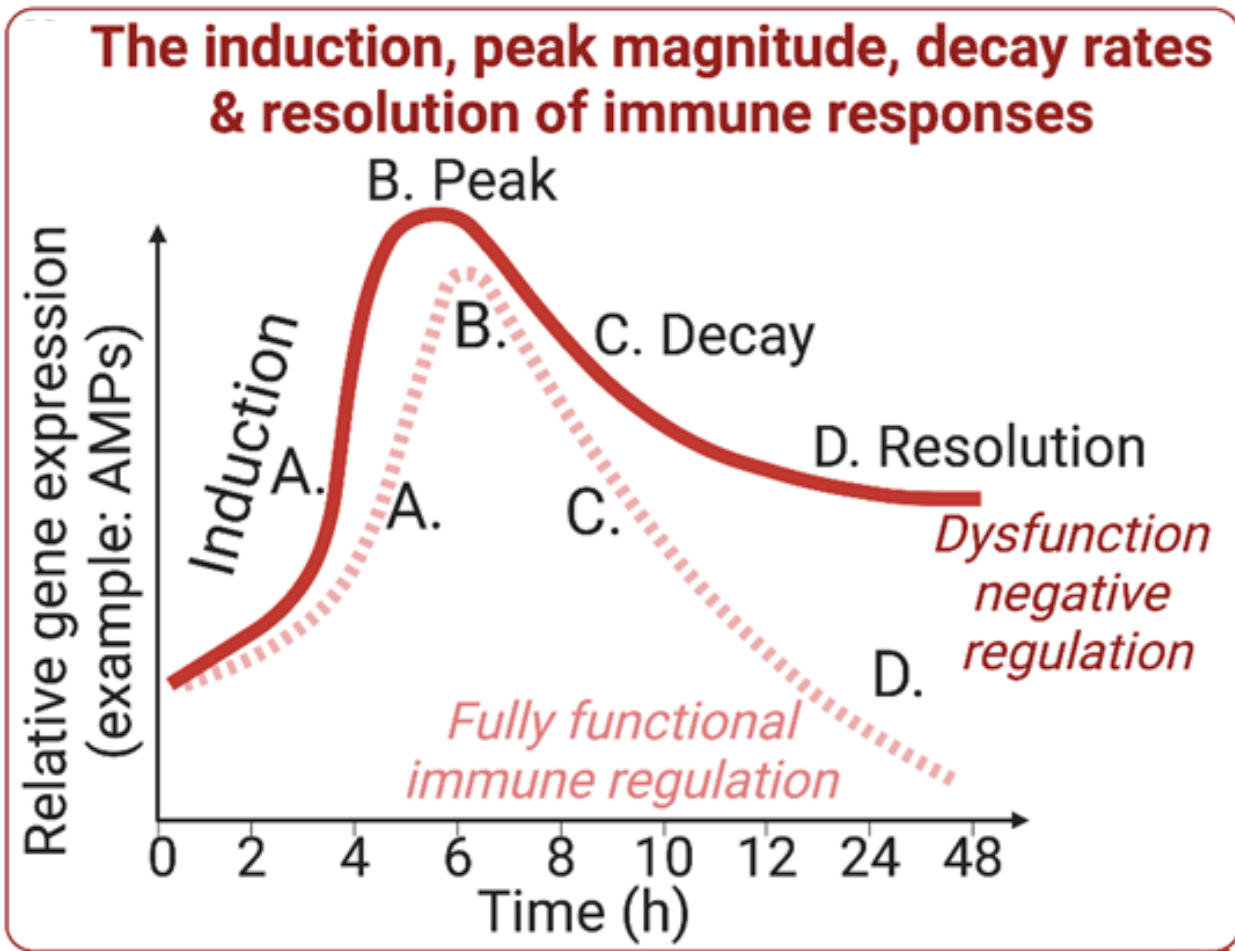


Figure 1. Simplified view of Toll and IMD signaling parameters. Production of AMPs from Toll and IMD signaling proceeds through a sequence of stages, starting with constitutive production before infection (A), induction upon parasite recognition (B), peak output (C), decay of transcript production, and finally resolution of the response (D). Dysfunction in negative regulators could potentially disturb signaling dynamics at any stage, leading to overproduction of immune effectors. Figure adapted from (Critchlow et al., 2023).

Dysregulation of immune signaling networks is associated with costs in humans, including excessive inflammation, tissue damage, and autoimmunity (Demetriou et al., 2001; Smits et al., 2005) and also in fruit flies (cites). Thus, insect immune systems serve as an ideal model for studying disruption in immune regulation, given their amenability to genetic modifications and the ability to measure energetic, immunopathological, and fitness-related costs to the host. For instance, while RNAi-mediated knockdown of *pirk* leads to increased AMP transcription and greater resistance to bacterial

infection in *D. melanogaster*, fly tolerance to infection is reduced since it takes significantly less bacteria for flies to perish from infection (Prakash et al., 2021). Since the benefits and costs to immune regulation can be so steep, negative regulators like *pirk* face conflicting evolutionary pressures to ensure a robust immune response that does not harm the host (Frank & Schmid-Hempel, 2019). Further understanding of the function of negative regulators and the consequences of their misregulation can provide insights into the costs and benefits of immunity and the situations that can lead to disease states. Extensive research has mapped the humoral immune response in *D. melanogaster*, but concentrating on a single species creates a large risk of overlooking unique immune strategies and mechanisms that other insects have evolved that other insects have developed due to their distinct ecological and evolutionary histories.

In this study we focus on identifying regulatory immune genes in the Toll and IMD immune pathways in the Coleopteran model organism, *Tribolium castaneum*, commonly known as the red flour beetle. The genome of *T. castaneum* is well characterized (Herndon et al., 2020; Richards et al., 2008) and since its assembly, a great deal of information about flour beetle immunology has been advanced (Behrens et al., 2014; Jent et al., 2019; Tate et al., 2017; Tate & Graham, 2017; Zou et al., 2007). *T. castaneum* is also highly amenable to RNA interference (RNAi) techniques, where septic injection of dsRNA provides systemic silencing of RNAi targeted genes (Linz & Tomoyasu, 2015; Miller et al., 2012; Tomoyasu et al., 2008). Although *T. castaneum*'s Toll and IMD pathways have many genes orthologous to *D. melanogaster* (Zou et al., 2007), the induction of AMPs in response to fungal and bacterial challenges, which in *D. melanogaster* are typically linked to either Toll or IMD activation respectively, appears to be less specific in *T. castaneum* (Yokoi et al., 2012; Zou et al., 2007). Thus, suggesting potential variations in immune regulation between the two species. By comparing *T. castaneum* and *D. melanogaster*, we can gain a deeper understanding of how distinct ecological and life-history

backgrounds influence the architecture of immune networks and shed light on the varied strategies species employ to manage the costs associated with immune responses. Furthermore, the ability to capture diverse populations of flour beetles in the wild (Jent et al., 2019) allows for future comparative studies to discern the drivers of natural immune variation (Tate & Graham, 2015a).

The primary objective of this study is to characterize the array of regulatory immune genes in *T. castaneum*, specifically on their role in both constitutive and inducible Toll and IMD signaling. Our focus was on understanding the distinct roles of these regulators dampening the IMD and Toll pathways due to their biological function within the signaling cascade. Based off experiments in *D. melanogaster*, we anticipated that silencing intracellular negative regulators would result in a constitutive upregulation of both Toll and IMD pathway signaling and greater peak induction (Kleino et al., 2008; Prakash et al., 2021), while silencing an extracellular regulator interacting directly with MAMPs would affect decay dynamics (Paredes et al., 2011). Interestingly, while we expected to replicate certain results observed in *D. melanogaster* and other organisms, our findings in *T. castaneum* did not align with these expectations. Given this discrepancy, we considered testing various parameters that might influence the manifestation of the anticipated phenotype. We investigated whether these discrepancies are from (1) potential redundancy in the Toll or IMD pathways due to crosstalk between the pathways, (2) changes to induction and decay patterns when responding to microbial challenge, (3) gut-specific regulatory functions, and (4) delayed RNAi phenotypes that require longer treatment periods. By further exploring the immune regulation differences between *T. castaneum* and *D. melanogaster*, we can gain a deeper insight into the diverse strategies organisms employ to manage their immune responses. Such a fundamental understanding of the factors that influence immune network architecture can enhance our knowledge of why autoimmune disorders persist in human populations. This knowledge can guide strategies to moderate overactive immune responses, potentially mitigating autoimmune diseases.

Materials and Methods

Beetle sources, rearing, and experimental grouping

In each experimental setup, we introduced roughly 200 age-matched parental beetles to fresh beetle media, consisting of whole-wheat flour from MP Biomedicals and 5% yeast. After allowing a 24-hour egg laying period, we relocated the parents to fresh media. Once the eggs matured into pupae, we segregated them by gender, transferring them into 100 mm petri dishes. Each dish contained either 100 unmated males or females, with media provided *ad libitum*. The beetles used for all experiments were sourced from the 'Snively' beetle population, initially gathered from a grain elevator in Pennsylvania in July 2013 and subsequently nurtured in our laboratory (Tate & Graham, 2015b). We housed all beetles in a walk-in incubator maintained at 30°C with a humidity level of 70%.

Primer sequences

For our initial investigation into characterizing the role of immune regulators in constitutive and inducible *T. castaneum* Toll and IMD signaling, we focused on the genes *tollip*, *dnr1*, *pgrp-sc2*, and *skpA* (Appendix Z). We chose to investigate Tollip, since it is an inhibitor of Toll-like-receptor signaling by preventing IRAK autophosphorylation and kinase activity in human kidney cells (Zhang & Ghosh, 2002). There is evidence that Tollip also regulates humoral signaling in weevils (Anselme et al., 2008) but does not have a corresponding orthologue in *D. melanogaster*. We selected the E3 ligase Dnr1 because, in *D. melanogaster*, it mediates the degradation of Dredd, where its silencing results in increased constitutive transcription of IMD related AMPs (Guntermann et al., 2009). *Pgrp-sc2* was chosen due to its role in *D. melanogaster* as an extracellular DAP-type PGN scavenger that delays IMD AMP decay rates by binding to and inactivating DAP-type PGN (Bischoff et al., 2006). Lastly, we

examined the E3 ligase SkpA, a component of the SCF complex that suppresses Relish by targeting it for ubiquitin-mediated degradation in *D. melanogaster* (Khush et al., 2002).

We designed dsRNA and qPCR primer sequences based on the iBeetle Database (Schmitt-Engel et al., 2015) as outlined in Appendix H. If the iBeetle database did not contain RNAi or qPCR primers for our gene of interest, we designed new primers using the NCBI primer-BLAST tool (Ye et al., 2012). To ensure the primers didn't produce secondary effects, we ran each primer set against the updated *T. castaneum* genome using NCBI's Primer-BLAST tool (Ye et al., 2012).

DsRNA synthesis

Using the Platinum Green Hot Start kit (Invitrogen), we derived T7 promoter sequence-tagged DNA from *T. castaneum* cDNA through PCR. This PCR product was cleaned using the QIAquick PCR Purification kit (Qiagen). We synthesized dsRNA overnight using the Megascript T7 kit (Invitrogen) as outlined by (Posnien et al., 2009). To control for RNAi induction from dsRNA injection, we utilized *E. coli* DNA to generate dsRNA targeting the maltose binding protein E (*malE*) sequence (Yokoi et al., 2012). We measured the dsRNA concentration with the Qubit™ microRNA Assay Kit (Invitrogen).

RNAi injections

In each experiment, beetles were randomly allocated to their designated dsRNA treatment groups. We administered injections of a 0.5 µL mixture with a concentration of 1 µg per µL using a Nanoeject II. Given that individual knockdowns did not alter constitutive AMP expression, we pursued dual knockdowns, targeting genes simultaneously in both the Toll and IMD pathways. This approach was motivated by evidence suggesting significant cross-talk between the two pathways. For combinatorial injections, 0.5 µg per µL for each target was used for a concentration of 1 µg per µL. We did not evaluate gene expression in naïve beetles (no dsRNA injection), given our previous findings

which indicated negligible differences in baseline expression between Male-RNAi and naïve beetles (Jent et al., 2019). For injections, we followed the methods detailed in (Posnien et al., 2009). For our 10-day incubation experiment, we injected adult beetles and allowed them to feed on beetle media for 10 days in individual 96 wells in a 30°C incubator. We refreshed beetle media on day 4 post injection. Then on day 10, we septicallly challenged beetles with heat-killed Bt.

Microbial challenge

To induce an immune response in the beetles, we septicallly infected beetles using heat-killed *Bacillus thuringiensis* (Bt). Bt is a gram-positive, sporulating, obligate killing bacterium that infects insects through oral ingestion or septic infection. Once it gains access to the insect hemolymph, it grows rapidly and eventually causes death after 12 to 24 hours (Nielsen-LeRoux et al., 2012; Raymond et al., 2010). For all infections, we used the Berliner strain of Bt (ATCC 55177) (Jent et al., 2019). Two days after RNAi injection, we cultured Bt overnight for 12-15 hours from a glycerol stock at -80°C in Luria Broth at 30°C. We transferred 200 uL of the overnight culture to 3 mL of new LB for 1.5 hours. We diluted the overnight and log cultures to OD600 values of 1.0 and 0.5, respectively. We then combined 500 uL of each culture and centrifuged the mixture at 4°C and 5,000 rpm for five minutes. We removed the supernatant and washed the Bt pellet twice with one mL of sterile insect saline. We then re-suspended the washed Bt pellet in 150 uL of insect saline and diluted 1:20 with insect saline to obtain an LD 50 dose (5×10^8 colony forming units (CFU)/mL). We inactivated Bt by heating to 90°C for 20 minutes. Beetles were infected by inserting an ultrafine insect pin dipped in the Bt mixture between the head and pronotum and were kept in individual wells in a 96-well plate after infection. Beetles were then flash frozen in -80°C for collections. For gut collections, the whole gut was extracted from the posterior end using forceps, followed by flash freezing on dry ice.

Immune gene expression via RT-qPCR

For RNA extractions, we used the Qiagen RNeasy kit, with a final elution volume of 30 μ L of nuclease-free water. We synthesized cDNA by incorporating 100-200 ng of RNA into a 5 μ L reaction, using the SuperScript IV VILO master mix (ThermoFisher Scientific). The resulting cDNA was diluted with 40 μ L of nuclease-free water. RT-qPCR was performed with the PowerUp SYBR Green master mix (Applied Biosystems) on a Biosystems QuantStudio 6 Flex instrument. The thermal cycling protocols started with a 95°C denaturation for 2 minutes, followed by 40 cycles of 95°C (15 seconds), 55°C (10 seconds), and 60°C (1 minute). Every sample was processed in duplicate, using the average Ct value for subsequent evaluations, provided the technical replicates had a difference of ≤ 1 Ct. Discrepancies beyond 1 Ct required repeated measurement.

We chose AMP genes for RT-qPCR analysis based on prior associations with Toll and IMD pathways in *T. castaneum* (Yokoi et al., 2012). To assay flux through the IMD pathway, we measured transcript abundance of *def-2* (TC010517) and *attacin-1* (TC007737). We chose *cec-2* (TC030482) and *thaumatin-1* (TC000518) to measure Toll pathway output (Altincicek et al., 2008; Herndon et al., 2020; Ntwasa et al., 2012). Reference gene expression was measured via the RPS18 primer pair (Lord et al., 2010) which demonstrated consistent RPS18 expression throughout infections.

Statistical analyses

For the visualization of constitutive knockdown efficiency and AMP transcription in the combinatorial experiment, we applied the formula $(2^{-(\Delta Ct(cactus) - \Delta Ct(malE))} * 100$ across all treatments to quantify the relative changes in mRNA abundance, with Male ΔCt denoting the mean ΔCt for all Male samples (Livak & Schmittgen, 2001). For statistical analysis, we applied the ΔCt approach to calculate relative expression on a log₂ scale by subtracting the average ct value of the target gene from the

reference mean ct value (Schmittgen & Livak, 2008). We then determined whether the Δ ct values for the target genes, *cec-2*, and *def-2* were normally distributed using the Shapiro–Wilk test (Shapiro & Wilk, 1965). If all Δ ct values for each treatment were normally distributed, we ran a one-way ANOVA - `aov(dct ~ treatment)` with a post-hoc Tukey HSD (Tukey, 1949). If any of the Δ ct were not non-parametric (*cec-2*), we ran a Kruskal Wallis test (Kruskal & Wallis, 1952).

For the time series experiments, we applied the Δ ct approach to calculate relative expression on a \log_2 scale by subtracting the average ct value of the target gene from the reference mean ct value (Schmittgen & Livak, 2008). This method of data representation allows for easier comparisons of gene expression across timepoints than the $\Delta\Delta$ ct method for fold change when the baseline treatment also changes (Critchlow et al., 2019). To discern the influence of each RNAi treatment on gene expression, we split our analysis into induction and decay phases depending on the AMP in question. Data normality was assured by inspecting histograms and Q-Q plots of standardized residuals. Gene expression underwent linear modeling, accounting for treatment, time, and their combined influence as determining factors, utilizing the `lme4` package in R (v. 4.3.0). We adjusted p-values for multiple tests using the Bonferroni approach (Dunn, 1961).

Results

Combinatorial knockdowns of *tollip* with either *dnr1* or *pgrp-sc2* do not significantly alter constitutive AMP transcription

Preliminary experiments indicated that RNAi for *pgrp-sc2*, *dnr1*, or *tollip* do not significantly alter constitutive transcription of *T. castaneum* AMPs (Zhong & Tate, 2023). To investigate whether this lack of transcriptional change is from the cross-talk between the Toll and IMD pathways (Yokoi et al., 2012), we combined *tollip* dsRNA with either *dnr1* or *pgrp-sc2* dsRNA and measured the constitutive

transcript abundance of the AMPs *cec-2* (Toll) and *def-2* (IMD). Our results indicate that dsRNA injection with a 3-day incubation resulted in substantial knockdown of the targeted genes compared to our MalE controls (**Appendix D, Figure 2a**). Despite significant gene silencing for all treatments, dsRNA treatment did not significantly change AMP expression for *cec-2* nor *def-2* compared to MalE for any treatment (tables x-y and figure Xb&c).

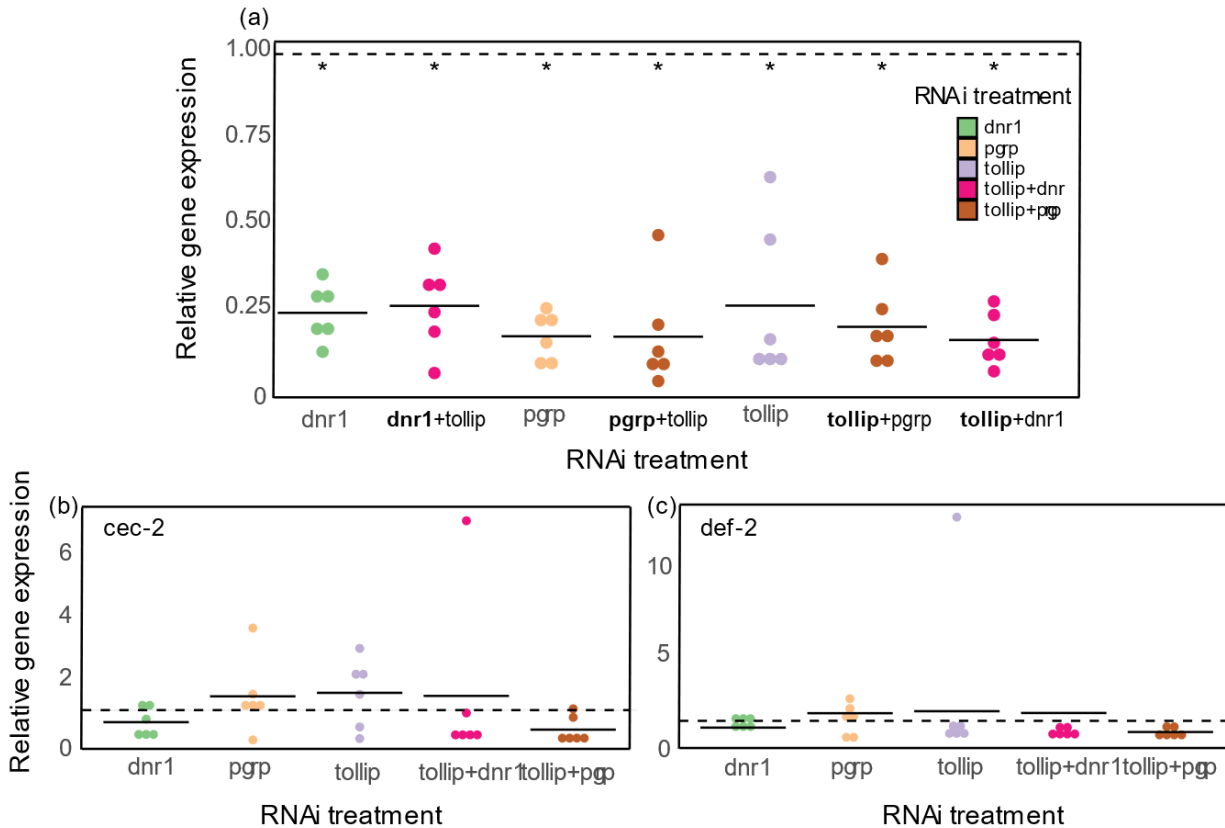


Figure 2. DsRNA-mediated knockdown of *dnr1*, *pgrp-sc2*, and *tollip* in combination does not constitutively increase *cec-2* nor *def-2* expression. a) Virgin adults were injected with 500 ng of dsRNA (250 ng if in combination) and given 3 days to incubate. Transcript abundance without microbial challenge was determined via RT-qPCR in whole adult beetles treated with 500 ng of target or *maleE* dsRNA. We used the $\Delta\Delta\text{Ct}$ method to determine the knockdown percentage compared to the average MaleE control (dotted line set at 1) for the RNAi targeted genes (a) and the antimicrobial peptides *cec-2* (b), and *def-2* (c). The * represents whether the transcript abundance was significantly altered compared to MaleE.

RNAi knockdown of *dnr1* does not significantly alter AMP transcription in response to microbial challenge

Since we did not observe changes in constitutive signaling, we hypothesized that the regulatory gene *dnr1* might influence IMD signaling only during the inducible response to microbial challenge. To investigate the role of *dnr1* in the constitutive, induction, decay, and resolution phases of humoral signaling, we injected 500 ng of *dnr1* or *maleE* (control) dsRNA into virgin adult beetles and then

septicaally challenged them three days later, using heat-killed *Bacillus thuringiensis* (Bt). We collected beetles at several time points over the next 48 hours, beginning before microbial challenge, and used RT-qPCR to measure *dnr1* knockdown efficiency (**Figure 3a**) and the transcriptional induction and decay of three AMPs (**Figure 3b-d**) associated with Toll and IMD signaling (*cec-2* (Toll), *def-2* & *att-1* (IMD) (Herndon et al., 2020; Yokoi et al., 2012). Our results indicate that our RNAi treatment significantly reduced *dnr1* transcript abundance (**Appendix E**). Our results also indicate that significant

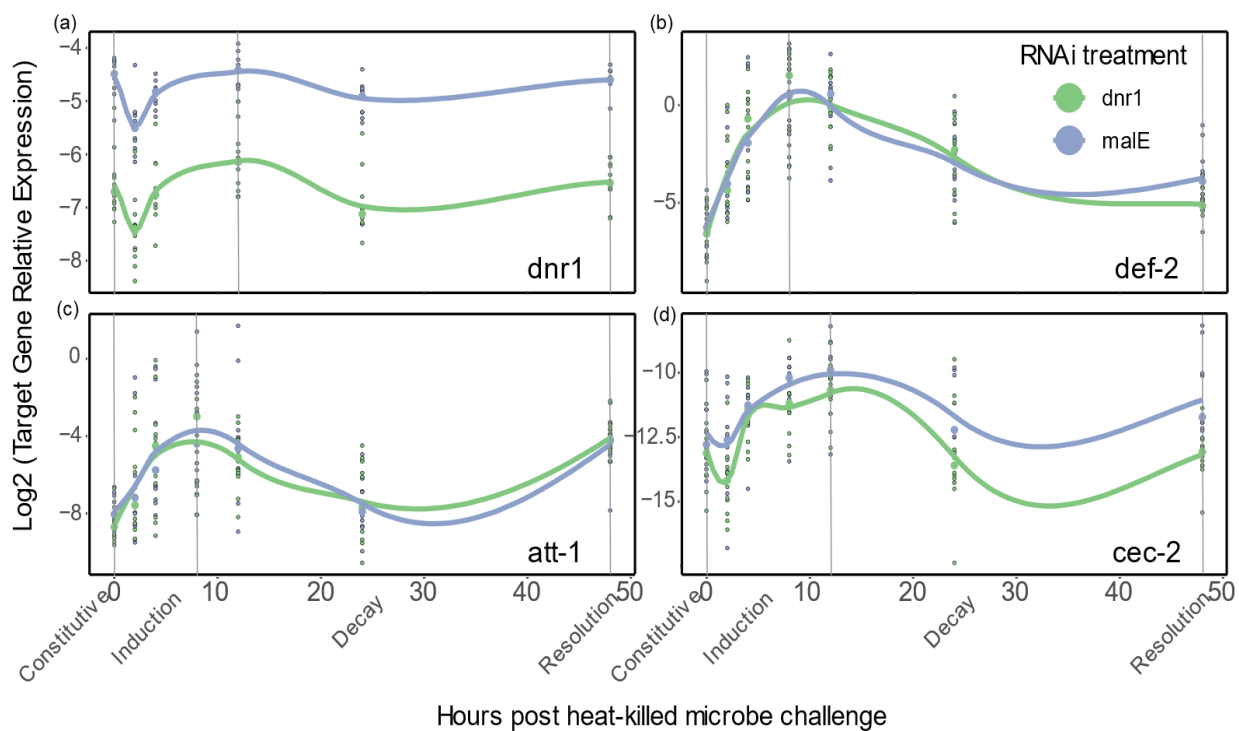


Figure 3. DsRNA-mediated knockdown of *dnr1* results no change in Toll nor IMD signaling. a-d) The expression of *dnr1* (a) and the antimicrobial peptides *def-2* (b), *att-1* (c) and *cec-2* (d) was determined by RT-qPCR to analyze whole adult beetles post-treatment given a 500 ng injection of *dnr1* or *malE* dsRNA, followed by a septic challenge using heat-inactivated Bt. Beetles were collected prior to the microbial challenge (hour 0) and at six subsequent time points over a 48-hour duration. Gene expression, relative to the reference gene RP18s, is depicted on a log₂ scale. To illustrate the induction and decay patterns post-RNAi treatment, splines were incorporated using the "loess" function (span 0.5) within the `geom_smooth` algorithm of `ggplot2` in R. The asterisk indicates significant alterations in the constitutive (hour 0), induction (rise from hour 0 to peak), decay (decline from peak to 48 hours), or resolution (hour 48) phases due to *dnr1* depletion ($\alpha = 0.0167$ for AMPs).

depletion in *dnr1* transcript abundance does not significantly increase whole body expression of *cec-2*, *def-2*, nor *att-1* (**Appendix E**). In fact, for the resolution phase, the malE treated beetles had significantly higher transcript abundance for AMPs *def-2* and *cec-2* ($p < 0.008$ and $p < 0.0005$, respectively).

DsRNA-mediated knockdown of *pgrp-sc2* and *tollip* does not alter humoral immune dynamics in beetle guts

In *D. melanogaster*, the silencing of *pgrp-sc2* results in increased gut specific IMD signaling that influences the fly intestinal microbial community (Guo et al., 2014). Additionally, in weevils *tollip*-mediated negative regulation of the Toll pathway is specific to a tissue that holds a high density of microbial symbionts (Anselme et al., 2008). We investigated whether these tissue specific effects on IMD and Toll signaling are present in the *T. castaneum* gut. Over a span of 48 hours, we collected beetles for gene expression at five time points, starting before septic heat-killed Bt challenge. Guts were removed from the adult beetles and flash-frozen on dry ice. Using RT-qPCR, we evaluated the knockdown efficiency and tracked the transcriptional induction and decay of three AMPs associated with Toll (*cec-2* & *thum-1*) and IMD (*def-2*) signaling (**Figure 4**). Our results indicate that systemic RNAi for *pgrp-sc2* and *tollip* do not alter IMD or Toll signaling in the gut (**Appendix F**).

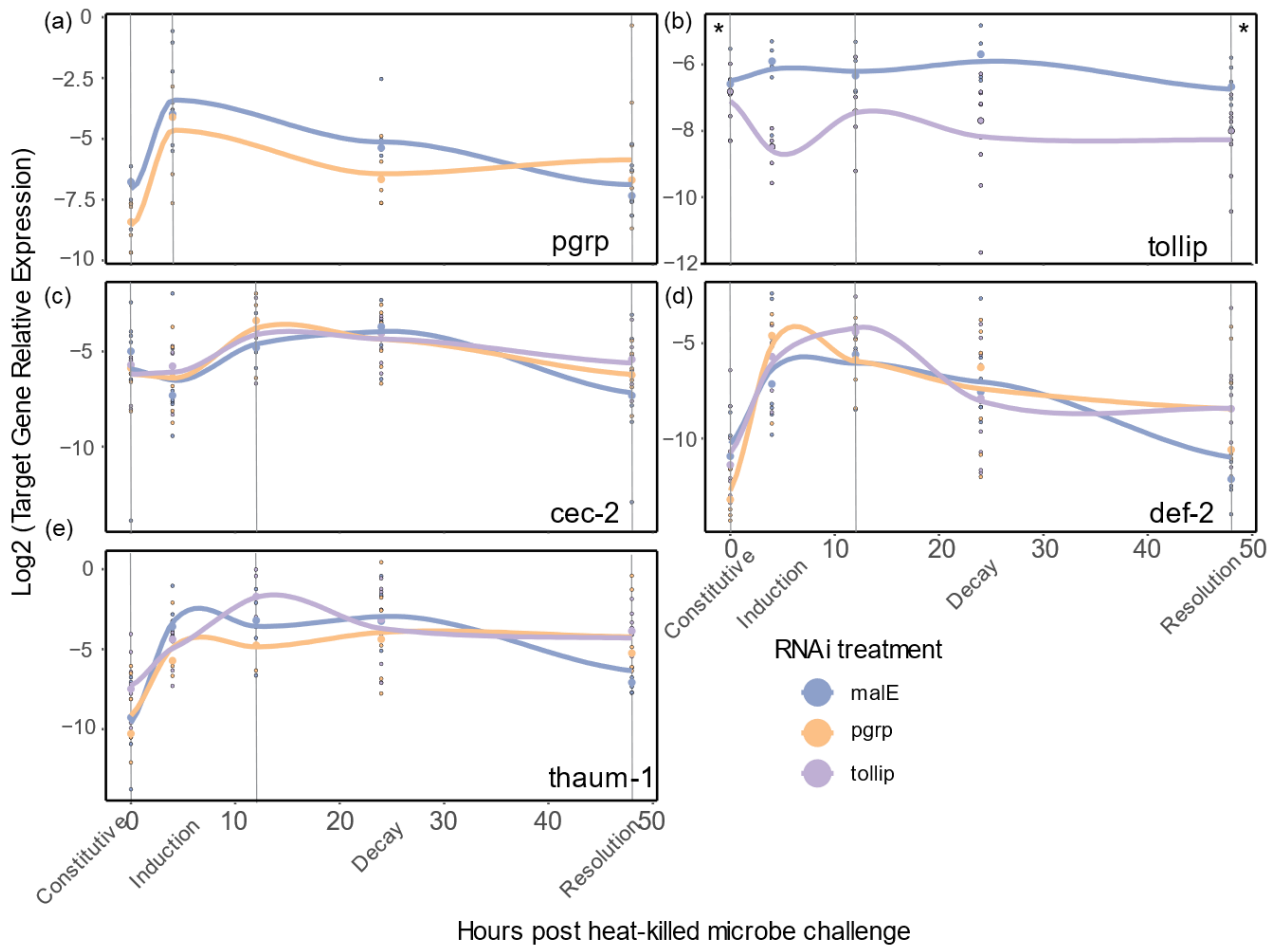


Figure 4. DsRNA-mediated knockdown of *tollip* and *pgrp-sc2* results no change in Toll nor IMD signaling in beetle guts. a-e) The expression of *pgrp-sc2* (a), *tollip* (b) and the antimicrobial peptides *cec-2* (c), *def-2* (d) and *thaum-1* (e) was determined by RT-qPCR to analyze adult beetle guts post a 500 ng injection of *pgrp-sc2*, *tollip*, or *malE* dsRNA, followed by a septic challenge using heat-inactivated Bt. Beetles were collected prior to the microbial challenge (hour 0) and at four subsequent time points over a 48-hour duration. Gene expression, relative to the reference gene RP18s, is depicted on a log2 scale. To illustrate the induction and decay patterns post-RNAi treatment, splines were incorporated using the "loess" function (span 0.5) within the *geom_smooth* algorithm of *ggplot2* in R. The asterisk indicates significant alterations in the constitutive (hour 0), induction (rise from hour 0 to peak), decay (decline from peak to 48 hours), or resolution (hour 48) phases due gene depletion ($\alpha = 0.0167$ for AMPs).

10-day RNAi-mediated knockdown of *skpA* decouples *T. castaneum* Toll and IMD signaling

Finally, we investigated whether the discrepancies in immune phenotypes between *T. castaneum* and *D. melanogaster* might be due to delayed protein turnover, giving us efficient knockdown when

viewing transcript abundance but hiding stable protein levels. Therefore, we extended the RNAi incubation time from 3 days to 10 days to allow more time for target proteins to turn over. We followed our same treatment protocol as in **Figure 3**, but instead used 10 days between RNAi injection and heat-killed Bt challenge. We then measured whole-body transcript abundance for our RNAi target genes (**Figure 5**) as well as AMPs *def-2* and *cec-2* (**Figure 6**) directly before and at five time points over 48 hours after microbial challenge. Our results indicate that our target genes exhibit significant reductions in gene expression after the 10 day incubation period similar to the 3 day period (**Appendix G**).

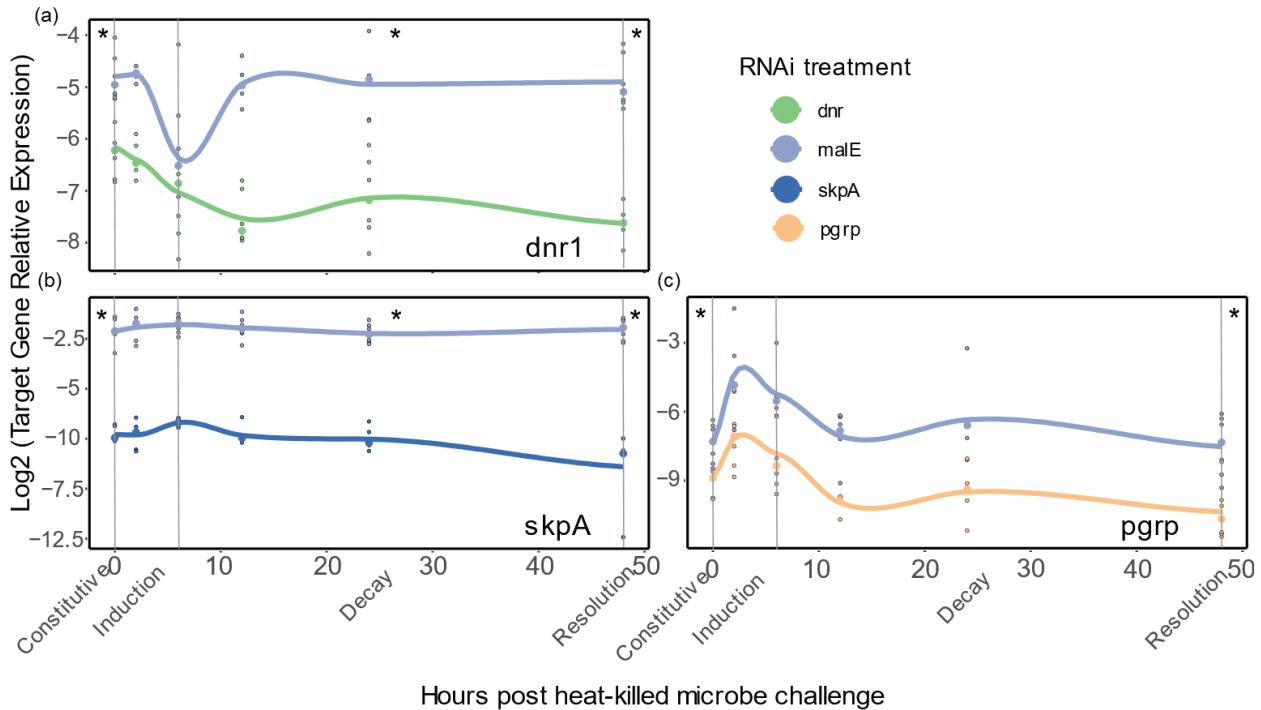


Figure 5. 10-day incubation after dsRNA injection significantly silences gene expression for *dnr1*, *skpA*, and *pgrp-sc2*. a-e) The expression of *dnr1* (a), *skpA* (b) and *pgrp-sc2* (c) was determined by RT-qPCR to analyze whole adult beetle transcript abundance after a 500 ng injection of *dnr1*, *skpA*, *pgrp-sc2*, or *malE* dsRNA, followed by a septic challenge using heat-inactivated Bt. Beetles were collected prior to the microbial challenge (hour 0) and at five subsequent time points over a 48-hour duration. Gene expression, relative to the reference gene RP18s, is depicted on a log2 scale. To illustrate the induction and decay patterns post-RNAi treatment, splines were incorporated using the "loess" function (span 0.5) within the `geom_smooth` algorithm of `ggplot2` in R. The asterisk indicates significant alterations in the constitutive (hour 0), induction (rise from hour 0 to peak), decay (decline from peak to 48 hours), or resolution (hour 48) phases due to gene depletion ($\alpha = 0.05$).

Our results also indicate that *skpA* RNAi with a 10-day incubation significantly increases *def-2* constitutive ($p < 0.01$) and resolution ($p < 0.01$) transcript abundance (**Appendix G**). Additionally, *skpA* RNAi significantly decreased *cec-2* expression at the constitutive ($p < 0.01$) and resolution ($p < 0.01$) phases. We also observe a trend of greater peak expression of *def-2* at 6 hours post infection when beetles are given *pgrp-sc2* RNAi ($p < 0.04$) (**Appendix G**); however, this result is not significant when adjusting the p value for multiple corrections.

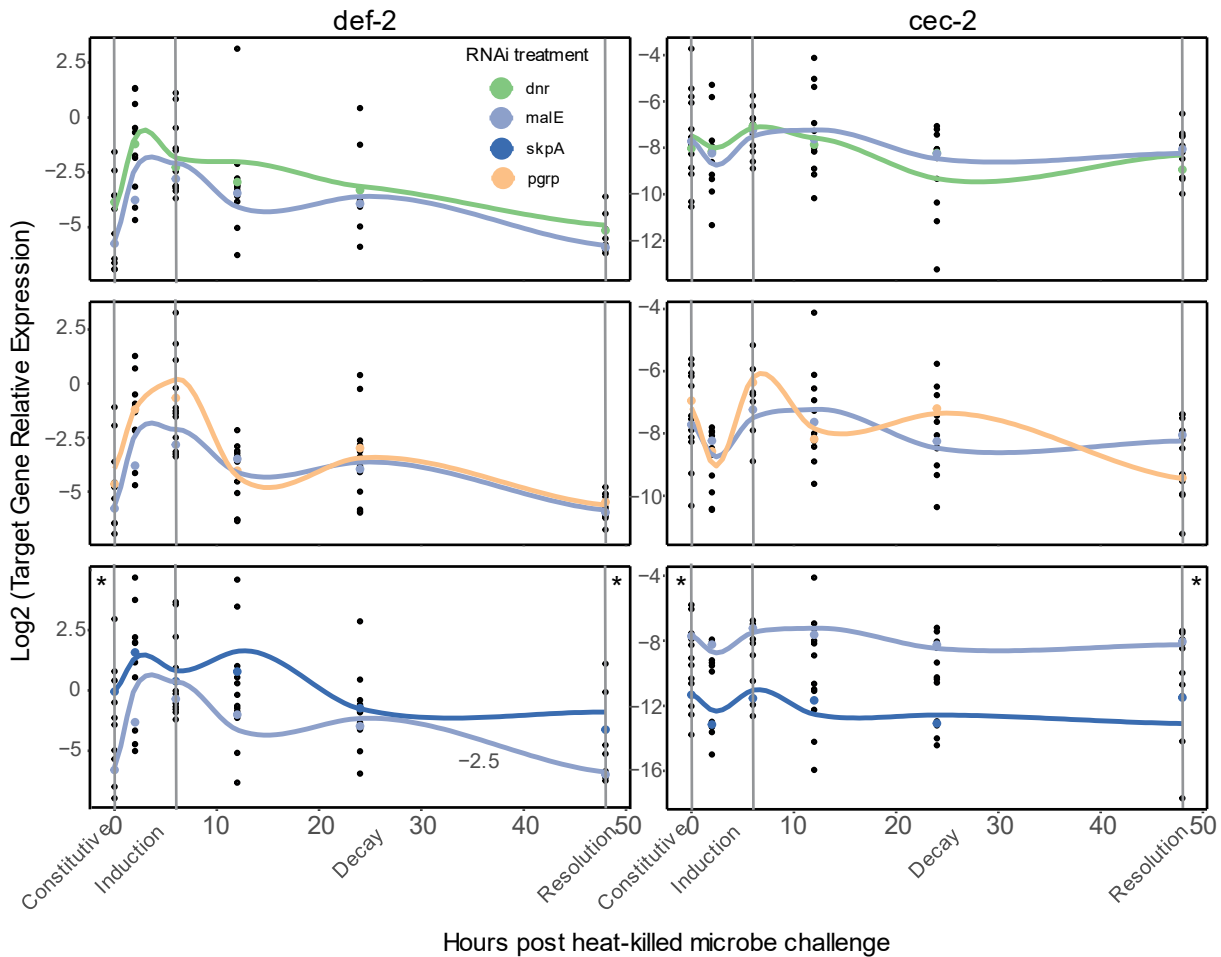


Figure 6. DsRNA-mediated knockdown of *skpA* significantly increases IMD signaling while decreasing Toll signaling. a-e) The expression of *pgrp-sc2* (a), *tollip* (b) and the antimicrobial peptides *cec-2* (c), *def-2* (d) and *thaum-1* (e) was determined by RT-qPCR to analyze adult beetle guts post a 500 ng injection of *pgrp-sc2*, *tollip*, or *malE* dsRNA, followed by a septic challenge using heat-inactivated Bt. Beetles were collected prior to the microbial challenge (hour 0) and at four subsequent time points over a 48-hour duration. Gene expression, relative to the reference gene RP18s, is depicted on a log2 scale. To illustrate the induction and decay patterns post-RNAi treatment, splines were incorporated using the "loess" function (span 0.5) within the *geom_smooth* algorithm of *ggplot2* in R. The asterisk indicates significant alterations in the constitutive (hour 0), induction (rise from hour 0 to peak), decay (decline from peak to 48 hours), or resolution (hour 48) phases due to gene depletion ($\alpha = 0.025$).

Discussion

We sought to identify regulatory genes governing the Toll and IMD pathways in *T. castaneum*.

Our focus was primarily on the regulatory genes *dnr1*, *pgrp-sc2*, and *skpA* from *D. melanogaster*, as well as *tollip* from the weevil *Sitophilus zeamais*. Surprisingly, our results revealed no significant alterations in the baseline Toll and IMD signaling in whole adult beetles subjected to RNAi treatments targeting *tollip*, *pgrp-sc2*, or *dnr1*. Similarly, *dnr1* silencing did not modify the induction and decay dynamics post-Bt septic infection. Furthermore, gut-specific signaling of the Toll and IMD pathways remained unchanged in beetles treated with dsRNA targeting *pgrp-sc2* or *tollip*. Yet, when the silencing duration was extended from 3 to 10 days, our data suggests that *skpA* acts as a negative regulator for the IMD pathway and a positive regulator for the Toll pathway. The extended incubation also hints at a potential role for *pgrp-sc2* in tempering the peak induction of IMD signaling. Intriguingly, our study makes the point that despite *T. castaneum* and *D. melanogaster* possessing orthologous genes in the IMD and Toll pathways, their impact on signaling dynamics can diverge considerably. These insights not only lay the foundation for a more comprehensive understanding of immune regulation mechanisms in *T. castaneum*, but they also shed light on the broader regulatory architecture of immune systems. By probing the conservation of these regulators across different species, we can gain valuable insights into the potential evolutionary selection pressures shaping immunity.

SkpA functions as a pathway-dependent regulator in *T. castaneum* humoral immune signaling

To better understand the regulation of the Toll and IMD pathways in *T. castaneum*, we investigated SkpA and its effect on AMP transcript abundance. Previous work in *D. melanogaster* showed that mutations in *skpA* led to constitutive expression of the IMD AMP *diptericin* but not for the Toll AMP *drosomycin* (Khush et al., 2002). Our study reveals that *skpA* silencing leads to an increase in *def-2* expression after a 10-day treatment period. Interestingly, while *D. melanogaster* exhibited no effect on the Toll pathway, our study found a significant reduction in *cec-2* expression, suggesting *skpA*'s role in positively regulating the Toll pathway. This pathway specific role for an E3 ligase is not

unprecedented. LUBAC, an E3 ligase in mammalian cells, helps activate signaling in response to TNF, but negatively regulates viral sensory receptors (Hu and Sun, 2016; Tokunaga, 2013). Our results suggest a similar dual role for the *T. castaneum* SCF complex. Future work should determine the influence *skpA* silencing has on the Toll and IMD transcription factors to see if the SCF complex partially mediates the cross-talk often seen between these pathways.

***Pgrp-sc2* silencing may influence the peak expression of IMD signaling**

In this study, we identified a potential role for *pgrp-sc2* in influencing the peak expression of IMD signaling in *T. castaneum* adults. Notably, after depleting *pgrp-sc2*, there was a discernible trend towards heightened *def-2* transcript levels 6 hours following a heat-killed Bt challenge. This observation contrasts with findings from *D. melanogaster*, where *pgrp-sc2* RNAi led to amplified IMD signaling but only 24 and 48 hours after septic challenge (Bischoff et al., 2006). A similar delay in decay rates was documented in *T. castaneum* pupae, where IMD signaling persisted at elevated levels 24 hours post septic challenge (Koyama et al., 2015). A crucial distinction between our study and previous ones is the combinatorial knockdown approach adopted in both the *D. melanogaster* and earlier *T. castaneum* experiments, where multiple PGRP genes were silenced concurrently. Prior research in *D. melanogaster* has demonstrated an additive effect of these extracellular amidases, with combined silencing intensifying the immune phenotype (Paredes et al., 2011). I anticipate that the differences between our results and previous findings stems from our singular knockdown approach. By simultaneously targeting redundant extracellular amidases, I expect to see not only significantly boosted peak IMD signaling but also extended decay rates. Future investigations could delve deeper into the redundancy of extracellular amidases across life stages and their implications for the intricate balance between development, reproduction, and immunity.

***Pgrp-sc2* silencing does not alter gut-specific IMD signaling**

In *D. melanogaster*, *pgrp-sc2* plays a crucial role in maintaining gut homeostasis. Its disruption escalates AMP transcription and triggers gut microbial imbalances (Guo et al., 2014). In contrast, our 3-day incubation study did not reflect these outcomes, as we observed no significant changes in gut-specific AMP transcript abundance after silencing *pgrp-sc2*. It is worth noting that this discrepancy might be from our reliance on septic challenges, while the *D. melanogaster* study utilized oral infections to probe the gut immune response. This distinction is consistent with previous work in flour beetles, showing that transcriptomic responses to oral infections differ markedly from septic infections. Additionally, our study involved a three-day incubation period post-RNAi treatment. However, the effects of *pgrp-sc2* on whole-body gene expression were observed after a 10-day incubation. To thoroughly assess *Pgrp-sc2*'s potential regulatory role in gut immune signaling, future studies should extend the incubation to 10 days and compare outcomes from both oral and septic challenges (Behrens et al., 2014). Furthermore, our methodology involved sterilizing the flour to avert contamination from protozoan parasites (Critchlow et al., 2019; Tate & Graham, 2015a). Yet, in the *D. melanogaster* study, the regulatory influence of *Pgrp-sc2* was not evident in axenically-reared flies (Guo et al., 2014). This raises the possibility that our beetles, devoid of access to a microbial community in their food, might lack the stimulus essential for *pgrp-sc2* production. Future endeavors investigating *T. castaneum* gut immune regulation should incorporate microbial communities.

***Dnr1* silencing does not alter humoral immune signaling**

Unlike the regulatory effects observed in *D. melanogaster* (Guntermann et al., 2009), our study found no conditions under which *dnr1* silencing significantly influenced AMP expression. Since DREDD is still necessary for proper IMD signaling in flour beetles, our findings suggest that the

network is responding to the disruption from our *dnr1* treatment to maintain homeostasis. Given that *T. castaneum* Dnr1 potentially has six paralogues (Zhong & Tate, 2023), it's plausible that these paralogues might compensate for any disruptions caused by our *dnr1* RNAi treatment.

The divergence in influence from the disruption of *dnr1* and the other immune regulators studied here between flour beetles and *D. melanogaster* highlights that even if proteins are conserved across species, their functional roles can differ significantly. Such differences hint at a broader variability in the immune responses of various insect species. Grasping this diversity in immune regulation between species can offer valuable insights into the trade-offs inherent in immune defense strategies. Given the vast array of parasites and environments hosts face, combined with the substantial costs of immunity, a better understanding of the unique balance required of immune networks might be pivotal in deciphering the evolutionary underpinnings of immune-related diseases.

CHAPTER 4

Mapping the functional form of the trade-off between infection resistance and reproductive fitness under dysregulated immune signaling

Preface

In this chapter, we develop an experimental methodology to explore the functional form between increased infection resistance and its trade-offs with other life history traits, from variation in expression of an inhibitor of transcription factors. This chapter reveals that while strengthening immune pathway activation enhances resistance and survival during bacterial infections, it also has a pronounced negative impact on reproduction and overall host health. These findings are significant since they detail the severe consequences from small changes in immune regulation and provide a framework for future studies to understand the relationship between immune investment and overall fitness. My advisor, Dr. Ann Thomas Tate, conceptualized and obtained funding for this study. Dr. Arun Prakash, Dr. Tate, and I designed the experiments. Dr. Prakash, Katherine Zhong, and I conducted the experiments. I statistically analyzed all of the data for this chapter. Dr. Tate and I wrote the manuscript. All authors critically reviewed the drafts and approved the final version. This work was supported by the National Institute of General Medical Sciences at the National Institutes of Health (grant number R35GM138007 to A.T.T.). This chapter was included in this dissertation with the permission of my collaborators, Dr. Arun Prakash, Katherine Zhong, and Dr. Ann Tate.

Abstract

Immune responses benefit organismal fitness by clearing parasites but also exact costs associated with immunopathology and energetic investment. Hosts manage these costs by tightly regulating the induction of immune signaling to curtail excessive responses and restore homeostasis. Despite the theoretical importance of turning off the immune response to mitigate these costs, experimentally connecting variation in the negative regulation of immune responses to organismal fitness remains a frontier in evolutionary immunology. In this study, we used a dose-response approach to manipulate the RNAi-mediated knockdown efficiency of *cactus* ($I\kappa B\alpha$), a central regulator of Toll pathway signal transduction in flour beetles (*Tribolium castaneum*). By titrating *cactus* activity along a continuous gradient, we derived the shape of the relationship between immune response investment and traits associated with host fitness, including infection susceptibility, lifespan, fecundity, body mass, and gut homeostasis. *Cactus* knock-down increased the overall magnitude of inducible immune responses and delayed their resolution in a dsRNA dose-dependent manner, promoting survival and resistance following bacterial infection. However, these benefits were counterbalanced by dsRNA dose-dependent costs to lifespan, fecundity, body mass, and gut integrity. Our results allowed us to move beyond the qualitative identification of a trade-off between immune investment and fitness to actually derive its functional form. This approach paves the way to quantitatively compare the evolution and impact of distinct regulatory elements on life-history trade-offs and fitness, filling a crucial gap in our conceptual and theoretical models of immune signaling network evolution and the maintenance of natural variation in immune systems.

Introduction

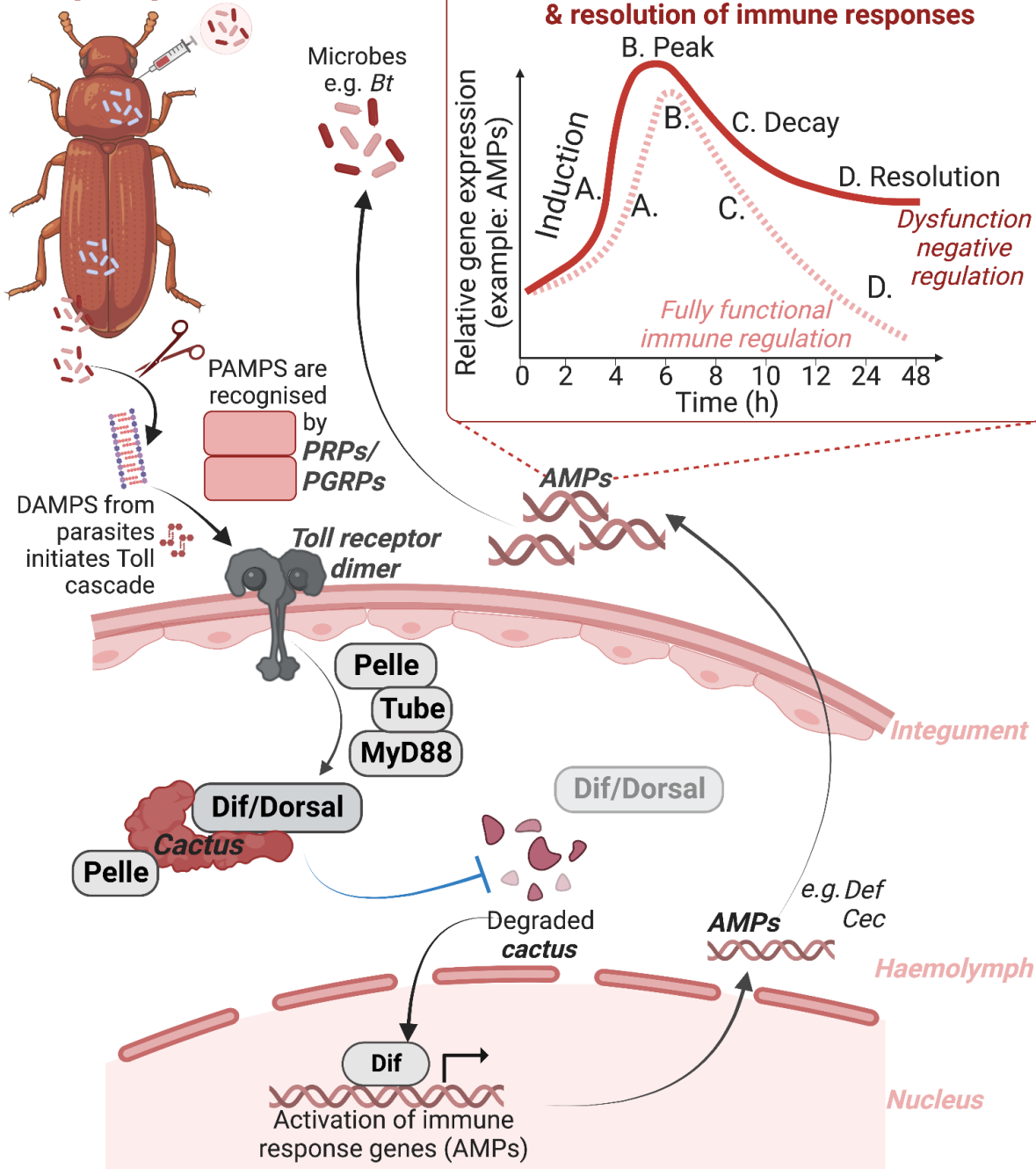
An effective immune response is essential for recognizing and clearing infections. Hosts produce immune effectors even in the absence of infection as part of the constitutive response, but once they recognize invaders they inducibly create immune effectors to stymie the infection and then deactivate the response once the infection is under control during the decay or resolution phase of an immune response (Jent et al., 2019; Sheldon & Verhulst, 1996). Failure to manage infections can result in parasite-mediated pathology and exploitation, but excessive immune activation can also exert significant immunopathological and energetic costs (Badinloo et al., 2018; Graham et al., 2005; Sears et al., 2011). To balance these costs, hosts must tightly control immunological responses before, during, and after infections (Lazzaro & Tate, 2022).

By reducing the probability of colonization and initial replication by pathogens and other parasites, constitutive immune defenses mitigate the opportunity for parasite-induced pathology and discourage parasite transmission (Boots & Best, 2018; Shudo & Iwasa, 2001; Westra et al., 2015). Since constitutive immunity requires continuous resource investment, its benefit to fitness diminishes as the risk of infection declines (Hamilton et al., 2008). In contrast, inducible defenses are predicted to limit immunological costs in the absence of infection but risk being overwhelmed by fast-growing parasites if the response is not robust enough (Hamilton et al., 2008). In *Drosophila melanogaster* flies infected with the bacterium *Providencia rettgeri*, for example, host death is determined by whether the fly produces enough antimicrobial peptides (AMPs) before *P. rettgeri* replicates to uncontrollable numbers (Duneau et al., 2017). Yet, failure to dampen an induced immune response can also pose serious risks to the host's health and lifespan, as seen when aged mealworm beetles overactivate the melanization response, damaging their Malpighian tubules (Khan et al., 2017). To prevent such runaway immunological costs, immune signaling pathways utilize negative feed-back loops (Ferrandon et al., 2007;

S. A. Frank & Schmid-Hempel, 2019).

Robust negative regulation is predicted to affect the constitutive levels of immune proteins as well as the rate of induction, total magnitude, and decay rate of inducible immune responses (**Figure 1**) (S. A. Frank, 2002; Lazzaro & Tate, 2022). Most invertebrate species rely on regulatory proteins to tightly govern the recognition, signaling, and output of the NF- κ B Imd and Toll pathways (Kleino & Silverman, 2014; Valanne et al., 2022; F. Wang & Xia, 2018; Zhai et al., 2018), and through genetic modification, researchers have started to characterize the consequences of their dysregulation (Lee & Ferrandon, 2011). For instance, the negative regulator Pirk interrupts the interaction of the transmembrane peptidoglycan recognition protein PGRP-LC and the intracellular signaling protein Imd (Aggarwal et al., 2008; Basbous et al., 2011; Kleino et al., 2008; Vincent & Dionne, 2021). When expression of *pirk* is disrupted via RNAi in the mosquito *Aedes aegypti*, survival against bacterial infection increases, but at a cost to female egg production (M. Wang et al., 2022). Cactus, the Toll inhibitor of nuclear factor kappa B ($\text{I}\kappa\text{B}\alpha$), prevents the translocation of the Toll pathway TFs Dif and Dorsal (Belvin & Anderson, 1996). Silencing and loss of function of the *cactus* gene in *D. melanogaster* disrupts Toll signaling resulting in increased production of AMPs and hemocyte proliferation (Qiu et al., 1998). While this Toll pathway dysregulation increases resistance and survival to infection (Garver et al., 2009; Lemaitre et al., 1996; Rhodes et al., 2018), it also shortens host lifespan (Ulrich et al., 2015), disrupts neuromuscular function (Beramendi et al., 2005), reduces lipid stores by suppressing insulin signaling (DiAngelo et al., 2009), and disrupts gut stability (Ryu et al., 2008).

I. A simplified version of Toll signaling in *T. castaneum*



Abbreviations:

PAMPs - Pathogen-associated molecular pattern molecules
DAMPs - Damage-associated molecular patterns
Toll - TLR-like receptor signaling
Bt - *Bacillus thuringiensis* (gram +ve bacteria)

PRRs - pathogen recognition receptors
PGRPs - peptidoglycan recognition proteins
Dif - Dorsal related immunity factor
AMPs - antimicrobial peptides
Def - Defensin
Cec - Cecropin

Figure 1. Simplified overview of the flour beetle Toll signaling pathway. I) Pattern Recognition Receptors (PRRs) identify pathogen or danger-associated molecular patterns (PAMPs or DAMPs) triggering signal transduction through Toll. This forms an intracellular signaling scaffold consisting of MyD88, Tube, and Pelle, resulting in Cactus phosphorylation by Pelle. The subsequent degradation of Cactus allows Dif and Dorsal transcription factors to translocate into the nucleus, initiating immune effector transcription. II) Production of AMPs from Toll signaling proceeds through a sequence of stages, starting with constitutive production before infection (A), induction upon parasite recognition (B), peak output (C), decay of transcript production, and finally resolution of the response (D). Dysfunction in negative regulators could potentially disturb signaling dynamics at any stage, leading to overproduction of immune effectors.

Unrestrained immune signaling clearly has consequences for host fitness, but how does every unit of gain in resistance translate into a cost to reproduction, and is the relationship linear or a case of diminishing returns?

We do not yet have an answer to this question because previous studies have typically employed binary treatments where genes are either expressed normally or maximally disrupted through mutation, deletion, or efficient RNAi knock-down (Clayton et al., 2013; Hou et al., 2014; Prakash et al., 2021). While these approaches are critical for establishing the presence of a trade-off, dichotomous experimental designs limit our ability to quantitatively assess the impact of variation in immune dynamics on host-parasite coevolutionary dynamics and the costs associated with immune activation (S. A. Frank & Schmid-Hempel, 2019). By adopting an approach that titrates the magnitude of genetic manipulation, we can capture the continuous relationship between negative immune regulators and host fitness traits. This would enable us to mimic the natural variation commonly seen in immune gene expression and function and gain a deeper understanding of the evolutionary constraints and selection pressures imposed on regulatory immune genes.

In the present study, we developed an experimental framework to establish the functional form

of the relationship between gains in infection resistance and costs to other life history traits for a specific regulatory node in immune signaling. We took advantage of dose-dependent RNAi knockdown efficiency in the red flour beetle (*Tribolium castaneum*) to quantitatively control the magnitude of dysregulation of Cactus. We measured the temporal dynamics of AMP transcription after exposure to fungal and bacterial microbes to parse apart the role of this individual regulator in fine tuning the rate of response to detection as well as the resolution of the response, both of which are predicted to determine an “optimal” immune response to infection (S. A. Frank, 2002). We also quantified functional metrics of infection susceptibility and resistance, including cellular immunity, hemolymph antimicrobial activity, bacterial load, and survival following live infection. At the same time, we quantified the impact of variation in Cactus activity on beetle fecundity, survival in the absence of infection, and gut homeostasis. Our results directly advance our understanding of immune system evolution and the complex feedbacks of host-parasite interactions on organismal fitness. These insights provide valuable information for understanding the pathogenesis of immune-related disorders and may guide the development of targeted therapeutic interventions, including siRNA-based therapies that aim to modulate immune responses for disease treatment.

Results

***Cactus* RNAi increases constitutive and total transcriptional activation and delays decay of Toll signaling**

To investigate the role of *cactus* on *T. castaneum* immune signaling, we injected 250 ng of *cactus* or *malE* (control) dsRNA into adult beetles and then septically challenged them three days later, using either heat-killed *Bacillus thuringiensis* (Bt) or heat-killed *Candida albicans*, which contain different sets of microbe-associated molecular patterns (MAMPs) that potentially stimulate differences

in recognition and subsequent immune signaling. We collected beetles at several time points over the next 48 hours, beginning before microbial challenge, and used RT-qPCR to measure *cactus* knockdown efficiency and the transcriptional induction and decay of three AMPs (**Figure 2a-h**) associated with Toll and IMD signaling (*cecropin-2* (Toll), *defensin-2* (IMD), and *defensin-3* (Toll & IMD) (Herndon et al., 2020; Yokoi, Koyama, Minakuchi, et al., 2012b)). We expected that our control (MalE) beetles would follow typical temporal dynamics (**Figure 1**), where AMP transcript abundance reaches maximum levels in 4-12 hours post septic challenge, then returns to baseline by 48 hours (Tate & Graham, 2017b; Zou et al., 2007b). Therefore, to statistically analyze differences in temporal dynamics among treatments, we considered four outputs for AMP expression: constitutive (hour 0), the rate of induction, the rate of decay from the peak magnitude of expression, and the magnitude of AMP production when the response should be resolved (hour 48).

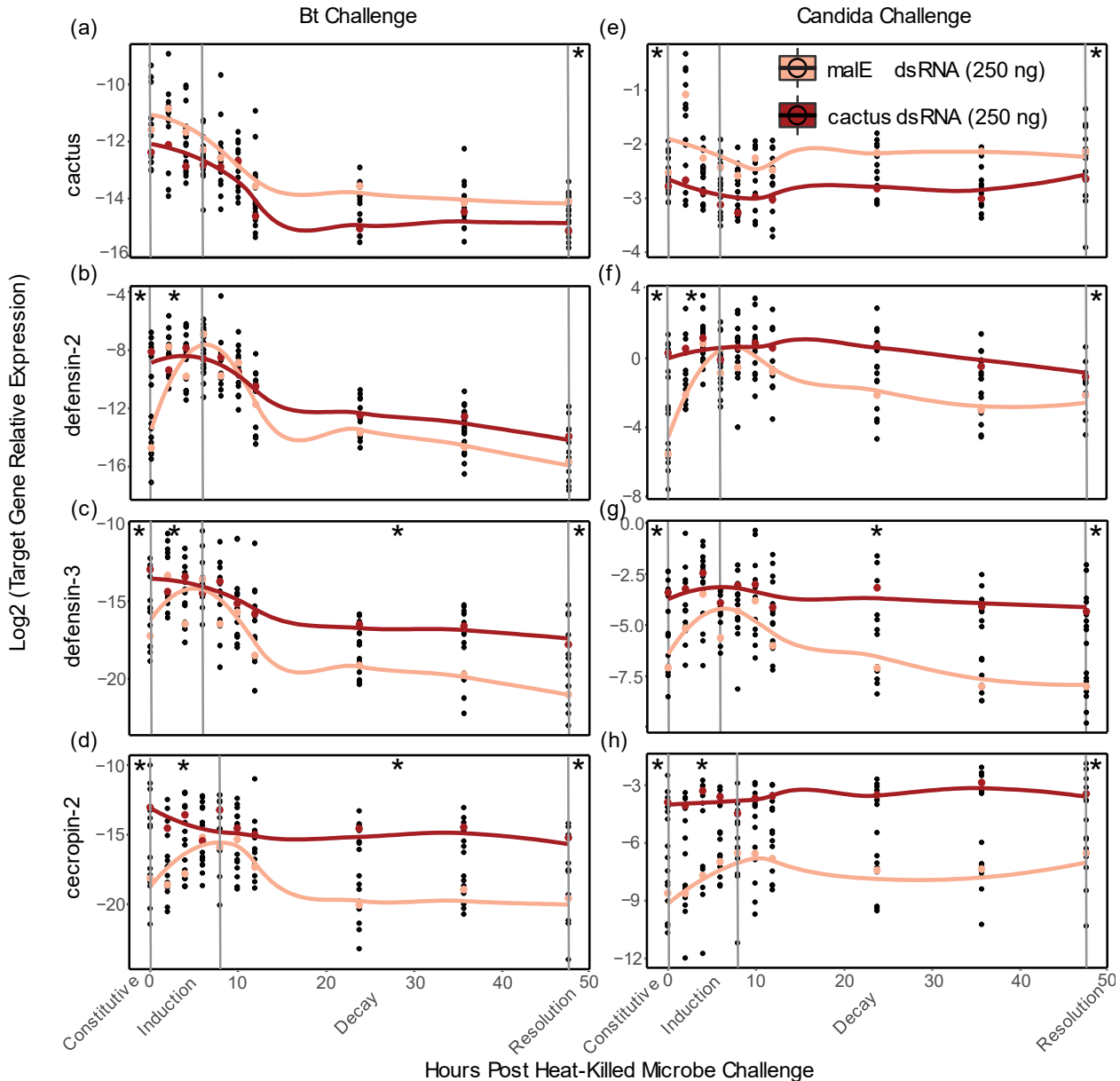


Figure 2. DsRNA-mediated knockdown of cactus results in increased Toll signaling. a-h) The expression of cactus (a, e) and the antimicrobial peptides defensin-2 (b, f), defensin-3 (c, g) and cecropin-2 (d, h) were assayed via RT-qPCR in whole adult beetles treated with 250 ng of cactus or malE dsRNA and then septically challenged with heat-killed Bt (left) or *C. albicans* (right). Beetles were sacrificed before microbial challenge (hour 0), and nine additional times after challenge over 48 hours. The expression of each gene relative to the reference gene RP18s is represented on a log2 scale. Splines have been added to visualize the induction and decay dynamics from RNAi treatment using “loess” function (span 0.25) in the `geom_smooth` algorithm of `ggplot2` in R. The * represents whether the constitutive (hour 0), induction (slope from hour 0 to peak expression), decay (slope from peak expression to 48 hours), or resolution (hour 48) windows were significantly altered by cactus depletion ($\alpha = 0.0167$).

Cactus RNAi treatment significantly reduced total *cactus* expression, relative to MalE RNAi-treated beetles, across the time course of the Bt ($p < .001$, **Appendix I**) and *Candida* exposure experiments ($p < 2 \times 10^{-16}$, **Appendix J**). Averaged across all time points, relative transcript abundance decreased by 39% (Bt) and 33% (*Candida*). For all three AMPs, constitutive expression and the overall magnitude of transcription after exposure were higher in *cactus*-depleted beetles, independent of the challenged microbe (**Figure 2b-d & 2f-h**) (**Appendix I & J**). AMP induction rates were significantly higher for *def-2*, *def-3*, and *cec-2* when challenged with Bt ($p < 0.01$) and for *def-2* and *cec-2* when challenged with *Candida* ($p < 0.01$). Additionally, *cactus* RNAi delayed decay for *def-3* and *cec-2* when challenged with Bt ($p < 0.01$), and delayed decay for *def-3* when challenged with *Candida* ($p < 0.01$). Resolution transcription levels at 48 hours post exposure were significantly higher for *def-3* and *cec-2* ($p < 0.001$) but not *def-2* ($p = 0.03$) when challenged with Bt and were higher for *def-3*, *cec-2*, and *def-2* ($p < 0.01$) when challenged with *Candida*.

Amplification of Toll Signaling via *cactus* RNAi increases total circulating hemocytes

To study the impact of enhanced Toll signaling on cellular immunity, we measured circulating hemocyte counts in adult beetles before and after heat-killed Bt challenge (**Figure 3a**). Circulating hemocytes did not constitutively increase in *cactus* RNAi (250 ng) treated beetles before Bt challenge or after a sham infection (**Appendix L**). However, *cactus* RNAi-treated beetles exhibited significantly higher numbers of hemocytes at all measured time points after bacterial exposure relative to their time-matched MalE counterparts (Wilcoxon rank sum test and FDR correction; **Appendix L**).

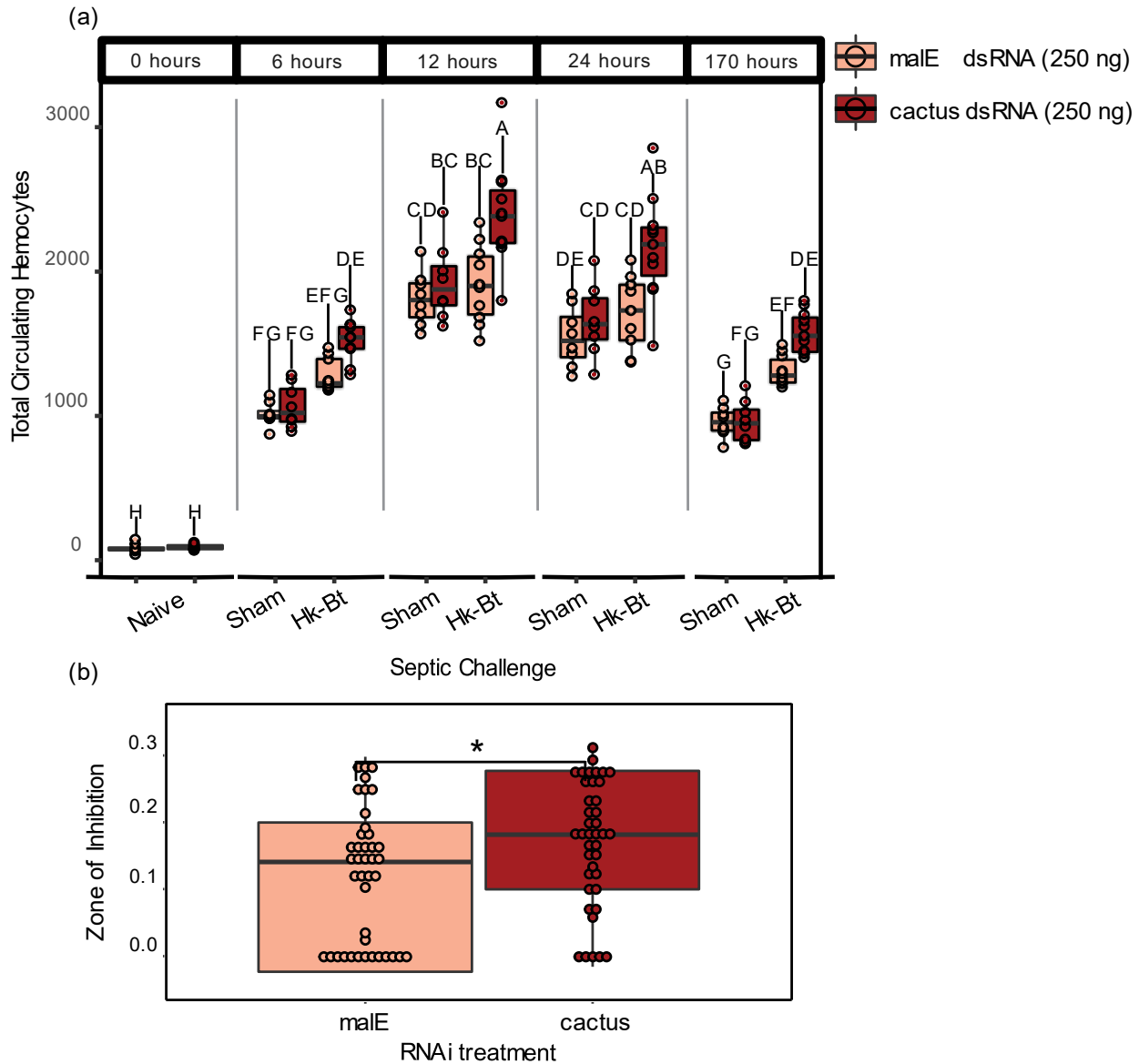


Figure 3. Toll signaling increases functional metrics of cellular immunity and antibacterial activity **a)** Circulating hemocytes were isolated, fixed, stained, and counted using a modified protocol from (King & Hilyer, 2013). Adult beetles received an injection of 250 ng of *cactus* or *malE* dsRNA, and after three days, they were septicly exposed to a heat-killed Bt or a sham infection. Medians not sharing the same letter are significantly different (Wilcoxon rank sum test and FDR correction, $P < 0.05$). **b)** The antibacterial activity of whole-beetle homogenates was assessed by measuring the mean diameter of the zone of inhibition of bacterial growth on agar plates.

Uninhibited Toll signaling enhances antibacterial activity

To measure whether unrestrained Toll signaling correlates with functional changes in antibacterial activity, we used a lytic zone assay to quantify the ability of beetle hemolymph to prevent Bt growth on Luria Broth agar (**Figure 3b**). Beetles treated with *cactus* dsRNA exhibited significantly increased hemolymph antibacterial activity relative to MalE controls (Kruskal-Wallis rank sum test, $N = 40-41$ beetles/treatment, $(\chi^2 = 6.08, Df = 1, P = 0.014)$).

The magnitude of Toll pathway activation depends on the dose of *cactus* dsRNA

To quantify the relationship between the magnitude of immune dysregulation and immune dynamics, we repeated the previous experiment but provided beetles with one of four *cactus* dsRNA doses: 0 ng (but 250 ng of *malE* dsRNA), 2.5 ng, 25 ng, or 250 ng. Using the linear model (expression \sim dose), the dose of *cactus* dsRNA was significantly associated with decreased total *cactus* transcription ($p < 0.001$) (**Figure 4a, Appendix K**). Total relative *cactus* transcript abundance was reduced by 25% (2.5 ng), 32% (25 ng), and 35% (250 ng) for each respective dose.

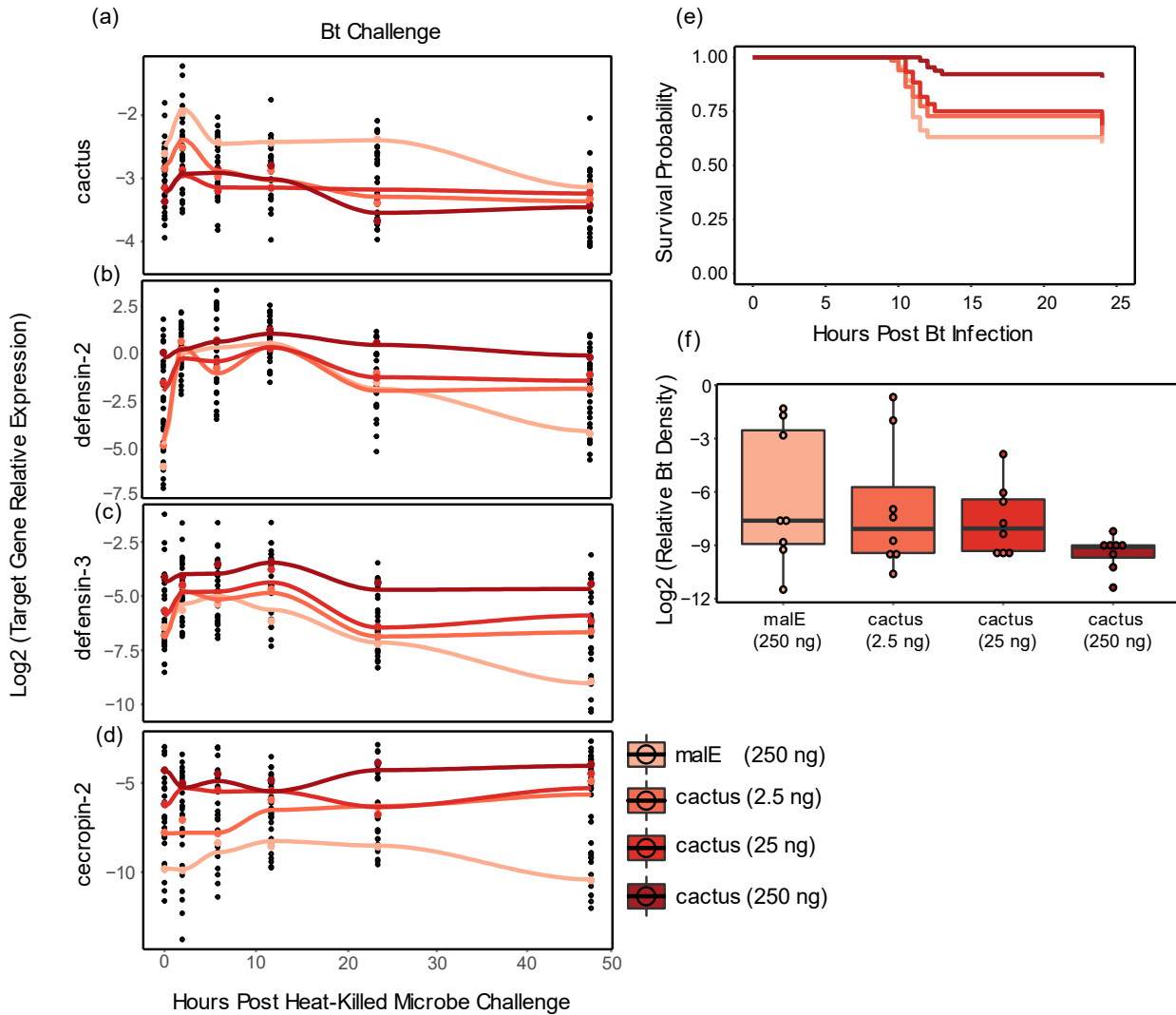


Figure 4. Quantitative knockdown of *cactus* transcripts benefits resistance and survival during infection. **a-d)** The expression of *cactus* (a) and the antimicrobial peptides *defensin-2* (b), *defensin-3* (c) and *cecropin-2* (d) were assayed via qRT-PCR in whole adult beetles treated with 250, 25, or 2.5 ng of *cactus* dsRNA or 250 ng of *malE* dsRNA and then septically challenged with heat-killed Bt. Beetles were frozen before microbial challenge, time 0, and five additional times over 48 hours. Splines have been added to visualize the induction and decay dynamics from RNAi treatment using “loess” function in the `geom_smooth` algorithm of ggplot2 (R). See Table 3 for significance. **e)** Survival to an LD₅₀ (6.5×10^8 /mL) Bt infection after RNAi treatment was monitored for 24 hours (N = 60-64 beetles/treatment and 29-34 per sex). **f)** To measure shifts in host resistance to bacterial infection from *cactus* RNAi treatment, beetles were given an LD-50 dose of Bt and sacrificed seven hours later. Relative bacterial density for each individual within each dsRNA treatment was quantified via RT-qPCR and calculated as the difference between Bt-specific and host reference gene expression (RP18s) on a log₂ scale.

Expression of the three AMPs significantly increased with each increasing dose during the constitutive, induction, and resolution windows (**Figure 4b-d, Appendix K**). For example, for every ng of *cactus* dsRNA, constitutive expression of *def-2* increased by 0.01 ($p < 0.001$), *def-3* increased by 0.01 ($p < 0.001$), and *cec-2* increased by 0.02 ($p < 0.0001$). Interestingly, non-significant interaction effects between dose and time indicate that increasing *cactus* dsRNA dose did not significantly alter induction and decay rates for the AMPs (**Appendix K**). This result is most likely due to the 2.5 ng, 25 ng, and 250 ng treatments converging upon maximum expression during the acute infection phase, since increasing *cactus* dsRNA dose significantly increases AMP expression during the constitutive and resolution hours for all three AMPs.

Elevated Toll pathway signaling increases survival to septic bacterial infection

We conducted a survival analysis to evaluate the relationship between *cactus* dsRNA dose and survival after live Bt infection. We administered one of four *cactus* dsRNA doses (N=60-65 per dose). After three days, beetles were septicallly challenged with an LD50 dose of Bt, which typically kills beetles within 12 hours. Weighted Cox Regression analysis revealed that for every ng of *cactus* dsRNA injected, the mortality risk from Bt declines by 0.69% (**Figure 4e**, Coef = -0.01, Se(coef) = 2×10^{-3} , hazard ratio = 0.993, lower 95% CI = 0.990, upper 95% CI = 0.997, Z = -3.94, $p < 8.1 \times 10^{-5}$). Furthermore, we assessed the impact of *cactus* dsRNA dose on *in vivo* bacterial loads at seven hours post-infection (**Figure 4f**). Since the data was non-normally distributed, we used the Kruskal-Wallis rank sum test, which did not reveal a significant difference between the *cactus* doses ($\chi^2 = 4.30$, Df = 3, $P = 0.23$). However, like previous experiments, our data displayed a bifurcating distribution of low and high Bt loads, complicating the statistical analysis (Duneau et al., 2017; Jent et al., 2019). When we repeated the experiment for 0 and 250 ng treatments to assay bacterial loads at a slightly earlier time

point (6 hours), we observed a significant reduction in Bt load in the 250 ng treated beetles (estimate = -2.02, st. error = 0.84, $t = -2.41$, $p = 0.03$) (**Appendix M**).

Increased Toll pathway signaling has severe fitness related costs

To assess the potential costs of enhanced Toll signaling, we measured changes to beetle lifespan, female egg laying, body mass, and gut integrity in response to all four *cactus* RNAi doses. We determined lifespan by monitoring beetle survival following RNAi injection, using the experimental setup from **Figure 4e** but without Bt infection (N = 30-32 beetles/dose, N=15-16 beetles/sex, **Figure 5a**). We then conducted a Weighted Cox Regression analysis and found that for every ng of *cactus* dsRNA the background mortality risk significantly increased by 0.89% (**Appendix N**, hazard ratio = 1.01, $Z = 16.25$, $p < 10^{-8}$). Additionally, our analysis revealed that male beetles had a significantly lower survival rate compared to female beetles (hazard ratio = 1.30, $Z = 16.25$, $p < 10^{-8}$). We did not investigate this further as sex did not prove to be a significant factor in any other experiments.

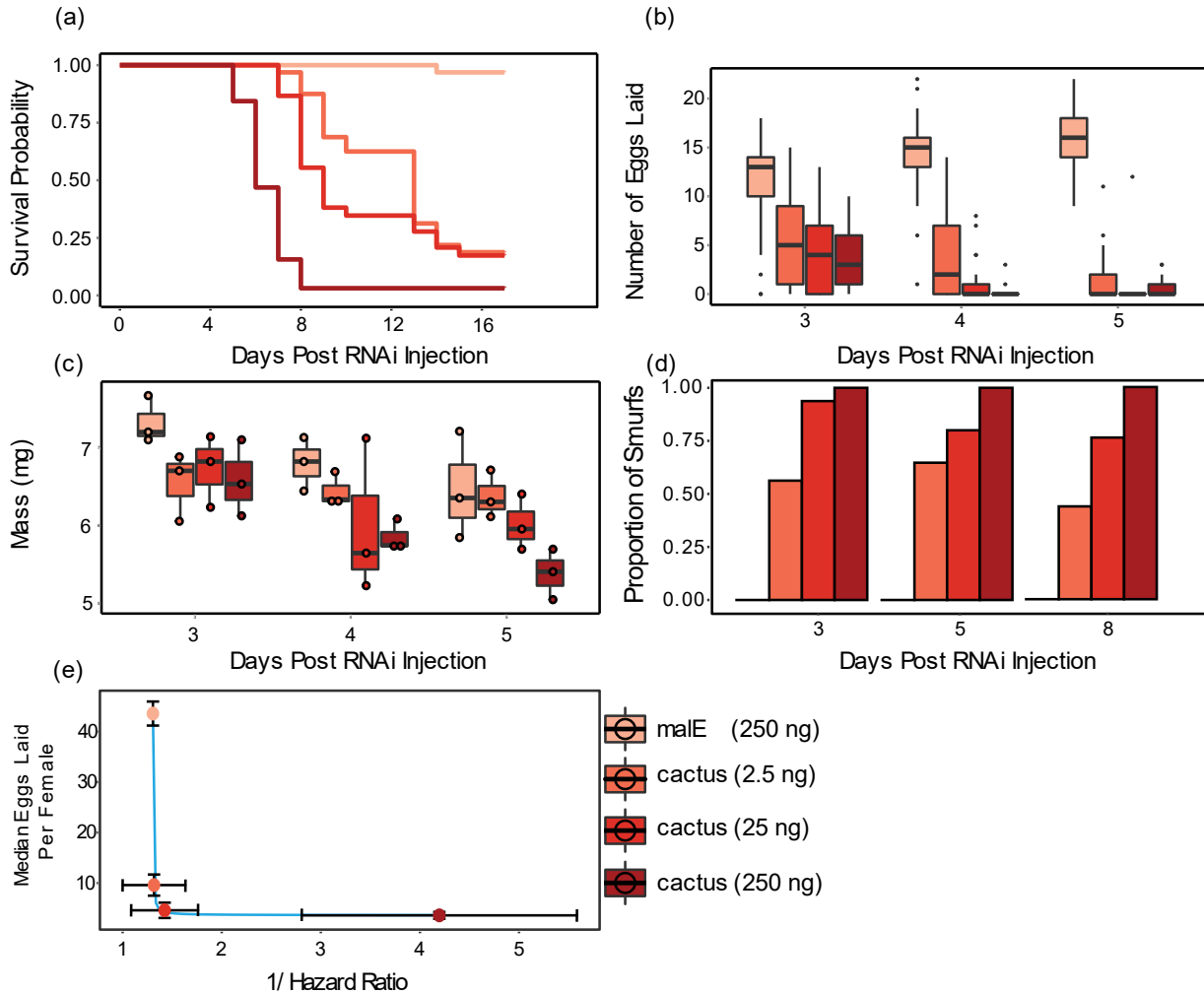


Figure 5. The costs of immune over-activation to fitness-associated traits. a) Beetle life-span after RNAi treatment was measured by monitoring survival in beetles given 250, 25, or 2.5 ng of cactus dsRNA or 250 ng of malE dsRNA for 17 days (N = 30-32 beetles/treatment and 15-16 beetles/sex). b) Female reproductive output after RNAi treatment was measured by allowing RNAi treated virgin female beetles 24 hours to mate and counting their number of eggs laid for three days. c) Female beetle mass after RNAi treatment was measured three to five days after cactus RNAi by pooling 3 individual beetles per measurement. Weighed beetles were discarded after measurement each day. d) Beetle gut integrity was measured by feeding adults flour stained blue and observing whether the blue dye entered the beetle hemolymph (N=15-21 beetles/day and 7-11 beetles/sex per day. e) The relationship between infection survival and fecundity ($y = 1 / (-8.09 + 8.12 * x) + 3.03$). Survival rate to infection for each RNAi treatment was calculated as 1/ (the hazard ratio relative to MalE). Reproductive output for each RNAi treatment is the median number of eggs laid for all three days measured per female.

Next, we investigated the impact of increased Toll signaling on female beetle reproductive output by measuring the number of eggs laid over consecutive 24 hour periods by females previously injected with *cactus* or *malE* dsRNA and then mated. Because the data is heteroscedastic, non-normal, and has an excess of 0 values, we analyzed the data using a Zero-Inflated Negative Binomial (ZINB) generalized linear model (dose + day + (1 | id)), which revealed that dose significantly reduced female egg laying (estimate = -3.57×10^{-3} , st. error = 7.4×10^{-4} , $t = -4.86$, $p < 1.1 \times 10^{-6}$) (**Figure 5b, Appendix O**).

Since Toll pathway activation is known to disrupt insulin signaling resulting in reduced larval and adult weights (DiAngelo et al., 2009; Suzawa et al., 2019), we investigated the metabolic demands of increasing Toll signaling on female beetle body mass. Beetles were given one of four *cactus* RNAi doses and weighed on day three, four, or five. Using the linear model (mass ~ dose + day), we found that *cactus* RNAi significantly decreased female body mass per ng of *cactus* dsRNA (estimate = -2.56×10^{-3} , st. error = -7.94×10^{-4} , $t = -3.23$, $p < 0.01$) (**Figure 5c, Appendix P**). Furthermore, our analysis indicated that beetles weighed significantly less at later dates regardless of treatment (estimate = -0.38, std error = 0.10, $t = -3.63$, $p < 0.001$). These results coincide with our qualitative observations that the fat bodies of *cactus* treated beetles are depleted compared to MalE controls by day five.

In *D. melanogaster*, overactivation of AMPs exacerbates gut dysfunction, correlating with reduced lifespan (Rera et al., 2012). We investigated if Toll signaling dysfunction in beetles affects gut stability and if the severity of this dysfunction relates to gut instability. Beetles were given one of four *cactus* RNAi treatments and fed a non-absorbable blue food dye. If gut integrity is disrupted, the blue dye leaks into the hemolymph, causing the beetles to turn blue, which are called “smurfs” (**Appendix S**) (Rera et al., 2011). Analysis using a binomial glm (smurfs ~ dose*day) showed that the dose of *cactus* dsRNA significantly influenced the proportion of smurf beetles (estimate = 0.18, st. error = 0.06, $t =$

3.13, $p < 0.01$) (**Figure 5d**). However, the number of days post RNAi injection and the interaction of dose and either day did not significantly influence the proportion of smurf beetles (**Appendix Q**).

Discussion

In this study, we implemented a novel experimental framework to map the fitness-related benefits and costs of failing to properly regulate an immune signaling pathway. Poorly restrained Toll pathway activation in *T. castaneum* resulted in increased constitutive and inducible expression of AMPs, delayed transcriptional decay of AMPs during the resolution of the response, and increased numbers of microbe-induced circulating hemocytes. By serially modulating the dose of *cactus* dsRNA, we manipulated the magnitude of Toll signaling, allowing us to extract the functional form of the relationship between increased parasite resistance via humoral and cellular immunity and fitness-related traits. This analysis revealed a steep convex relationship between the benefits of immune investment against infection and the costs to fitness-associated traits like reproduction, reflecting the importance of Cactus as a central node in immune signaling as well as the pleiotropic impact of Toll pathway signaling on physiological homeostasis in insects. This experimental design can serve as a valuable blueprint for future studies to quantify the relationship between immune investment and reproductive fitness or to compare the relative roles of different regulatory checkpoints for the cost-benefit calculus of immune response regulation.

Small increases in Toll signaling have massive costs to reproductive potential

Our results reaffirm the well-established trade-off between immunity and reproduction (Schwenke et al., 2016), but also emphasize the sensitivity of this relationship (**Figure 5e**). Specifically, injecting beetles with the smallest dose of *cactus* dsRNA led to just a four-fold increase in constitutive

cec-2 expression and a similarly modest increase in beetles surviving Bt infection but resulted in a severe reduction in reproductive output. This is not surprising, considering previously documented costs to Toll overexpression (Beramendi et al., 2005; DiAngelo et al., 2009; Ryu et al., 2008) and the role of Cactus as a direct inhibitor of Toll transcription factors, representing a potent and costly form of chronic immune activation. Is immune dysregulation always this costly? When the negative regulator *pirk-like* in *Aedes aegypti* is completely knocked-out, there is an approximately 30% increase in final survival probability to *E. coli* infection but only an approximately 52% decrease in female egg laying (M. Wang et al., 2022), representing a far less costly process to increase resistance. We are not aware of any additional studies that directly investigate these attributes of negative regulators on host reproduction, but we expect that such studies will reveal unique trade-off relationships (e.g., concave or exponential) compared to our results, which will provide key empirical data for theoreticians to incorporate real-life trade-offs and mechanistic detail into models of host-parasite and life history evolution.

Theoretical models of immune system evolution, for example, generally incorporate the cost of increased resistance to fitness traits like reproduction, growth, or mortality (Boots et al., 2009). To keep things simple, models tend to stay agnostic to the molecular underpinnings behind changes in immune output (Schmid-Hempel, 2003). They often assume small mutational steps that increase immune output and infection resistance, which coincides with equal reductions to fitness traits (Best et al., 2014; Boots & Bowers, 2004; Buckingham & Ashby, 2022; Schmid-Hempel, 2003). However, our results clearly show that the cost of increasing parasite resistance is not always linear. Rather, the trade-off between resistance and reproduction from elevated Toll signaling follows a convex decay form (**Figure 5e**). While this relationship certainly does not reflect outcomes across all immune genes, future models could benefit from assessing multiple trade-off shapes beyond linear forms (Buckingham & Ashby, 2022; Hoyle et al., 2008; Jessup & Bohannan, 2008). Furthermore, integration of additional empirical examples would enable

models to better mirror real-life consequences of immune variation. Researchers could then manipulate environmental parameters as needed and superimpose the most influential trade-offs onto fitness landscapes (Jessup & Bohannan, 2008), potentially aiding in understanding phenomena such as the natural variation of macrophage activation, which modulates the trade-off between enhanced cancer survival and increased susceptibility to autoimmune diseases like rheumatoid arthritis (Buscher et al., 2017).

Dose dependent *Cactus* depletion regulates Toll signaling

We found that *cactus* depletion affects the expression of AMPs associated with both IMD (*def-2* & *3*) and Toll (*cec-2* and *def-3*) pathways. This is consistent with previous studies highlighting the cross-talk between the TFs Dif-Dorsal (Toll) and Relish (IMD) in *T. castaneum* (Altincicek et al., 2008b; Behrens et al., 2014; Tate & Graham, 2017b; Yokoi et al., 2022; Yokoi, Koyama, Ito, et al., 2012b; Yokoi, Koyama, Minakuchi, et al., 2012b). Pathway cross-talk is an increasingly appreciated feature of immune signaling across Insecta, including in the Hemipteran *Plautia stali* (Nishide et al., 2019) and Hymenopteran *Apis mellifera* (Lourenço et al., 2013) and has even been described in *D. melanogaster* (Tanji et al., 2007), indicating less pathway specificity than predicted by early studies in fruit flies (Lemaitre et al., 1997). At the same time, our data indicate the existence of distinct negative regulatory elements that differentially affect decay rates within these two pathways. Following *cactus* depletion, for example, the expression of *def-2* shows a delay in decay rate after microbial challenge but still ultimately resolves by 48 hours post exposure. Regardless of the magnitude of Toll activation, on the other hand, *cec-2* maintains maximum expression, suggesting the existence of IMD-specific negative regulators compensating for NF- κ B dysregulation that do not compensate for Toll pathway-mediated effectors. In *D. melanogaster*, microbial challenges are also necessary for extracellular amidases, zinc finger proteins, and the JAK/STAT, JNK, and MAPK pathways to suppress the IMD pathway (F. Wang & Xia, 2018). It is intriguing to consider whether the IMD-specific decay we observe is driven by

conserved mechanisms with *D. melanogaster* or novel regulatory factors. Such studies could shed light on conserved or novel mechanisms of immune modulation and provide a deeper understanding of genetic network robustness and resiliency, providing potential therapeutic targets for diseases characterized by overactive immune responses.

Toll signaling increases circulating hemocytes after microbe challenge

Prior research in *D. melanogaster* larvae indicates that overactivation of Toll via *cactus* RNAi triggers hemocyte proliferation, melanotic tumors, and lamellocyte differentiation (Banerjee et al., 2019; Lemaitre et al., 1995; Qiu et al., 1998). In our study, we explored whether adult *T. castaneum* beetles exhibit similar proliferation from increased Toll signaling. Unlike *D. melanogaster* larvae, we observed no increase in circulating hemocytes prior to challenge. Interestingly, heightened Toll signaling did increase circulating hemocytes after microbial challenge, but not after septic wounding. This suggests a Toll-dependent hemocyte proliferation mechanism outside of the beetle wounding response that is enhanced by unrestricted Dif-Dorsal translocation. Our results also differ from a study in adult *Anopheles gambiae*, which found Toll overactivation did not significantly alter circulating hemocyte numbers two days post microbe challenge (Barletta et al., 2022). These disparate results highlight an interesting possibility that different mechanisms may regulate hemocyte proliferation and differentiation in these three model organisms.

Increasing Toll signaling amplifies damage to host health

Toll overactivation results in severe costs to host health through neuromuscular destabilization (Beramendi et al., 2005), fat body depletion (DiAngelo & Birnbaum, 2009), and gut instability (Ryu et al., 2008). Similarly, our study revealed that the dysregulation of Toll signaling in beetles resulted in shorter

lifespans, greater body mass depletion, and increased probability of gut barrier instability. While these results align with our expectations, the differences observed between the doses introduce intriguing questions regarding the underlying mechanisms and factors influencing these outcomes.

In our study, we found that beetles treated with *cactus* RNAi became increasingly lethargic until their early death. We also found that by mitigating Toll dysregulation with lower doses, lethargy is delayed, and death is less prevalent. Toll dysregulation in *D. melanogaster* also leads to lethargy, which is associated with destabilized neuromuscular junctions (NMJs) (Beramendi et al., 2005). NMJ disruption is linked to the alternative splicing of *dorsal* and *cactus*, which creates two distinct protein isoform pairs that mediate development and immunity (Dorsal-Cactus A) or NMJs (Dorsal-Cactus B) (Zhou et al., 2015). Surprisingly, Dorsal B, Pelle, and Cactus B work together, not in opposition, for proper NMJ functioning (Heckscher et al., 2007). Since our *cactus* RNAi targets both isoforms, subsequent research should evaluate whether the concentration of this particular Cactus isoform dictates the observed delayed phenotype, thereby improving our understanding of how organisms employ alternative splicing to circumvent costs from varying expression of pleiotropic genes (Williams et al., 2023).

To dramatically increase AMP production, *D. melanogaster* modifies its metabolic pathways by reducing insulin hormone levels, shifting from anabolic lipid metabolism to phospholipid synthesis and endoplasmic reticulum (ER) expansion (Martínez et al., 2020). This metabolic shift enhances triglyceride synthesis and lipid droplet formation while decreasing insulin signaling and hormonal levels (Cheon et al., 2006; Harsh et al., 2019; Suzawa et al., 2019). As a result, pupal triglyceride stores halve when Toll signaling is genetically induced (Martínez et al., 2020). Our findings suggest that even small levels of Toll activation can cause metabolic stress, resulting in lower body mass and egg production in female beetles. Dissecting the relationship between immune activation, metabolism, and egg production

could offer crucial insights into immune-metabolic interplay and its evolutionary implications (Gupta et al., 2022).

Intestinal barrier dysfunction in *D. melanogaster* predicts metabolic defects in insulin signaling, shifts in immune signaling, and fly death more accurately than chronological age (Rera et al., 2012). This gut barrier instability is linked to excessive AMP expression, changes to the composition of gut microbiota composition, and stem cell hyper-proliferation, resulting in shorter fly lifespans (Guo et al., 2014; Ryu et al., 2008). Our study aligns with these findings, as we noticed significant gut instability from increased Toll signaling. We also observe that milder *cactus* depletion results in a lower incidence of destabilized guts. Unexpectedly, as the lower dosed beetles approached their mortality window, the proportion of dysfunctional guts did not increase, suggesting that even though gut dysfunction could contribute to mortality, it is not the primary driver of it. Using RNAi in *T. castaneum* causes mRNA depletion across all tissues (Posnien et al., 2009), and while this complicates distinguishing gut immunopathology from other dysfunctions in life history traits, it's a challenge shared across the field requiring innovative solutions. Considering our findings, it would be interesting to explore whether gut instability is associated with AMP concentration, or if tolerance mechanisms effectively mitigate damage from immune signaling dysregulation at these low doses.

Conclusion

Using our *cactus* RNAi experimental framework, we conducted a novel quantitative assessment of the benefits of increased immunity and the significant fitness costs incurred by immune dysregulation in the absence of infection (**Appendix T**). Specifically, we investigated the effects of increased Toll pathway signaling in *T. castaneum*, which resulted in increased AMP transcription and the number of circulating hemocytes leading to functional increases in resistance. By serially increasing the strength of

Toll signaling, we demonstrated that the magnitude of Toll activation correlates with the ability of *T. castaneum* to resist and survive parasitic infection. Our findings reveal the costs of increased parasite resistance, as beetle lifespan, reproduction, mass, and gut integrity reduced as the degree of immune activation increased. Our results align with previously identified phenotypes from Toll pathway overactivation (Anjum et al., 2013; Beramendi et al., 2005; Bingsohn et al., 2017; Germani et al., 2018; Liu et al., 2016; Nicolas et al., 1998; Qiu et al., 1998; Roth et al., 1991; Sneed et al., 2022), but reveal the steep sensitivity of their relationship with immune activation. Our results stress the need for future empirical studies to adopt this type of experimental framework to quantify the benefits and costs of immune regulation.

Materials and Methods

Beetle rearing and experimental groups

For each experiment we put approximately 200 age-matched parental beetles on fresh beetle media (whole-wheat flour from MP Biomedicals and 5% yeast) to lay eggs for 24 hours and then we removed the parents onto new media. Once the eggs developed into pupae, we separated them by sex and transferred them to petri dishes (100 mm) containing either 100 unmated males or females with *ad libitum* media. We derived all experimental beetles from the ‘Snavely’ beetle population, originally collected from a Pennsylvania grain elevator in July 2013 and subsequently maintained in the laboratory since (Tate & Graham, 2015e). We kept all beetles in a walk-in incubator at 30°C and 70% humidity.

DsRNA synthesis

We designed the *T. castaneum cactus* primer sequences for dsRNA synthesis from the iBeetle

Database (Ulrich et al., 2015) (**Appendix R**). We then verified the primer pair for the absence of secondary effects by comparing phenotypes with a non-overlapping dsRNA fragment (Ulrich et al., 2015) and by blasting the primer pair against the new *T. castaneum* genome using NCBI's Primer-BLAST (Ye et al., 2012b). Next, we generated T7 promoter sequence-tagged DNA from *T. castaneum* cDNA via PCR using the Platinum Green Hot Start kit (Invitrogen). We then purified the PCR product using the QIAquick PCR Purification kit (Qiagen). Using the Megascript T7 kit (Invitrogen), we synthesized dsRNA overnight (Posnien et al., 2009). As a control for the induction of beetle RNAi, we used *E. coli* DNA as a template to produce dsRNA against a maltose binding protein E (*malE*) sequence (Yokoi, Koyama, Ito, et al., 2012b). Finally, we quantified dsRNA concentration using the Qubit™ microRNA Assay Kit (Invitrogen).

RNAi treatments

Recently, (Bingsohn et al., 2017) demonstrated that by diluting the dose of *cactus* dsRNA to as little as 0.001 nanograms, the RNAi induced mortality in adult *T. castaneum* was reduced from 100% to 75%, illustrating a system capable of quantitatively modulating RNAi-mediated phenotypes based on knockdown efficiency. For each experiment, we randomly assigned beetles to their respective dsRNA treatment groups and injected them with 0.5 uL of injection mixture. For the *cactus* RNAi group, we dissolved dsRNA in sterile insect saline at concentrations of 500, 50, or 5 ng/uL, while for the *MalE* control group, all injections used the 500 ng/uL concentration. We did not test gene expression for naïve beetles because our prior study showed no significant difference in constitutive expression between *MalE*-RNAi and naïve beetles (Jent et al., 2019). For injections, we followed the methods detailed in (Posnien et al., 2009). We applied the formula $(2^{-(\Delta Ct(cactus) - \Delta Ct(malE))}) * 100$ across all time points to quantify RNAi treatment knockdown efficiency. By averaging these values, we determined the overall

relative knockdown percentage for the entire experiment, with Male Δ Ct denoting the mean Δ Ct for all Male samples (Livak & Schmittgen, 2001).

Microbial infections

Bacillus Thuringiensis (Bt)

Bt, a sporulating, gram-positive, and obligate-killing bacterium, can infect insects through oral ingestion or septic injection, and once it gains access to insect hemolymph, it grows rapidly, causing death within 12-24 hours (Nielsen-LeRoux et al., 2012; Raymond et al., 2010). For all infections, we used the Berliner strain of Bt (ATCC 55177)(Jent et al., 2019). Two days after RNAi injections, we cultured Bt overnight for 12-15 hours from a glycerol stock at -80°C in Luria Broth at 30°C. We transferred 200 uL of the overnight culture to 3 mL of new LB for 1.5 hours. We diluted the overnight and log cultures to OD₆₀₀ values of 1.0 and 0.5, respectively. We then combined 500 uL of each culture and centrifuged the mixture at 4°C and 5,000 rpm for five minutes. We removed the supernatant and washed the Bt pellet twice with one mL of sterile insect saline. We then re-suspended the washed Bt pellet in 150 uL of insect saline and diluted 1:20 with insect saline to obtain an LD 50 dose (5×10^8 colony forming units (CFU)/mL). For the gene expression experiments, we inactivated Bt by heating to 90°C for 20 minutes. Beetles were infected by inserting an ultrafine insect pin dipped in the Bt mixture between the head and pronotum and were kept in individual wells in a 96-well plate after infection.

Candida albicans

Candida albicans is a common opportunistic fungal parasite that has MAMPs typical of insect fungal parasites sensed by the Toll pathway. For our fungal challenge experiment, we used the *C.*

albicans strain (ATCC 18804). Two days after RNAi injections, we cultured *C. albicans* overnight for 12-15 hours from a glycerol stock at -80°C in Luria Broth at 30°C. We diluted the overnight culture to an OD₆₀₀ of 1.0. We then centrifuged one mL of the culture at 4°C and 5,000 rpm for five minutes. After washing twice, we re-suspended the fungal pellet in 150 uL of insect saline (1.89 x 10⁸ colony forming units (CFU)/mL) and heat-killed at 90°C for 20 minutes.

Immune gene expression and Bt load quantification via RT-qpcr

To isolate RNA, we used the Qiagen RNeasy kit and eluted with 30 µL of nuclease-free water. For cDNA synthesis, we used 100-200 ng of RNA in a 5 µL reaction using the SuperScript IV VILO master mix (ThermoFisher Scientific). We then diluted the resulting cDNA with 40 µL of nuclease-free water. We conducted RT-qPCR using the PowerUp SYBR Green master mix (Applied Biosystems) on a Biosystems QuantStudio 6 Flex machine. The thermal cycling conditions consisted of an initial denaturation step at 95°C for 2 minutes, followed by 40 cycles of 95°C (15 seconds), 55°C (10 seconds), and 60°C (1 minute). We ran all samples in duplicate, and we used the average Ct value for subsequent analyses, if the technical replicates were within 1 Ct. If the technical replicates differed by more than 1 Ct, we repeated the reaction.

We selected immune genes for RT-qPCR analysis based on their previous correlation to Toll and IMD output in *T. castaneum*, as reported in a study by (Yokoi, Koyama, Minakuchi, et al., 2012b). Specifically, we assayed the expression of *defensin-2* (TC010517), *defensin-3* (TC012469), and *cecropin-2* (TC030482) to represent the IMD, IMD and Toll combined, and Toll pathways, respectively (Herndon et al., 2020). To assess reference gene expression, we used the RPS18 primer pair provided in (Lord et al., 2010b), which showed RPS18 expression is constant during fungal infection.

For all gene expression analyses, we used the Δ ct method to calculate relative expression values on a

log₂ scale for each gene in each sample by subtracting the mean ct value of the target gene from the reference mean ct value (Schmittgen & Livak, 2008b). This method of data representation allows for easier comparisons of gene expression across timepoints than the $\Delta\Delta$ ct method for fold change when the baseline treatment also changes (Critchlow et al., 2019). To analyze the effect of RNAi treatment on gene expression, we split the analysis into induction (0-6 hours) and decay (8-48 hours) stages, except for *cecropin-2*, where peak induction occurred at eight hours post-infection. We ensured normality of data by examining histograms and Q-Q plots of the standardized residuals. We performed linear modeling on gene expression using treatment, time, and their interaction as factors with the lme4 package in R (v. 4.3.0) and adjusted *p*-values for multiple comparisons using the Bonferroni method (Dunn, 1961). A significant effect for treatment indicates a difference in gene expression magnitude between treatments, while a significant effect for hour indicates differential gene induction or decay over time from microbial challenge. A significant interaction denotes a difference in induction or decay rates for the target gene in *cactus*-treated beetles relative to control-treated beetles. To investigate the impact of *cactus* RNAi dosage on the induction and decay of target AMPs, we employed a linear model (expression ~ dose * hour), where "dose" is a continuous variable, and the MalE treatment group serves as a reference point with zero ng of *cactus* dsRNA. A significant effect for dose indicates a linear increase in the total transcription of the gene with increasing dose. A significant effect for hour denotes significant gene induction or decay. A significant interaction term indicates that the rate of induction or decay is dependent on *cactus* dsRNA dose. See **Appendix U** for experimental design.

Hemocyte proliferation quantification

We isolated total circulating blood cells (hemocytes) by perfusion bleeding the hemolymph in adult beetles. For this, we used a modified protocol from (King & Hillyer, 2013). Briefly, we made an

incision through the lateral edge of the abdominal tergite segments V and VII using a feather blade, while the beetle was held dorsally with abdomen pointing downwards. We then inserted a glass microinjection needle into the thorax region and 50 μ L of insect saline buffer was injected, and the diluted hemolymph that exited the posterior abdomen was collected onto one of the three 1-cm diameter etched rings on Rite-On glass slides (Fisher Scientific, Epremia). We perfused at a rate of 15-20 seconds per RNAi treated beetle, with the first 50 μ L collected in one etched ring, followed by second and third in the other wells. We allowed the hemocytes to adhere to the slide for 20 min at room temperature and were fixed and stained for 20 min using 4% paraformaldehyde in phosphate buffer saline (1xPBS) and Hoechst 33342 nuclear stain (Invitrogen, Carlsbad, CA, USA) in phosphate buffered saline (PBS). We then mounted the slides using coverslips with Aqua Poly/Mount (Polysciences; Warrington, PA, USA). We captured images with a Nikon Ti-E inverted microscope and Zyla sCMOS digital camera, then we counted hemocytes using the NIS-Elements software (Nikon). We performed the experiment over a course of three biological blocks/trials, with each composed of 3-4 beetles per treatment combination. We aggregated data from all the trials. Given the non-normal distribution of residuals, we used a series of Wilcoxon rank sum tests for all combinations of treatment, time, and infection. We corrected for multiple tests using the False Discovery Rate (FDR) (Benjamini et al., 2001).

Antibacterial activity

To measure AB activity, we closely followed the protocol from (Khan et al., 2016), modified from Roth et al., 2010 by measuring the inhibition zones produced by the whole-body homogenate of RNAi treated beetles on a lawn of Bt bacterial growth. To eliminate the confounding effects of quinones (secreted from the odoriferous defensive stink glands) on the AB activity, we froze beetles for 20 minutes at -80°C 3-days post RNAi treatment (N = 40-41 beetles per treatment & sex combinations).

Freezing at -80°C triggers the release of quinones from the thorax and abdomen, which can otherwise prevent microbial growth and confound the results of the AB activity. We then cleaned the frozen beetles using 70% ethanol (surface sterilization) to remove any remaining quinones and washed twice with 100 µL insect saline. We prepared whole body homogenates of individual RNAi treated beetles using 30 µL sterile filtered Bis-Tris buffer (0.1 M, pH adjusted to 7.5, Sigma-Aldrich ltd) supplemented with 0.01% Phenylthiourea acid (PTU; Sigma-Aldrich ltd) to inhibit melanization. We then centrifuged the homogenate at 7500 rpm at 4°C for 10 minutes and separated the supernatant (on ice).

We prepared LB agar plates, using the overnight *Bt* culture in LB Broth at 30°C to an optical density of 1.0. Meanwhile, we separately autoclaved a LB broth with 1% agar and allowed it to cool in a water bath held at 45°C. Following this, we added the *Bt* bacterial culture to the agar medium and mixed by shaking, giving a final OD concentration of 0.001. We poured 6 mL of the mixture into each 75 mm Petri dish, with constant swirling to obtain homogenous distribution of bacterial culture. We then punched 4 wells (2x2 mm diameter) in each plate and added 4 µl homogenate from RNAi treated beetles to each of the wells. We added 2 µl Kanamycin (2 mg/ml) to every plate as positive control. We incubated the plates at 30°C for 16 h, at which point we measured the clear zones of inhibition of *Bt* bacterial growth around wells. We used the mean value by calculating the average of the horizontal and vertical diameters around each well as a proxy for the AB activity. Since the data is not normally distributed, we used a non-parametric Wilcoxon rank sum test to analyze the AB activity.

Host survival experiments

For survival to parasite infection, we gave beetles an LD50 dose (6.5×10^8 CFUs/mL) of live *Bt* and monitored survival every 30 minutes for 12.5 hours and again at 24 hours post infection (N = 60-65/dose), We censored individuals that died at or before four hours post infection, since mortality most

likely resulted from stab trauma. For estimating lifespan, we randomly assigned beetles to the four RNAi treatment groups (N = 30-32 beetles/dose, N = 15-16 beetles/sex), put them into individual wells in a 96-well plate with *ad libitum* media, and monitored them daily for 17 days. To compare survival among treatments for both experiments, we used weighted Cox Proportional Hazard tests (R package *coxphw*) to obtain a hazard ratio (Dunkler et al., 2018). The use of weighted Cox regression allowed us to obtain an average hazard ratio, despite our data not meeting the assumptions of the Cox proportional hazards model.

Resistance to live Bt infection

To quantify Bt load during infection, we used the previously validated and published primers by (Tate & Graham, 2015e, 2017b) (Table S6), which correlate with bacterial CFU counts on agar plates. We performed a Kruskal-Wallis rank sum test to determine whether there were significant differences in Bt load for the four *cactus* dsRNA doses, since the data is non-parametric.

Female reproductive output

We randomly assigned 7-day old unmated female beetles to one of four RNAi treatments, injected dsRNA, and allowed for 24 hours of recovery in individual wells in a 96-well plate with media. We paired females with a single aged-matched unmated male in a 2.0 mL centrifuge tube with 0.5 mL volume of media for 24 hours. We then separated the females and put them in their own petri dish with flour. After 24 hours, we counted the eggs for each individual and put the females on new flour. We allowed the eggs to develop for 21-days and counted the total number of viable larva for each female individual. We employed a zero-inflated negative binomial (ZINB) generalized linear model (R package MASS) to analyze the effect of dose and day on fecundity (fecundity ~ dose*day), since the data is non-

parametric and the ZINB model showed the lowest AIC score among all the tested glm types. We interpreted a significant effect for dose as indicating that the dosage of *cactus* dsRNA affected the number of eggs laid, while a significant effect for day indicated whether each day was unique from the others in terms of egg-laying behavior. A significant interaction term was interpreted as indicating whether the effect of dose on egg-laying changed over time.

Body mass and fat body dissections

We cleaned female beetles twice by vortexing in 5 mL sterile insect saline and dried via Kimwipe. We measured average body mass changes on days three, four and five post RNAi injection. We then stored beetles in individual wells in a 96-well plate with beetle media until weighed. To analyze the changes in beetle mass, we used a linear model (mass ~ dose + day). A significant main effect of dose indicates that the dosage of *cactus* dsRNA linearly changes the weight of female beetles. A significant effect of day indicates whether there are significant differences in weight among individual days.

Gut/intestinal integrity quantification (Smurf assay)

We assessed gut barrier integrity of RNAi treated beetles by placing the beetles on blue food (n = 10-12 beetles per condition) prepared using 2.5% (w/v) FD&C blue dye no. 1 (Spectrum Chemicals) and sterilized wheat flour, prepared using the previously described protocol by (Rera et al., 2012). We examined the distribution of blue food dye after 24 h feeding. We randomly assigned beetles (females and males separately) to one of four RNAi treatment groups (*malE*-250 ng, *cactus*-0 ng, *cactus*-25 ng, *cactus*-250 ng) and held them in individual wells in a 96-well plate. On days three, five, and eight following RNAi treatment, we removed a subset of beetles from flour and starved them for four-six

hours. We then put the starved beetles back on flour mixed with blue food dye. After 24 hours of exposure to blue food, we dissected each beetle by removing both wings and looked for any leakiness in the gut-intestine barrier and scored the beetles as blue “smurf” phenotype (**Appendix S**). We used a binomial generalized linear model (glm) (smurfs ~ dose * day) to analyze the effect of *cactus* dsRNA dosage on gut integrity. A significant effect of dose indicates that the dosage of *cactus* dsRNA determines the number of smurf beetles, while a significant effect for day is interpreted as changes in gut integrity over time. A significant interaction indicates that the number of smurfs over time is affected by the dose of *cactus* dsRNA.

CHAPTER 5

Efficient methods for experimental evolution of *Bacillus thuringiensis* isolated against variable immune defenses in flour beetles

Preface

This chapter introduces and implements a serial passaging protocol that examines the relationship between inducible immunity and the microbial parasite, *Bacillus thuringiensis* (Bt), in the flour beetle, *T. castaneum*. My findings reveal that when Bt is experimentally evolved within a highly susceptible beetle population, its potency to kill its host diminishes. This protocol is significant since it offers a structured approach to bypass initial resistance mechanisms to isolate the influence of downstream inducible immunity on parasite evolution. My advisor, Dr. Ann Tate, obtained funding for this study. Dr. Tate and I conceptualized this study. I conducted all experiments with assistance from our former lab manager Derrick Jent. I analyzed the data and created the figures. Dr. Tate and I wrote the manuscript. This chapter has been reproduced with the permission of Dr. Tate and Derrick Jent.

Abstract

Parasites can evolve to increase or decrease the damage to their host, replicate faster, evade the immune system, or survive longer, but the alteration of one trait can come at a cost to the others. While theory predicts that increased host immune resistance should drive the evolution or phenotypic plasticity of parasites towards greater host exploitation, most empirical studies to date neglect to account for variably structured interactions between immunity and parasites at different phenotypic stages. To study potential trade-offs between parasite traits under variable immune pressure, experiments need to isolate their interactions over the course of infection. Here we present an *in vivo* serial passaging protocol that isolates the interaction between *Bacillus thuringiensis* (Bt) and the immune defenses of flour beetles. We then validate our protocol by taking advantage of natural variation in flour beetle susceptibility to Bt infection to quantify the impact of immunological variability on bacterial life history evolution. We passaged Bt through 6 generations of either highly resistant (Marshall) or highly susceptible (Green River) flour beetle strains. We then tested evolved bacterial virulence and the change in bacterial growth rates *in vitro*. We found that serial passaging in the highly susceptible hosts resulted in Bt isolates with reduced virulence. Additionally, we found that passaging in the highly resistant hosts was associated with Bt isolates with increased *in vitro* lag phases.

Introduction

During infection parasites need to overcome myriad resistance mechanisms. For example, animal immune defenses can be constitutively expressed or induced by detection of non-self for activation, but the maintenance of each can be costly to host development and host reproduction and can cause immunopathology (Sheldon & Verhulst, 1996). Site-specific defenses prevent entrance, followed by wound healing and resistance mechanisms induced by the recognition of non-self. This is followed by signaling for immune cells and initiation of immune cascades (e.g. Toll or IMD pathways in insects) that induce the expression of infection-specific immune factors like antimicrobial peptides, AMPs (Hamilton et al., 2008). Hosts can naturally vary in the specificity, intensity, and speed of these immune defenses, leading to a wide range of selection pressures during parasite development (i.e., lag, exponential growth, and transmission phases). As a result, variation in immune defenses can lead to differences in microenvironments that parasites experience, stimulating the evolution in parasite virulence and transmission.

Recent work with the water-flea (*Daphnia magna*) parasite, *Pasteuria ramosa*, illustrates how immune variation can influence parasite life history and virulence evolution. To infect *Daphnia*, *P. ramosa* spores attach to the intestinal lining after ingestion, penetrate the host's body cavity, grow and reproduce, castrate the host, and finally kill the host, spreading spores to infect the next generation of hosts (Ebert et al., 2016). *P. ramosa* requires a specific host receptor to attach to the esophagus cells after ingestion and then encounters different selection pressures from the invertebrate immune response upon entering the body cavity (Ebert et al., 2016). Successful attachment is determined by the interaction of a single host allele and the infecting parasite strain and represents 64% of observed variance in castration and death from infection (Hall et al., 2019). This is defined as a *qualitative resistance* mechanism because variation in the allele results in binary outcomes of infection or no infection (Corwin & Kliebenstein, 2017). While this type of resistance influences some coevolutionary

outcomes in *Daphnia-P. ramosa* infections, selection on this allele does not explain why the average time until castration has decreased over evolutionary time (Decaestecker et al., 2007). Among *Daphnia* susceptible to *P. ramosa* attachment, 23 loci represent 5-16% of the remaining variance in castration, which may explain the reduction in time until castration (Hall et al., 2019). This is defined as *quantitative resistance* where many loci influence resistance, and variation within a single locus slightly changes the probability of transmission rather than mediating an all or nothing outcome (Corwin & Kliebenstein, 2017).

Coevolutionary studies in model systems often gravitate toward studying qualitative resistance because the resulting phenotypes are so unambiguous: a host either succumbs to the parasite or succeeds in evading infection entirely. However, they mask the impact of quantitative resistance (e.g. inducible immunity) on parasite evolution in many host-parasite systems (Hall et al., 2019). In both maize-*Bipolaris maydis* (southern corn leaf blight) and *Drosophila-sigma virus* infections, important mechanisms responsible for quantitative variation were found only after people studying these models moved beyond qualitative resistance (Balint-Kurti et al., 2006; Bangham et al., 2008; Cogni et al., 2016). Strategies to parse these mechanisms apart and define their influence on parasite evolution, however, remain a frontier for evolutionary studies.

To investigate the role of variable immunity on parasite fitness, we created a protocol that isolates the interaction between an entomopathogenic pathogen and hosts with genetically modified immune defenses. In this study, we detail our serial passaging protocol and feasibility study using the powerful flour beetle-*Bacillus thuringiensis* system. Flour beetles (including *Tribolium castaneum* & *T. confusum*) are stored grain pests originating from Indo-Australia but now spoil stored grain across the world (Pointer et al., 2021). The genome of *T. castaneum* is well characterized and since its assembly, a great deal of information about flour beetle immunology and development of new genetic augmentation

techniques have been advanced and used to characterize the immune response during Bt infection (Behrens et al., 2014; Ferro et al., 2019; Jent et al., 2019; Tate & Graham, 2017a). Once Bt is in the hemolymph, it transitions through distinct phases of arrested growth (lag time), exponential replication (growth phase), a plateau of within host density (stationary phase), survival in its dead host (necrotrophic), and a transmission stage (sporulation phase) (Slamti et al., 2014). At each life-history phase, Bt encounters an innate immune response by flour beetles where genetic diversity influences the intensity of immune effectors (Jent et al., 2019; Tate & Graham, 2017a). When studying Bt evolution using only the oral infection route, the gut-toxin interaction overwhelms selection forces from inducible immune effectors and occludes our understanding of how Bt adapts to variation in immune defenses (Masri et al., 2015; Papkou et al., 2019). However, this interaction can be circumvented by directly inserting Bt into the hemolymph through a septic infection. Here, we detail our methods to bypass this well-defined qualitative resistance mechanism by serially passaging Bt via septic infection across beetle populations that vary in susceptibility to Bt mortality. This protocol could also be applied to our RNAi knockdown populations in chapters III and IV to investigate the influence of variation in quantitative resistance on pathogen evolution.

Methods

The detailed protocol is described in **Appendix X**. In this protocol, I detail the methods to sidestep the gut-toxin qualitative resistance phase by employing septic infections in either adult beetles or larvae. The procedure outlines the steps to infect beetles, collect deceased beetles, extract and cultivate Bt to achieve a viable infectious dose, and to preserve DNA and glycerol samples. Throughout the protocol, I detail the decisions made and controls implemented to isolate the interaction of Bt with the beetle's immune response, minimizing and accounting for undesired selection forces.

While developing our Bt serial passaging protocol, we made a few strategic choices to isolate the

influence of immunity on parasite fitness while allowing researchers to probe multiple evolutionary questions (see Appendix V for full protocol). One primary decision regards which life stage researchers should use. When compared to larvae, adult beetles necessitate the removal of the odoriferous glands containing antimicrobial quinones, which lengthens the passaging time. Adults do, however, allow for the incorporation of sex and mating factors that could influence parasite evolution. In larvae, the absence of the stink glands enables faster and simpler passaging by eliminating the need to culture Bt. Larval passaging also offers the flexibility of either standardizing the dose of Bt via culturing or allowing it to vary. Using a standardized dose allows researchers to identify the per parasite effects of different immune environments. Conversely, researchers can passage Bt without culturing, allowing for variations in cadaver loads. This variation alters the infection dose for the next passaging event, reflecting transmission dynamics in nature. This flexibility enables researchers to tease apart the between-host and within-host forces on parasite evolution. Nevertheless, there are constraints. Manipulating immune genes in larvae can result in developmental defects because of the pleiotropic roles these genes play, thereby reducing the number of targetable genes (cite). When choosing between the life stages, we recommend using larvae if you are incorporating between-host variation in transmission dynamics. Meanwhile, adults are superior for investigating sex-specific effects or manipulating immune genes essential for development.

Because Bt forms biofilms and sporulates, our protocol emphasizes the importance of passaging before its stationary phase. This is because biofilm formation and sporulation occur heterogeneously, resulting in significant variation between cells (). To prevent this variability, our methodology serially passages Bt before it forms biofilms in the beetle carcass and at the mid log phase when culturing. For experimental evolution approaches, it is vital to account for selection pressures that arise from the act of serial passaging. This is because parasites are known to increase their host killing abilities from

just *in vitro* passaging (Duangurai et al., 2020). Without *in vitro* controls during Bt serial passaging, researchers cannot determine if changes in Bt phenotypes and genotypes arise from variation in immune environments or from passaging itself. Therefore, it's essential to include *in vitro* passaging as a control. Additionally, our protocol uses a negative RNAi control to ensure changes in the immune environment are from knockdowns of the gene of interest rather than stimulation of the RNAi pathway (Yokoi, Koyama, Ito, et al., 2012c). We suggest including this control with serial passaging. This would allow researchers to tease apart the influence of gene silencing on Bt evolution from non-specific RNAi induction.

Lastly, to statistically observe the extent of parallel evolution in different immune environments, researchers need to replicate their passaging in multiple isolates with enough serial passaging events. Each Bt infection results in conservatively 9.5 replication events for Bt (Milutinović et al., 2015). Since statistically significant changes to *E. coli* fitness are observed within a minimum of 200 generations from *in vitro* passaging (Arjan G. et al., 1999). For our pilot experiment, we conducted only 6 passaging events. However, we recommend a minimum of 21 passaging events, equivalent to approximately 200 generations, before concluding the experiment to enhance the chances of observing significant changes in Bt fitness (McDonald, 2019). Serial passaging experiments also require multiple replicate isolates passaged in the same RNAi treatment for statistical power (Fox & Lenski, 2015). Because of the high degree of effort and the number of mandatory controls, we suggest performing this protocol in multiple experimental blocks. This will ensure a project capable of statistically evaluating parallel evolution in key Bt fitness traits, such as killing rates, growth rates, and final spore loads, with insights into their genetic underpinnings.

Representative Results

As a pilot study to validate that our serial passaging methods can influence key Bt phenotypic traits, we took advantage of the natural variation in flour beetle susceptibility to Bt infection mortality (Jent et al., 2019) to quantify the impact of immunological variability on Bt killing rates and *in vitro* growth rates (**Figure 1**). We passaged Bt through 6 events of either highly resistant (Marshall) or highly susceptible (Green River) flour beetle strains. We then tested the evolved bacterial virulence by infecting the same population the Bt isolate had been passaged through, or a moderately susceptible genotype (Snively). We measured changes in Bt killing rates because, as an obligate killing bacterium, Bt's ability to kill its host profoundly impacts its overall fitness. We also assessed changes in *in vitro* maximum growth rate and lag time to identify possible virulence-growth trade-offs. We focused on maximum growth rate since it can be positively (Acevedo et al., 2019) or negatively correlated (Leggett et al., 2017) with parasite virulence. We also investigated changes in Bt lag time since parasites, such as *Staphylococcus aureus*, can evolve longer lag phases to tolerate exposure to certain AMPs (Makarova et al., 2018).

Serial passaged strains evolve lower virulence to their passaged population

To evaluate changes in the killing efficacy of each Bt replicate after serial passaging, we septically infected hosts with Bt that had undergone passaging within the same beetle population (homologous) or in a population that exhibited moderate Bt susceptibility (Snively) as a common garden genotype. We then used a Weighted Cox Regression analysis (Dunkler et al., 2018) to analyze whether Bt killing rates significantly changed from the ancestral stock isolate. Survival analysis indicates that the Bt isolates serially passaged in the low susceptibility hosts (Marshall) showed no significant change in killing rates when injected into either the Marshall beetles (**Figure 2a**, hazard ratio = 1.16, 95% CI: 0.65 - 2.06, Z = 0.50, $p = 0.61$) or the Snively beetles (**Figure 2c**, Coef = 0.18, Se(coef)

= 0.21, hazard ratio = 1.2, lower 95% CI = 0.80, upper 95% CI = 1.80, Z = 0.88, $p = 0.38$). However, the analysis does indicate a significant decrease in killing rates for Bt isolates serially passaged in the highly susceptible hosts (Green River) when infecting the same Green River population (**Figure 2b**, Coef = -0.01, Se(coef) = 2×10^{-3} , hazard ratio = 0.993, lower 95% CI = 0.990, upper 95% CI = 0.997, Z = -3.94, $p < 8.1 \times 10^{-5}$) but not when infecting the Snavelly beetles (**Figure 2c**, Coef = 0.10, Se(coef) = 0.21, hazard ratio = 1.11, lower 95% CI = 0.73, upper 95% CI = 1.70, Z = 0.48, $p = 0.62$). Interestingly, the *in vitro* passaging significantly increased Bt killing rates when infecting the Snave population (**Figure 2c**, Coef = 0.54, Se(coef) = 0.20, hazard ratio = 1.71, lower 95% CI = 1.15, upper 95% CI = 2.56, Z = 2.63, $p < 0.01$) but not the Marshall (**Figure 2a**, Coef = 0.55, Se(coef) = 0.31, hazard ratio = 1.73, lower 95% CI = 0.95, upper 95% CI = 3.17, Z = 1.78, $p = 0.07$) or Green River populations (**Figure 2b**, Coef = 0.01, Se(coef) = 0.27, hazard ratio = 1.01, lower 95% CI = 0.60, upper 95% CI = 1.70, Z = 0.04, $p = 0.97$).

Additionally, we compared the hazard ratios of individual isolates by contrasting the mortality rates in homologous beetles with the killing rates in Snavelly beetles by regressing Snavelly hazard ratios over the homologous population hazard ratios. Analysis indicates that there is no significant correlation between killing rates in homologous and Snavelly beetles for our Bt isolates (**Figure 2d & e**, Green River – estimate = -0.51, std. error = 1.59, $t = -0.32$, $p = 0.77$ and Marshall – estimate = 0.24, std. error = 0.46, $t = 0.53$, $p = 0.64$).

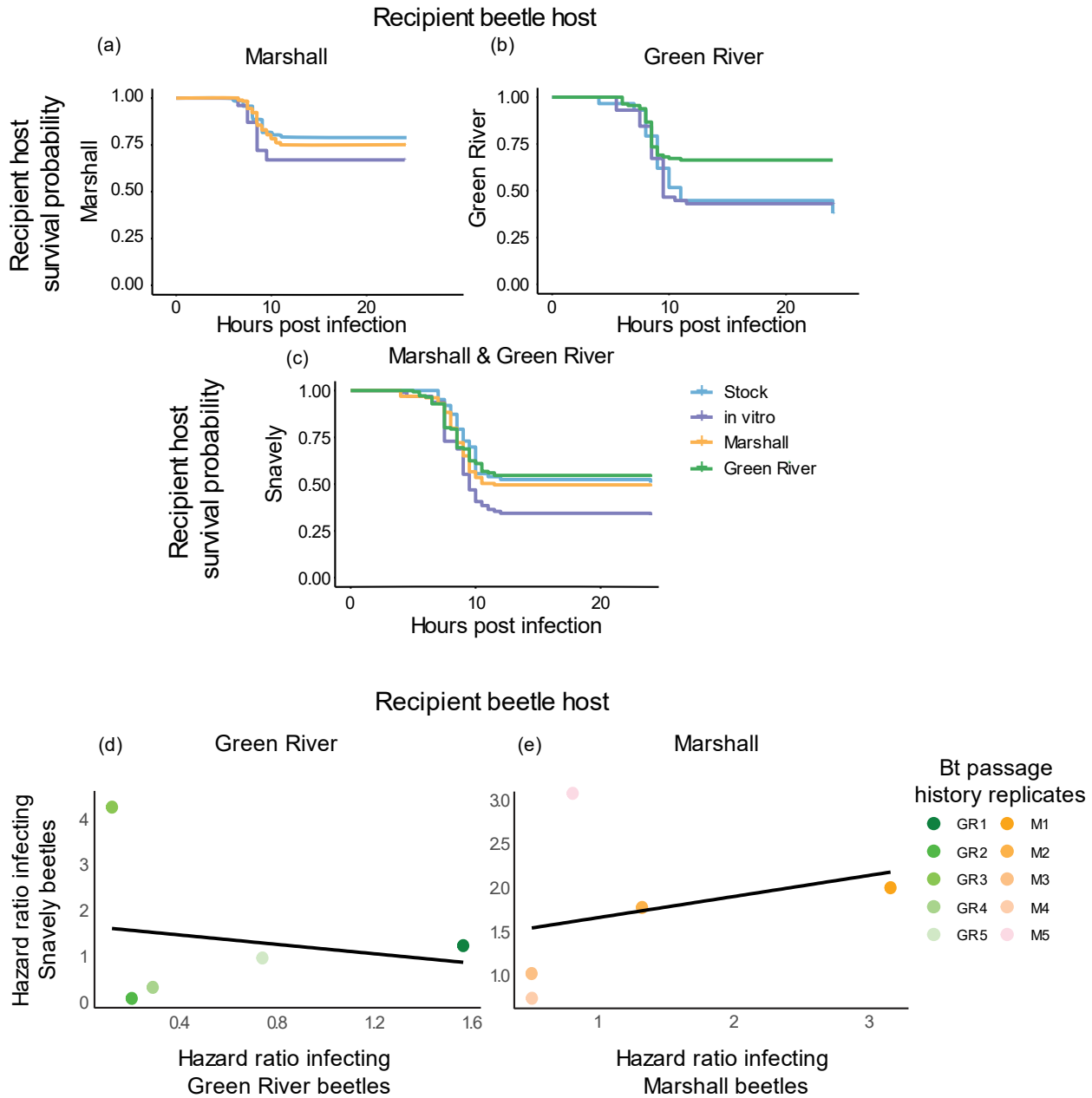


Figure 1. Bt killing rate after serial passaging. Survival curves for the passaged bacteria infecting the genotype they were passaged in (a & b) or in a naïve genotype with moderate Bt susceptibility (Snavelly, c). Figures d & e show the linear regression of the hazard ratios for the homologous genotype versus the naïve Snavelly genotype. Regression analysis indicates that killing rates in the serial passaging host does not significantly predict killing rates in the Snavelly population.

Serial passaging in a low-susceptibility host increases *in vitro* lag time

To assess how serial passaging affects Bt growth rates, we generated growth curves for all isolates using the protocol in **Appendix V**. Using the GrowthRates package (Mira et al., 2017), we extracted lag time and maximum growth rates (**Figure 3**) and evaluated differences with the Kruskal-Wallis rank sum tests and subsequent Dunn's post-hoc tests with an FDR correction using the FSA package in R. Serial passaging in the low susceptibility Marshall population showed a non-significant delay after multiple correction in lag time compared to the ancestral stock (**Figure 3a**, $z = 2.20$, $p = 0.08$) and displayed a non-significant increase in maximum growth rate (**Figure 3b**, $z = 1.97$, $p = 0.15$). Passaging in the high susceptibility Green River hosts also showed no significant changes in lag time nor maximum growth rate ($z = 0.96$, $p = 0.34$ & $z = 1.53$, $p = 0.19$, respectively).

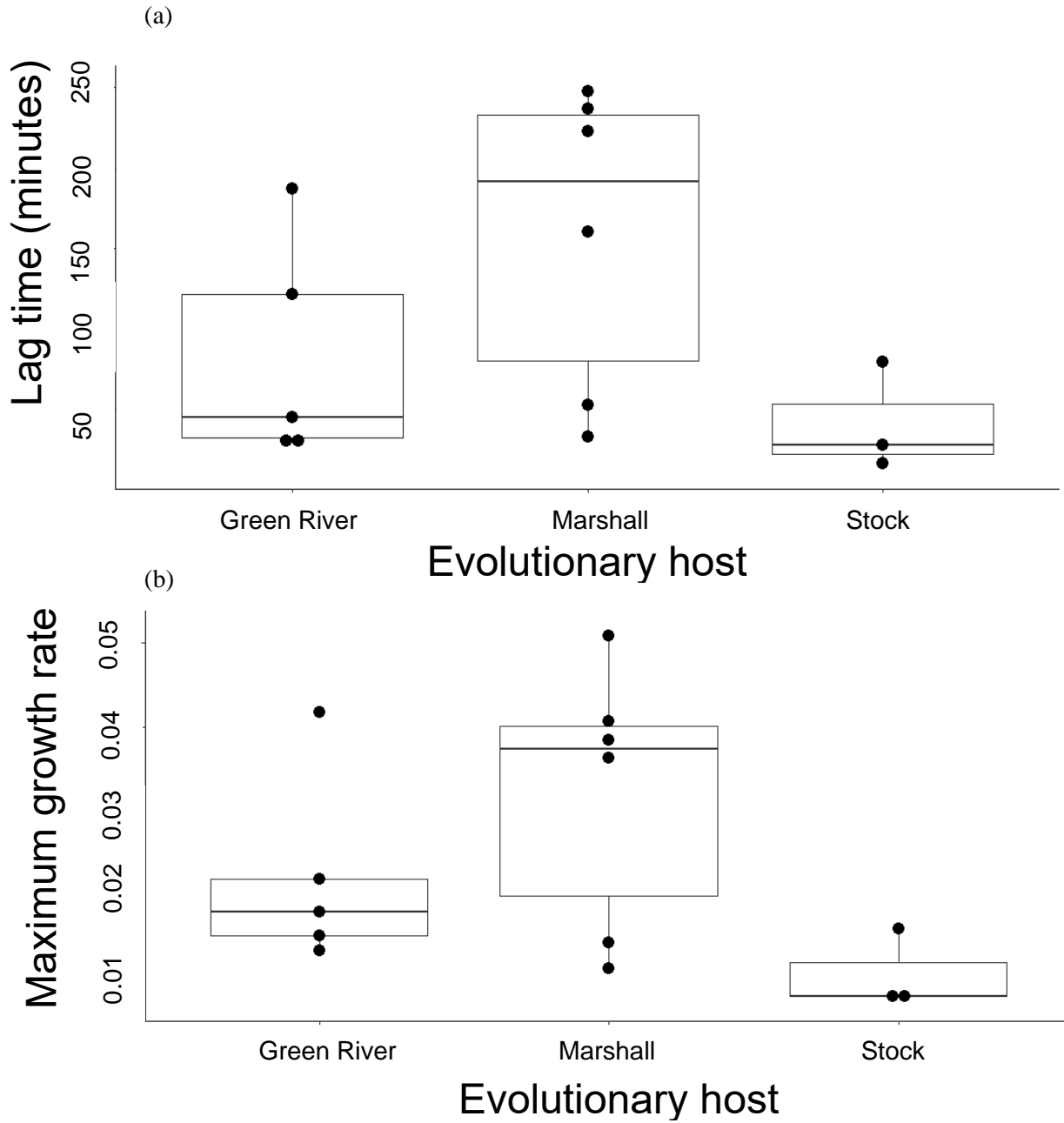


Figure 2. Shifts in Bt growth parameters after serial passaging. *In vitro* lag time (a) and maximum growth rate (b) for Bt after serial passaging in highly susceptible (Green River) and highly resistant (Marshall) hosts.

Discussion

To validate our *in vivo* serial passaging protocol, we took the approach of serially passaging Bt in *Tribolium* beetles with varying susceptibility to Bt infection. By bypassing the initial major gut receptor-toxin qualitative resistance infection stage and passaging Bt prior to its necrotrophic and sporulation phases, our protocol specifically targets the selective pressures from quantitative immunity while ensuring feasibility. The flexibility of our protocol permits modifications to either control the infectious dose or allow Bt to naturally adjust its transmission potential from final cadaver loads. In our preliminary tests using this approach, Bt passaged through flour beetle populations significantly altered their killing rates.

Our findings show that Bt isolates that underwent serial passaging in a highly susceptible host (Green River) had reduced killing rates in Green River beetles. In contrast, no significant change was noted in killing rates in moderately susceptible hosts (Snaveley). Additionally, no changes were detected in lag time and maximum growth rate for Bt evolved within Green River. One possible explanation is that reduced selective pressure from inducible immunity might have led to the increase in traits that trade off with host killing rates, like when two Bt strains were serially passaged in *Plutella xylostella*. These evolved strains exhibited improved *in vitro* growth competition but at the expense of their efficacy in killing *P. xylostella* (Garbutt et al., 2011). While our study did not reveal statistically significant changes in *in vitro* growth rates, further exploration into the competition between isolates and the influence of different culturing mediums on *in vitro* growth rates could unveil a similar trade-off.

When Bt was passaged through hosts less susceptible to septic infection (Marshall), there was a trend towards longer *in vitro* lag time and a trend towards increased maximum growth rates. Yet, killing rates were unchanged when infecting the Marshall and Snaveley populations compared to the ancestral stock. We speculate that to counter heightened immune resistance, the Marshall isolates extended their

lag phase duration. Indeed, by changing the proficiency of essential enzymes involved during lag phase, bacteria can increase their survivorship from exposure to certain AMPs and antibiotics (Bertrand, 2019; Li et al., 2016; Sandín et al., 2022). We anticipate these isolates would similarly have greater resistance to *in vitro* AMP and antibiotic exposure and that further serial passaging would result in isolates with increased killing ability when infecting the less susceptible Marshall population.

FUTURE DIRECTIONS

By integrating the RNAi techniques from chapters III, IV, and **Appendix V** with our serial passaging protocol, researchers can elucidate the selective pressures exerted by immune genes on parasite fitness. Using our RNAi protocol, future work can knock down the major positive and negative regulating host immune genes during septic Bt infection to determine the immune mechanisms that influence Bt fitness traits. For example, our previous work shows that RNAi-mediated knockdown of *imd* reduces the ability of *T. castaneum* to resist infection through induced expression of the IMD pathway but does not result in a reduction in beetle survival (Jent et al., 2019). Once the influence of the remaining arms of the beetle immune response on Bt are determined, these results will clarify the influence of insect immune defense mechanisms on parasite fitness.

The identification of these major immune genes can then be paired with the serial passaging protocol to investigate how life-history traits of parasites change in response to varying immune resistance across evolutionary timescales and the trade-offs associated with these adaptations. For example, enhanced virulence associated with faster growth rates are predicted when parasites evolve under increased immune resistance (Anderson & May, n.d.; Ewald, 1983; S. A. Frank, 1996; Gandon & Michalakis, 2000; Read, 1994). However, experimental observations of this correlation are inconsistent (Barclay et al., 2012; Gandon et al., 2001; Mackinnon & Read, 2004; Tardy et al., 2019) with little empirical evidence detailing the mechanisms used to achieve increased virulence. Using our protocol, Bt can be passaged through hosts that differ in immunological resistance via RNAi-mediated knockdown. Evolved Bt isolates can then be tested for shifts over evolutionary time in key Bt fitness related traits like killing rates and final spore loads. By combining these two traits, one can approximate an isolate's transmission potential as an indicator of Bt fitness (Ben-Ami, 2017; Papkou et al., 2019; Raymond et al., 2009).

Additionally, researchers could measure Bt growth and gene expression *in vitro* to identify virulence-growth trade-offs that correlate with changes in Bt gene expression (Zhu et al., 2015).

This work would indicate which specific parasite traits immunological variation selects for and if these traits could become liabilities in other conditions, which can inform rational intervention designs that factor in parasite evolution. Such insights would also refine epidemiological models, enabling them to factor in realistic evolutionary trade-offs when predicting parasite evolution across diverse populations.

Finally, after serially passaging Bt in these diverse immune environments, the saved glycerol stocks and DNA samples can be used to connect the shifting phenotypes with their genetic underpinnings. For example, if researchers observe parallel evolution of increased host-killing rates under increased host immune resistance among multiple replicates, researchers could use the saved glycerol stocks to identify at which passage this phenotype was introduced (Blount et al., 2020). Then researchers could use the saved DNA samples to analyze the single nucleotide polymorphisms, indels, and copy number variation for each isolate. Completion of such a study would facilitate the identification of the genetic basis of adaptation and identify the degree of parallel evolution across replicates or even strains in nature. It also may better our understanding of why the same mutation can have different phenotypic effects given a slightly different genetic background (Bleuven & Landry, 2016).

REFERENCES

- Acevedo, M. A., Dillemoth, F. P., Flick, A. J., Faldyn, M. J., & Elder, B. D. (2019). Virulence-driven trade-offs in disease transmission: A meta-analysis*. *Evolution*, 73(4), 636–647. <https://doi.org/10.1111/evo.13692>
- Aggarwal, K., Rus, F., Vriesema-Magnuson, C., Ertürk-Hasdemir, D., Paquette, N., & Silverman, N. (2008). Rudra interrupts receptor signaling complexes to negatively regulate the IMD pathway. *PLoS Pathogens*, 4(8), e1000120. <https://doi.org/10.1371/journal.ppat.1000120>
- Ahn, H.-M., Lee, K.-S., Lee, D.-S., & Yu, K. (2012). JNK/FOXO mediated PeroxiredoxinV expression regulates redox homeostasis during *Drosophila melanogaster* gut infection. *Developmental & Comparative Immunology*, 38(3), 466–473. <https://doi.org/10.1016/j.dci.2012.07.002>
- Alizon, S., Hurford, A., Mideo, N., & Van Baalen, M. (2009). Virulence evolution and the trade-off hypothesis: history, current state of affairs and the future. *Journal of Evolutionary Biology*, 22(2), 245–259. <https://doi.org/10.1111/j.1420-9101.2008.01658.x>
- Altincicek, B., Knorr, E., & Vilcinskis, A. (2008a). Beetle immunity: Identification of immune-inducible genes from the model insect *Tribolium castaneum*. *Developmental & Comparative Immunology*, 32(5), 585–595. <https://doi.org/10.1016/j.dci.2007.09.005>
- Altincicek, B., Knorr, E., & Vilcinskis, A. (2008b). Beetle immunity: Identification of immune-inducible genes from the model insect *Tribolium castaneum*. *Developmental & Comparative Immunology*, 32(5), 585–595. <https://doi.org/10.1016/j.dci.2007.09.005>
- Anderson, R. M., & May, R. M. (n.d.). *Coevolution of hosts and parasites*. <https://doi.org/10.1017/S0031182000055360>
- Anderson, R. M., & May, R. M. (1986). The invasion, persistence and spread of infectious diseases within animal and plant communities. *Philosophical Transactions of the Royal Society of London. Series B, Biological Sciences*, 314(1167), 533–570. <http://www.ncbi.nlm.nih.gov/pubmed/2880354>
- Anjum, S. G., Xu, W., Nikkholgh, N., Basu, S., Nie, Y., Thomas, M., Satyamurti, M., Budnik, B. A., Ip, Y. T., & Veraksa, A. (2013). Regulation of toll signaling and inflammation by β -Arrestin and the SUMO protease Ulp1. *Genetics*, 195(4), 1307–1317. <https://doi.org/10.1534/GENETICS.113.157859-/DC1/GENETICS.113.157859-5.PDF>
- Anselme, C., Pérez-Brocal, V., Vallier, A., Vincent-Monegat, C., Charif, D., Latorre, A., Moya, A., & Heddi, A. (2008). Identification of the Weevil immune genes and their expression in the bacteriome tissue. *BMC Biology*, 6, 43. <https://doi.org/10.1186/1741-7007-6-43>
- Antonson, N. D., Rubenstein, D. R., Hauber, M. E., & Botero, C. A. (2020). Ecological uncertainty favours the diversification of host use in avian brood parasites. *Nature Communications*, 11(1), 4185. <https://doi.org/10.1038/s41467-020-18038-y>
- Arjan G., J., Visser, M. de, Zeyl, C. W., Gerrish, P. J., Blanchard, J. L., & Lenski, R. E. (1999). Diminishing Returns from Mutation Supply Rate in Asexual Populations. *Science*, 283(5400), 404–406. <https://doi.org/10.1126/science.283.5400.404>
- Armitage, S. A., Genersch, E., McMahon, D. P., Rafaluk-Mohr, C., & Rolff, J. (2022). Tripartite interactions: how immunity, microbiota and pathogens interact and affect pathogen virulence evolution. *Current Opinion in Insect Science*, 50, 100871. <https://doi.org/10.1016/J.COIS.2021.12.011>
- Arnot, C. J., Gay, N. J., & Gangloff, M. (2010). Molecular Mechanism That Induces Activation of Spätzle, the Ligand for the *Drosophila* Toll Receptor. *Journal of Biological Chemistry*, 285(25), 19502–19509. <https://doi.org/10.1074/JBC.M109.098186>
- Ashby, B., & Bruns, E. (2018). The evolution of juvenile susceptibility to infectious disease. *Proceedings of the Royal Society B: Biological Sciences*, 285(1881), 20180844. <https://doi.org/10.1098/rspb.2018.0844>
- Badinloo, M., Nguyen, E., Suh, W., Alzahrani, F., Castellanos, J., Klichko, V. I., Orr, W. C., & Radyuk, S. N.

- (2018). Overexpression of antimicrobial peptides contributes to aging through cytotoxic effects in *Drosophila* tissues. *Archives of Insect Biochemistry and Physiology*, 98(4), e21464. <https://doi.org/10.1002/ARCH.21464>
- Balint-Kurti, P. J., Krakowsky, M. D., Jines, M. P., Robertson, L. A., Molnár, T. L., Goodman, M. M., & Holland, J. B. (2006). Identification of quantitative trait loci for resistance to southern leaf blight and days to anthesis in a maize recombinant inbred line population. *Phytopathology*, 96(10), 1067–1071. <https://doi.org/10.1094/PHYTO-96-1067>
- Balka, K. R., & De Nardo, D. (2019). Understanding early TLR signaling through the Myddosome. *Journal of Leukocyte Biology*, 105(2), 339–351. <https://doi.org/10.1002/JLB.MR0318-096R>
- Banerjee, U., Girard, J. R., Goins, L. M., & Spratford, C. M. (2019). *Drosophila* as a Genetic Model for Hematopoiesis. *Genetics*, 211(2), 367–417. <https://doi.org/10.1534/genetics.118.300223>
- Bangham, J., Knott, S. A., Kim, K. W., Young, R. S., & Jiggins, F. M. (2008). Genetic variation affecting host-parasite interactions: Major-effect quantitative trait loci affect the transmission of sigma virus in *Drosophila melanogaster*. *Molecular Ecology*, 17(17), 3800–3807. <https://doi.org/10.1111/j.1365-294X.2008.03873.x>
- Barclay, V. C., Sim, D., Chan, B. H. K., Nell, L. A., Rabaa, M. A., Bell, A. S., Anders, R. F., & Read, A. F. (2012). The evolutionary consequences of blood-stage vaccination on the rodent malaria *Plasmodium chabaudi*. *PLoS Biology*, 10(7), e1001368. <https://doi.org/10.1371/journal.pbio.1001368>
- Barletta, A. B. F., Saha, B., Trisnadi, N., Talyuli, O. A. C., Raddi, G., & Barillas-Mury, C. (2022). Hemocyte differentiation to the megacyte lineage enhances mosquito immunity against *Plasmodium*. *ELife*, 11. <https://doi.org/10.7554/eLife.81116>
- Basbous, N., Coste, F., Leone, P., Vincentelli, R., Royet, J., Kellenberger, C., & Roussel, A. (2011). The *Drosophila* peptidoglycan-recognition protein LF interacts with peptidoglycan-recognition protein LC to downregulate the Imd pathway. *EMBO Reports*, 12(4), 327–333. <https://doi.org/10.1038/embor.2011.19>
- Behrens, S., Peuß, R., Milutinović, B., Eggert, H., Esser, D., Rosenstiel, P., Schulenburg, H., Bornberg-Bauer, E., & Kurtz, J. (2014). Infection routes matter in population-specific responses of the red flour beetle to the entomopathogen *Bacillus thuringiensis*. *BMC Genomics*, 15(1), 445. <https://doi.org/10.1186/1471-2164-15-445>
- Belvin, M. P., & Anderson, K. V. (1996). A conserved signaling pathway: the *Drosophila* toll-dorsal pathway. *Annual Review of Cell and Developmental Biology*, 12(1), 393–416. <https://doi.org/10.1146/annurev.cellbio.12.1.393>
- Ben-Ami, F. (2017). The virulence-transmission relationship in an obligate killer holds under diverse epidemiological and ecological conditions, but where is the tradeoff? *Ecology and Evolution*, 7(24), 11157–11166. <https://doi.org/10.1002/ece3.3532>
- Benjamini, Y., Drai, D., Elmer, G., Kafkafi, N., & Golani, I. (2001). Controlling the false discovery rate in behavior genetics research. *Behavioural Brain Research*, 125(1–2), 279–284. [https://doi.org/10.1016/S0166-4328\(01\)00297-2](https://doi.org/10.1016/S0166-4328(01)00297-2)
- Benjamini, Y., & Yekutieli, D. (2001). The control of the false discovery rate in multiple testing under dependency. *The Annals of Statistics*, 29(4). <https://doi.org/10.1214/aos/1013699998>
- Beramendi, A., Peron, S., Megighian, A., Reggiani, C., & Cantera, R. (2005). The inhibitor kappaB-ortholog Cactus is necessary for normal neuromuscular function in *Drosophila melanogaster*. *Neuroscience*, 134(2), 397–406. <https://doi.org/10.1016/j.neuroscience.2005.04.046>
- Bertrand, R. L. (2019). Lag Phase Is a Dynamic, Organized, Adaptive, and Evolvable Period That Prepares Bacteria for Cell Division. *Journal of Bacteriology*, 201(7). <https://doi.org/10.1128/JB.00697-18>
- Best, A., White, A., & Boots, M. (2014). The coevolutionary implications of host tolerance. *Evolution; International Journal of Organic Evolution*, 68(5), 1426–1435. <https://doi.org/10.1111/evo.12368>
- Bingsohn, L., Knorr, E., Billion, A., Narva, K. E., & Vilcinskis, A. (2017). Knockdown of genes in the Toll pathway reveals new lethal RNA interference targets for insect pest control. *Insect Molecular Biology*, 26(1), 92–102. <https://doi.org/10.1111/imb.12273>
- Bischoff, V., Vignal, C., Duvic, B., Boneca, I. G., Hoffmann, J. A., & Royet, J. (2006). Downregulation of the *Drosophila* Immune Response by Peptidoglycan-Recognition Proteins SC1 and SC2. *PLoS Pathogens*, 2(2), e14. <https://doi.org/10.1371/journal.ppat.0020014>

- Blaser, M., & Schmid-Hempel, P. (2005). Determinants of virulence for the parasite *Nosema whitei* in its host *Tribolium castaneum*. *Journal of Invertebrate Pathology*, 89(3), 251–257. <https://doi.org/10.1016/j.jip.2005.04.004>
- Bleuven, C., & Landry, C. R. (2016). Molecular and cellular bases of adaptation to a changing environment in microorganisms. In *Proceedings of the Royal Society B: Biological Sciences* (Vol. 283, Issue 1841). Royal Society of London. <https://doi.org/10.1098/rspb.2016.1458>
- Blount, Z. D., Maddamsetti, R., Grant, N. A., Ahmed, S. T., Jagdish, T., Baxter, J. A., Sommerfeld, B. A., Tillman, A., Moore, J., Slonczewski, J. L., Barrick, J. E., & Lenski, R. E. (2020). Genomic and phenotypic evolution of *Escherichia coli* in a novel citrate-only resource environment. *ELife*, 9, 1–64. <https://doi.org/10.7554/ELIFE.55414>
- Boots, M., & Best, A. (2018). The evolution of constitutive and induced defences to infectious disease. *Proceedings of the Royal Society B: Biological Sciences*, 285(1883), 20180658. <https://doi.org/10.1098/rspb.2018.0658>
- Boots, M., Best, A., Miller, M. R., & White, A. (2009). The role of ecological feedbacks in the evolution of host defence: what does theory tell us? *Philosophical Transactions of the Royal Society of London. Series B, Biological Sciences*, 364(1513), 27–36. <https://doi.org/10.1098/rstb.2008.0160>
- Boots, M., & Bowers, R. G. (2004). The evolution of resistance through costly acquired immunity. *Proceedings. Biological Sciences*, 271(1540), 715–723. <https://doi.org/10.1098/rspb.2003.2655>
- Bou Aoun, R., Hetru, C., Troxler, L., Doucet, D., Ferrandon, D., & Matt, N. (2011). Analysis of Thioester-Containing Proteins during the Innate Immune Response of *Drosophila melanogaster*. *Journal of Innate Immunity*, 3(1), 52–64. <https://doi.org/10.1159/000321554>
- Buckingham, L. J., & Ashby, B. (2022). Coevolutionary theory of hosts and parasites. *Journal of Evolutionary Biology*, 35(2), 205–224. <https://doi.org/10.1111/jeb.13981>
- Buscher, K., Ehinger, E., Gupta, P., Pramod, A. B., Wolf, D., Tweet, G., Pan, C., Mills, C. D., Lusic, A. J., & Ley, K. (2017). Natural variation of macrophage activation as disease-relevant phenotype predictive of inflammation and cancer survival. *Nature Communications*, 8, 16041. <https://doi.org/10.1038/ncomms16041>
- Chakaya, J., Khan, M., Ntoumi, F., Aklillu, E., Fatima, R., Mwaba, P., Kapata, N., Mfinanga, S., Hasnain, S. E., Katoto, P. D. M. C., Bulabula, A. N. H., Sam-Agudu, N. A., Nachega, J. B., Tiberi, S., McHugh, T. D., Abubakar, I., & Zumla, A. (2021). Global Tuberculosis Report 2020 – Reflections on the Global TB burden, treatment and prevention efforts. *International Journal of Infectious Diseases*, 113, S7–S12. <https://doi.org/10.1016/j.ijid.2021.02.107>
- Chen, J., Almo, S. C., & Wu, Y. (2017). General principles of binding between cell surface receptors and multi-specific ligands: A computational study. *PLoS Computational Biology*, 13(10), e1005805. <https://doi.org/10.1371/journal.pcbi.1005805>
- Cheon, H.-M., Shin, S. W., Bian, G., Park, J.-H., & Raikhel, A. S. (2006). Regulation of lipid metabolism genes, lipid carrier protein lipophorin, and its receptor during immune challenge in the mosquito *Aedes aegypti*. *The Journal of Biological Chemistry*, 281(13), 8426–8435. <https://doi.org/10.1074/jbc.M510957200>
- Clayton, A. M., Cirimotich, C. M., Dong, Y., & Dimopoulos, G. (2013). Caudal is a negative regulator of the Anopheles IMD pathway that controls resistance to *Plasmodium falciparum* infection. *Developmental and Comparative Immunology*, 39(4), 323–332. <https://doi.org/10.1016/j.dci.2012.10.009>
- Clopton, R. E. (2009). Phylogenetic Relationships, Evolution, and Systematic Revision of the Septate Gregarines (Apicomplexa: Eugregarinorida: Septatorina). *Comparative Parasitology*, 76(2), 167–190. <https://doi.org/10.1654/4388.1>
- Cogni, R., Cao, C., Day, J. P., Bridson, C., & Jiggins, F. M. (2016). The genetic architecture of resistance to virus infection in *Drosophila*. *Molecular Ecology*, 25(20), 5228. <https://doi.org/10.1111/MEC.13769>
- Corwin, J. A., & Kliebenstein, D. J. (2017). Quantitative resistance: More than just perception of a pathogen. In *Plant Cell* (Vol. 29, Issue 4, pp. 655–665). <https://doi.org/10.1105/tpc.16.00915>
- Costantino, R. F., Desharnais, R. A., Cushing, J. M., & Dennis, B. (1997). Chaotic Dynamics in an Insect Population. *Science*, 275(5298), 389–391. <https://doi.org/10.1126/science.275.5298.389>
- Cotter, S. C., Kruuk, L. E. B., & Wilson, K. (2004). Costs of resistance: genetic correlations and potential trade-offs in an insect immune system. *Journal of Evolutionary Biology*, 17(2), 421–429.

<https://doi.org/10.1046/j.1420-9101.2003.00655.x>

- Critchlow, J. T., Norris, A., & Tate, A. T. (2019). The legacy of larval infection on immunological dynamics over metamorphosis. *Philosophical Transactions of the Royal Society B: Biological Sciences*, 374(1783), 20190066. <https://doi.org/10.1098/rstb.2019.0066>
- Day, T. (2003). Virulence evolution and the timing of disease life-history events. *Trends in Ecology & Evolution*, 18(3), 113–118. [https://doi.org/10.1016/S0169-5347\(02\)00049-6](https://doi.org/10.1016/S0169-5347(02)00049-6)
- de Martino, M., Lodi, L., Galli, L., & Chiappini, E. (2019). Immune Response to Mycobacterium tuberculosis: A Narrative Review. *Frontiers in Pediatrics*, 7, 350. <https://doi.org/10.3389/fped.2019.00350>
- de Roode, J. C., Yates, A. J., & Altizer, S. (2008). Virulence-transmission trade-offs and population divergence in virulence in a naturally occurring butterfly parasite. *Proceedings of the National Academy of Sciences of the United States of America*, 105(21), 7489–7494. <https://doi.org/10.1073/pnas.0710909105>
- Decaestecker, E., Gaba, S., Raeymaekers, J. A. M., Stoks, R., Van Kerckhoven, L., Ebert, D., & De Meester, L. (2007). Host-parasite “Red Queen” dynamics archived in pond sediment. *Nature*, 450(7171), 870–873. <https://doi.org/10.1038/nature06291>
- Detwiler, J., & Janovy, J. (2008). The Role of Phylogeny and Ecology in Experimental Host Specificity: Insights from a Eugregarine–Host System. *Journal of Parasitology*, 94(1), 7–12. <https://doi.org/10.1645/GE-1308.1>
- DiAngelo, J. R., & Birnbaum, M. J. (2009). Regulation of fat cell mass by insulin in *Drosophila melanogaster*. *Molecular and Cellular Biology*, 29(24), 6341–6352. <https://doi.org/10.1128/MCB.00675-09>
- DiAngelo, J. R., Bland, M. L., Bambina, S., Cherry, S., & Birnbaum, M. J. (2009). The immune response attenuates growth and nutrient storage in *Drosophila* by reducing insulin signaling. *Proceedings of the National Academy of Sciences of the United States of America*, 106(49), 20853–20858. <https://doi.org/10.1073/pnas.0906749106>
- Diard, M., Garcia, V., Maier, L., Remus-Emsermann, M. N. P., Regoes, R. R., Ackermann, M., & Hardt, W. D. (2013). Stabilization of cooperative virulence by the expression of an avirulent phenotype. *Nature*, 494(7437), 353–356. <https://doi.org/10.1038/nature11913>
- Diard, M., & Hardt, W.-D. (2017). Evolution of bacterial virulence. *FEMS Microbiology Reviews*, 41(5), 679–697. <https://doi.org/10.1093/femsre/fux023>
- Duangurui, T., Reamtong, O., Rungruengkitkun, A., Srinon, V., Boonyuen, U., Limmathurotsakul, D., Chantratita, N., & Pumirat, P. (2020). In vitro passage alters virulence, immune activation and proteomic profiles of *Burkholderia pseudomallei*. *Scientific Reports*, 10(1), 8320. <https://doi.org/10.1038/s41598-020-64914-4>
- Duneau, D., Ferdy, J.-B., Revah, J., Kondolf, H., Ortiz, G. A., Lazzaro, B. P., & Buchon, N. (2017). Stochastic variation in the initial phase of bacterial infection predicts the probability of survival in *D. melanogaster*. *eLife*, 6. <https://doi.org/10.7554/eLife.28298>
- Dunkler, D., Ploner, M., Schemper, M., & Heinze, G. (2018). Weighted Cox Regression Using the R Package **coxphw**. *Journal of Statistical Software*, 84(2), 1–26. <https://doi.org/10.18637/jss.v084.i02>
- Dunn, O. J. (1961). Multiple Comparisons among Means. *Journal of the American Statistical Association*, 56(293), 52–64. <https://doi.org/10.1080/01621459.1961.10482090>
- Dussurget, O., Pizarro-Cerda, J., & Cossart, P. (2004). Molecular Determinants of *Listeria monocytogenes* Virulence. *Annual Review of Microbiology*, 58(1), 587–610. <https://doi.org/10.1146/annurev.micro.57.030502.090934>
- Ebert, D., Duneau, D., Hall, M. D., Luijckx, P., Andras, J. P., Du Pasquier, L., & Ben-Ami, F. (2016). A Population Biology Perspective on the Stepwise Infection Process of the Bacterial Pathogen *Pasteuria ramosa* in *Daphnia*. In *Advances in parasitology* (Vol. 91, pp. 265–310). <https://doi.org/10.1016/bs.apar.2015.10.001>
- El-Khoury, N., Majed, R., Perchat, S., Kallassy, M., Lereclus, D., & Gohar, M. (2016). Spatio-Temporal Evolution of Sporulation in *Bacillus thuringiensis* Biofilm. *Frontiers in Microbiology*, 7(AUG), 212601. <https://doi.org/10.3389/fmicb.2016.01222>
- Engström, Y. (1999). Induction and regulation of antimicrobial peptides in *Drosophila*. *Developmental & Comparative Immunology*, 23(4–5), 345–358. [https://doi.org/10.1016/S0145-305X\(99\)00016-6](https://doi.org/10.1016/S0145-305X(99)00016-6)
- Ewald, P. W. (1983). Host-Parasite Relations, Vectors, and the Evolution of Disease Severity. *Annual Review of*

- Ecology and Systematics*, 14(1), 465–485. <https://doi.org/10.1146/annurev.es.14.110183.002341>
- Farrugia, M., & Baron, B. (2016). The role of TNF- α in rheumatoid arthritis: a focus on regulatory T cells. *Journal of Clinical and Translational Research*, 2(3), 84–90.
- FELLOUS, S., & LAZZARO, B. P. (2011). Potential for evolutionary coupling and decoupling of larval and adult immune gene expression. *Molecular Ecology*, 20(7), 1558–1567. <https://doi.org/10.1111/j.1365-294X.2011.05006.x>
- FENTON, A., LAMB, T., & GRAHAM, A. L. (2008). Optimality analysis of Th1/Th2 immune responses during microparasite-macroparasite co-infection, with epidemiological feedbacks. *Parasitology*, 135(7), 841–853. <https://doi.org/10.1017/S0031182008000310>
- Ferrandon, D., Imler, J.-L., Hetru, C., & Hoffmann, J. A. (2007). The *Drosophila* systemic immune response: sensing and signalling during bacterial and fungal infections. *Nature Reviews. Immunology*, 7(11), 862–874. <https://doi.org/10.1038/nri2194>
- Ferro, K., Peuß, R., Yang, W., Rosenstiel, P., Schulenburg, H., & Kurtz, J. (2019). Experimental evolution of immunological specificity. *Proceedings of the National Academy of Sciences*, 116(41), 20598–20604. <https://doi.org/10.1073/pnas.1904828116>
- Fox, J. W., & Lenski, R. E. (2015). From Here to Eternity--The Theory and Practice of a Really Long Experiment. *PLoS Biology*, 13(6), e1002185. <https://doi.org/10.1371/journal.pbio.1002185>
- Frank, C. L., Michalski, A., McDonough, A. A., Rahimian, M., Rudd, R. J., & Herzog, C. (2014). The Resistance of a North American Bat Species (*Eptesicus fuscus*) to White-Nose Syndrome (WNS). *PLoS ONE*, 9(12), e113958. <https://doi.org/10.1371/journal.pone.0113958>
- Frank, S. A. (1996). Models of parasite virulence. *The Quarterly Review of Biology*, 71(1), 37–78. <https://doi.org/10.1086/419267>
- Frank, S. A. (2002). Immune response to parasitic attack: Evolution of a pulsed character. *Journal of Theoretical Biology*, 219(3), 281–290. <https://doi.org/10.1006/JTBI.2002.3122>
- Frank, S. A., & Schmid-Hempel, P. (2008). Mechanisms of pathogenesis and the evolution of parasite virulence. *Journal of Evolutionary Biology*, 21(2), 396–404. <https://doi.org/10.1111/j.1420-9101.2007.01480.x>
- Frank, S. A., & Schmid-Hempel, P. (2019). Evolution of negative immune regulators. *PLoS Pathogens*, 15(8), e1007913. <https://doi.org/10.1371/journal.ppat.1007913>
- Gandon, S., Mackinnon, M. J., Nee, S., & Read, A. F. (2001). Imperfect vaccines and the evolution of pathogen virulence. *Nature* 2001 414:6865, 414(6865), 751–756. <https://doi.org/10.1038/414751a>
- Gandon, S., & Michalakakis, Y. (2000). Evolution of parasite virulence against qualitative or quantitative host resistance. *Proceedings. Biological Sciences*, 267(1447), 985–990. <https://doi.org/10.1098/rspb.2000.1100>
- Garbutt, J., Bonsall, M. B., Wright, D. J., & Raymond, B. (2011). Antagonistic competition moderates virulence in *Bacillus thuringiensis*. *Ecology Letters*, 14(8), 765–772. <https://doi.org/10.1111/j.1461-0248.2011.01638.x>
- Garver, L. S., Dong, Y., & Dimopoulos, G. (2009). Caspar Controls Resistance to *Plasmodium falciparum* in Diverse Anopheline Species. *PLoS Pathogens*, 5(3), e1000335. <https://doi.org/10.1371/journal.ppat.1000335>
- Germani, F., Hain, D., Sternlicht, D., Moreno, E., & Basler, K. (2018). The Toll pathway inhibits tissue growth and regulates cell fitness in an infection-dependent manner. *ELife*, 7. <https://doi.org/10.7554/eLife.39939>
- Giglio, A., & Giulianini, P. G. (2013). Phenoloxidase activity among developmental stages and pupal cell types of the ground beetle *Carabus* (*Chaetocarabus*) *lefebvrei* (Coleoptera, Carabidae). *Journal of Insect Physiology*, 59(4), 466–474. <https://doi.org/10.1016/j.jinsphys.2013.01.011>
- Graham, A. L., Allen, J. E., & Read, A. F. (2005). Evolutionary Causes and Consequences of Immunopathology. <https://doi.org/10.1146/annurev.ecolsys.36.102003.152622>, 36(1), 373–397. <https://doi.org/10.1146/ANNUREV.ECOLSYS.36.102003.152622>
- Graham, A. L., Schrom, E. C., & Metcalf, C. J. E. (2021). The evolution of powerful yet perilous immune systems. *Trends in Immunology*. <https://doi.org/10.1016/J.IT.2021.12.002>
- Grenfell, B. T., Pybus, O. G., Gog, J. R., Wood, J. L. N., Daly, J. M., Mumford, J. A., & Holmes, E. C. (2004). Unifying the Epidemiological and Evolutionary Dynamics of Pathogens. In *Science* (Vol. 303, Issue 5656, pp. 327–332). American Association for the Advancement of Science. <https://doi.org/10.1126/science.1090727>

- Guirado, E., Schlesinger, L. S., & Kaplan, G. (2013). Macrophages in tuberculosis: friend or foe. *Seminars in Immunopathology*, 35(5), 563–583. <https://doi.org/10.1007/s00281-013-0388-2>
- Gulley, M. M., Zhang, X., & Michel, K. (2013). The roles of serpins in mosquito immunology and physiology. *Journal of Insect Physiology*, 59(2), 138–147. <https://doi.org/10.1016/J.JINSPHYS.2012.08.015>
- Guntermann, S., Primrose, D. A., & Foley, E. (2009). Dnr1-dependent regulation of the *Drosophila* immune deficiency signaling pathway. *Developmental and Comparative Immunology*, 33(1), 127–134. <https://doi.org/10.1016/j.dci.2008.07.021>
- Guo, L., Karpac, J., Tran, S. L., & Jasper, H. (2014). PGRP-SC2 promotes gut immune homeostasis to limit commensal dysbiosis and extend lifespan. *Cell*, 156(1–2), 109–122. <https://doi.org/10.1016/j.cell.2013.12.018>
- Gupta, V., Frank, A. M., Matolka, N., & Lazzaro, B. P. (2022). Inherent constraints on a polyfunctional tissue lead to a reproduction-immunity tradeoff. *BMC Biology*, 20(1), 127. <https://doi.org/10.1186/s12915-022-01328-w>
- Ha, E.-M., Oh, C.-T., Bae, Y. S., & Lee, W.-J. (2005). A Direct Role for Dual Oxidase in *Drosophila* Gut Immunity. *Science*, 310(5749), 847–850. <https://doi.org/10.1126/science.1117311>
- Hakim, R. S., Baldwin, K., & Smagghe, G. (2010). Regulation of Midgut Growth, Development, and Metamorphosis. *Annual Review of Entomology*, 55(1), 593–608. <https://doi.org/10.1146/annurev-ento-112408-085450>
- Haldane, J. B. S. (1932). The Time of Action of Genes, and Its Bearing on some Evolutionary Problems. *The American Naturalist*, 66(702), 5–24. <https://doi.org/10.1086/280406>
- Hall, M. D., Routtu, J., & Ebert, D. (2019). Dissecting the genetic architecture of a stepwise infection process. *Molecular Ecology*, mec.15166. <https://doi.org/10.1111/mec.15166>
- Hamilton, R., Siva-Jothy, M., & Boots, M. (2008). Two arms are better than one: parasite variation leads to combined inducible and constitutive innate immune responses. *Proceedings. Biological Sciences*, 275(1637), 937–945. <https://doi.org/10.1098/rspb.2007.1574>
- Harsh, S., Heryanto, C., & Eleftherianos, I. (2019). Intestinal lipid droplets as novel mediators of host-pathogen interaction in *Drosophila*. *Biology Open*, 8(7). <https://doi.org/10.1242/bio.039040>
- Hawley, D. M., & Altizer, S. M. (2011). Disease ecology meets ecological immunology: understanding the links between organismal immunity and infection dynamics in natural populations. *Functional Ecology*, 25(1), 48–60. <https://doi.org/10.1111/j.1365-2435.2010.01753.x>
- Hayden, M. S., & Ghosh, S. (2004). Signaling to NF-kappaB. *Genes & Development*, 18(18), 2195–2224. <https://doi.org/10.1101/gad.1228704>
- Heckscher, E. S., Fetter, R. D., Marek, K. W., Albin, S. D., & Davis, G. W. (2007). NF-κB, IκB, and IRAK Control Glutamate Receptor Density at the *Drosophila* NMJ. *Neuron*, 55(6), 859–873. <https://doi.org/10.1016/j.neuron.2007.08.005>
- Hedengren, M., Asling, B., Dushay, M. S., Ando, I., Ekengren, S., Wihlborg, M., & Hultmark, D. (1999). Relish, a central factor in the control of humoral but not cellular immunity in *Drosophila*. *Molecular Cell*, 4(5), 827–837. [https://doi.org/10.1016/s1097-2765\(00\)80392-5](https://doi.org/10.1016/s1097-2765(00)80392-5)
- Herndon, N., Shelton, J., Gerischer, L., Ioannidis, P., Ninova, M., Dönitz, J., Waterhouse, R. M., Liang, C., Damm, C., Siemanowski, J., Kitzmann, P., Ulrich, J., Dippel, S., Oberhofer, G., Hu, Y., Schwirz, J., Schacht, M., Lehmann, S., Montino, A., ... Bucher, G. (2020). Enhanced genome assembly and a new official gene set for *Tribolium castaneum*. *BMC Genomics*, 21(1), 47. <https://doi.org/10.1186/s12864-019-6394-6>
- Hou, F., He, S., Liu, Y., Zhu, X., Sun, C., & Liu, X. (2014). RNAi knock-down of shrimp *Litopenaeus vannamei* Toll gene and immune deficiency gene reveals their difference in regulating antimicrobial peptides transcription. *Developmental & Comparative Immunology*, 44(2), 255–260. <https://doi.org/10.1016/j.dci.2014.01.004>
- Howles, P., Lawrence, G., Finnegan, J., McFadden, H., Ayliffe, M., Dodds, P., & Ellis, J. (2005). Autoactive Alleles of the Flax *L6* Rust Resistance Gene Induce Non-Race-Specific Rust Resistance Associated with the Hypersensitive Response. *Molecular Plant-Microbe Interactions®*, 18(6), 570–582. <https://doi.org/10.1094/MPMI-18-0570>

- Hoyle, A., Bowers, R. G., White, A., & Boots, M. (2008). The influence of trade-off shape on evolutionary behaviour in classical ecological scenarios. *Journal of Theoretical Biology*, 250(3), 498–511. <https://doi.org/10.1016/j.jtbi.2007.10.009>
- Jacot, A., Scheuber, H., & Brinkhof, M. W. G. (2004). COSTS OF AN INDUCED IMMUNE RESPONSE ON SEXUAL DISPLAY AND LONGEVITY IN FIELD CRICKETS. *Evolution*, 58(10), 2280–2286. <https://doi.org/10.1111/j.0014-3820.2004.tb01603.x>
- Jaenike, J. (1996). Suboptimal Virulence of an Insect-Parasitic Nematode. *Evolution; International Journal of Organic Evolution*, 50(6), 2241–2247. <https://doi.org/10.1111/j.1558-5646.1996.tb03613.x>
- Janovy, Jr., J., Detwiler, J., Schwank, S., Bolek, M. G., Knipes, A. K., & Langford, G. J. (2007). NEW AND EMENDED DESCRIPTIONS OF GREGARINES FROM FLOUR BEETLES (TRIBOLIUM SPP. AND PALORUS SUBDEPRESSUS: COLEOPTERA, TENEBRIONIDAE). *Journal of Parasitology*, 93(5), 1155–1170. <https://doi.org/10.1645/GE-1090R.1>
- Jent, D., Perry, A., Critchlow, J., & Tate, A. T. (2019). Natural variation in the contribution of microbial density to inducible immune dynamics. *Molecular Ecology*, 28(24), 5360–5372. <https://doi.org/10.1111/mec.15293>
- Jessup, C. M., & Bohannan, B. J. M. (2008). The shape of an ecological trade-off varies with environment. *Ecology Letters*, 11(9), 947–959. <https://doi.org/10.1111/j.1461-0248.2008.01205.x>
- Johnston, P. R., & Rolff, J. (2015). Host and Symbiont Jointly Control Gut Microbiota during Complete Metamorphosis. *PLOS Pathogens*, 11(11), e1005246. <https://doi.org/10.1371/journal.ppat.1005246>
- Kaneko, T., Goldman, W. E., Mellroth, P., Steiner, H., Fukase, K., Kusumoto, S., Harley, W., Fox, A., Golenbock, D., & Silverman, N. (2004). Monomeric and polymeric gram-negative peptidoglycan but not purified LPS stimulate the Drosophila IMD pathway. *Immunity*, 20(5), 637–649. [https://doi.org/10.1016/s1074-7613\(04\)00104-9](https://doi.org/10.1016/s1074-7613(04)00104-9)
- Karasov, T. L., Chae, E., Herman, J. J., & Bergelson, J. (2017). Mechanisms to Mitigate the Trade-Off between Growth and Defense. *The Plant Cell*, 29(4), 666–680. <https://doi.org/10.1105/tpc.16.00931>
- Khan, I., Agashe, D., & Rolff, J. (2017). Early-life inflammation, immune response and ageing. *Proceedings of the Royal Society B: Biological Sciences*, 284(1850). <https://doi.org/10.1098/RSPB.2017.0125>
- Khan, I., Prakash, A., & Agashe, D. (2016). Immunosenescence and the ability to survive bacterial infection in the red flour beetle *Tribolium castaneum*. *The Journal of Animal Ecology*, 85(1), 291–301. <https://doi.org/10.1111/1365-2656.12433>
- Khush, R. S., Cornwell, W. D., Uram, J. N., & Lemaitre, B. (2002). A Ubiquitin-Proteasome Pathway Represses the Drosophila Immune Deficiency Signaling Cascade. *Current Biology*, 12(20), 1728–1737. [https://doi.org/10.1016/S0960-9822\(02\)01214-9](https://doi.org/10.1016/S0960-9822(02)01214-9)
- King, J. G., & Hillyer, J. F. (2013). Spatial and temporal in vivo analysis of circulating and sessile immune cells in mosquitoes: hemocyte mitosis following infection. *BMC Biology*, 11(1), 55. <https://doi.org/10.1186/1741-7007-11-55>
- Kleino, A., Myllymäki, H., Kallio, J., Vanha-aho, L.-M., Oksanen, K., Ulvila, J., Hultmark, D., Valanne, S., & Rämet, M. (2008). Pirk is a negative regulator of the Drosophila Imd pathway. *Journal of Immunology (Baltimore, Md. : 1950)*, 180(8), 5413–5422. <https://doi.org/10.4049/jimmunol.180.8.5413>
- Kleino, A., & Silverman, N. (2014). The Drosophila IMD pathway in the activation of the humoral immune response. *Developmental and Comparative Immunology*, 42(1), 25–35. <https://doi.org/10.1016/j.dci.2013.05.014>
- Koyama, H., Kato, D., Minakuchi, C., Tanaka, T., Yokoi, K., & Miura, K. (2015a). Peptidoglycan recognition protein genes and their roles in the innate immune pathways of the red flour beetle, *Tribolium castaneum*. *Journal of Invertebrate Pathology*, 132, 86–100. <https://doi.org/10.1016/j.jip.2015.09.003>
- Koyama, H., Kato, D., Minakuchi, C., Tanaka, T., Yokoi, K., & Miura, K. (2015b). Peptidoglycan recognition protein genes and their roles in the innate immune pathways of the red flour beetle, *Tribolium castaneum*. *Journal of Invertebrate Pathology*, 132, 86–100. <https://doi.org/10.1016/j.jip.2015.09.003>
- Kruskal, W. H., & Wallis, W. A. (1952). Use of Ranks in One-Criterion Variance Analysis. *Journal of the American Statistical Association*, 47(260), 583–621. <https://doi.org/10.1080/01621459.1952.10483441>
- Laughton, A. M., Boots, M., & Siva-Jothy, M. T. (2011). The ontogeny of immunity in the honey bee, *Apis mellifera* L. following an immune challenge. *Journal of Insect Physiology*, 57(7), 1023–1032.

<https://doi.org/10.1016/j.jinsphys.2011.04.020>

- Laut, C. L., Leasure, C. S., Pi, H., Carlin, S. M., Chu, M. L., Hillebrand, G. H., Lin, H. K., Yi, X. I., Stauff, D. L., & Skaar, E. P. (2022). DnaJ and ClpX Are Required for HitRS and HssRS Two-Component System Signaling in *Bacillus anthracis*. *Infection and Immunity*, *90*(1), e0056021. <https://doi.org/10.1128/IAI.00560-21>
- Lazzaro, B. P., & Tate, A. T. (2022). Balancing sensitivity, risk, and immunopathology in immune regulation. *Current Opinion in Insect Science*, *50*, 100874. <https://doi.org/10.1016/J.COIS.2022.100874>
- League, G. P., Estévez-Lao, T. Y., Yan, Y., Garcia-Lopez, V. A., & Hillyer, J. F. (2017). Anopheles gambiae larvae mount stronger immune responses against bacterial infection than adults: evidence of adaptive decoupling in mosquitoes. *Parasites & Vectors*, *10*(1), 367. <https://doi.org/10.1186/s13071-017-2302-6>
- Lee, K.-Z., & Ferrandon, D. (2011). Negative regulation of immune responses on the fly. *The EMBO Journal*, *30*(6), 988–990. <https://doi.org/10.1038/emboj.2011.47>
- Leggett, H. C., Cornwallis, C. K., Buckling, A., & West, S. A. (2017). Growth rate, transmission mode and virulence in human pathogens. *Philosophical Transactions of the Royal Society of London. Series B, Biological Sciences*, *372*(1719). <https://doi.org/10.1098/rstb.2016.0094>
- Lemaitre, B., Meister, M., Govind, S., Georgel, P., Steward, R., Reichhart, J. M., & Hoffmann, J. A. (1995). Functional analysis and regulation of nuclear import of dorsal during the immune response in *Drosophila*. *The EMBO Journal*, *14*(3), 536–545. <https://doi.org/10.1002/j.1460-2075.1995.tb07029.x>
- Lemaitre, B., Nicolas, E., Michaut, L., Reichhart, J. M., & Hoffmann, J. A. (1996). The dorsoventral regulatory gene cassette *spätzle/Toll/cactus* controls the potent antifungal response in *Drosophila* adults. *Cell*, *86*(6), 973–983. [https://doi.org/10.1016/s0092-8674\(00\)80172-5](https://doi.org/10.1016/s0092-8674(00)80172-5)
- Lemaitre, B., Reichhart, J. M., & Hoffmann, J. A. (1997). *Drosophila* host defense: differential induction of antimicrobial peptide genes after infection by various classes of microorganisms. *Proceedings of the National Academy of Sciences of the United States of America*, *94*(26), 14614–14619. <https://doi.org/10.1073/pnas.94.26.14614>
- Leulier, F., Parquet, C., Pili-Floury, S., Ryu, J.-H., Caroff, M., Lee, W.-J., Mengin-Lecreulx, D., & Lemaitre, B. (2003). The *Drosophila* immune system detects bacteria through specific peptidoglycan recognition. *Nature Immunology*, *4*(5), 478–484. <https://doi.org/10.1038/ni922>
- Leulier, F., Rodriguez, A., Khush, R. S., Abrams, J. M., & Lemaitre, B. (2000). The *Drosophila* caspase Dredd is required to resist gram-negative bacterial infection. *EMBO Reports*, *1*(4), 353–358. <https://doi.org/10.1093/embo-reports/kvd073>
- Leulier, F., Vidal, S., Saigo, K., Ueda, R., & Lemaitre, B. (2002). Inducible expression of double-stranded RNA reveals a role for dFADD in the regulation of the antibacterial response in *Drosophila* adults. *Current Biology: CB*, *12*(12), 996–1000. [https://doi.org/10.1016/s0960-9822\(02\)00873-4](https://doi.org/10.1016/s0960-9822(02)00873-4)
- Li, B., Qiu, Y., Shi, H., & Yin, H. (2016). The importance of lag time extension in determining bacterial resistance to antibiotics. *The Analyst*, *141*(10), 3059–3067. <https://doi.org/10.1039/C5AN02649K>
- Ligoxygakis, P., Pelte, N., Ji, C., Leclerc, V., Duvic, B., Belvin, M., Jiang, H., Hoffmann, J. A., & Reichhart, J. M. (2002). A serpin mutant links Toll activation to melanization in the host defence of *Drosophila*. *The EMBO Journal*, *21*(23), 6330. <https://doi.org/10.1093/EMBOJ/CDF661>
- Linz, D. M., & Tomoyasu, Y. (2015). RNAi screening of developmental toolkit genes: a search for novel wing genes in the red flour beetle, *Tribolium castaneum*. *Development Genes and Evolution*, *225*(1), 11–22. <https://doi.org/10.1007/S00427-015-0488-1>
- Liu, B., Zheng, Y., Yin, F., Yu, J., Silverman, N., & Pan, D. (2016). Toll Receptor-Mediated Hippo Signaling Controls Innate Immunity in *Drosophila*. *Cell*, *164*(3), 406–419. <https://doi.org/10.1016/J.CELL.2015.12.029>
- Livak, K. J., & Schmittgen, T. D. (2001). Analysis of relative gene expression data using real-time quantitative PCR and the 2(-Delta Delta C(T)) Method. *Methods (San Diego, Calif.)*, *25*(4), 402–408. <https://doi.org/10.1006/meth.2001.1262>
- Loeb, M. J., Martin, P. A. W., Hakim, R. S., Goto, S., & Takeda, M. (2001). Regeneration of cultured midgut cells after exposure to sublethal doses of toxin from two strains of *Bacillus thuringiensis*. *Journal of Insect Physiology*, *47*(6), 599–606. [https://doi.org/10.1016/S0022-1910\(00\)00150-5](https://doi.org/10.1016/S0022-1910(00)00150-5)

- Long, G. H., & Boots, M. (2011). How can immunopathology shape the evolution of parasite virulence? *Trends in Parasitology*, 27(7), 300–305. <https://doi.org/10.1016/J.PT.2011.03.012>
- Lord, J. C., Hartzler, K., Toutges, M., & Oppert, B. (2010a). Evaluation of quantitative PCR reference genes for gene expression studies in *Tribolium castaneum* after fungal challenge. *Journal of Microbiological Methods*, 80(2), 219–221. <https://doi.org/10.1016/j.mimet.2009.12.007>
- Lord, J. C., Hartzler, K., Toutges, M., & Oppert, B. (2010b). Evaluation of quantitative PCR reference genes for gene expression studies in *Tribolium castaneum* after fungal challenge. *Journal of Microbiological Methods*, 80(2), 219–221. <https://doi.org/10.1016/j.mimet.2009.12.007>
- Lorrain, C., Gonçalves dos Santos, K. C., Germain, H., Hecker, A., & Duplessis, S. (2019). Advances in understanding obligate biotrophy in rust fungi. *New Phytologist*, 222(3), 1190–1206. <https://doi.org/10.1111/nph.15641>
- Lourenço, A. P., Guidugli-Lazzarini, K. R., Freitas, F. C. P., Bitondi, M. M. G., & Simões, Z. L. P. (2013). Bacterial infection activates the immune system response and dysregulates microRNA expression in honey bees. *Insect Biochemistry and Molecular Biology*, 43(5), 474–482. <https://doi.org/10.1016/j.ibmb.2013.03.001>
- Luecke, S., Sheu, K. M., & Hoffmann, A. (2021). Stimulus-specific responses in innate immunity: Multilayered regulatory circuits. *Immunity*, 54(9), 1915–1932. <https://doi.org/10.1016/j.immuni.2021.08.018>
- Mackinnon, M. J., & Read, A. F. (2004). Immunity promotes virulence evolution in a malaria model. *PLoS Biology*, 2(9), E230. <https://doi.org/10.1371/journal.pbio.0020230>
- Makarova, O., Johnston, P., Rodriguez-Rojas, A., El Shazely, B., Morales, J. M., & Rolff, J. (2018). Genomics of experimental adaptation of *Staphylococcus aureus* to a natural combination of insect antimicrobial peptides. *Scientific Reports*, 8(1), 1–8. <https://doi.org/10.1038/s41598-018-33593-7>
- Malinczak, C.-A., Lukacs, N. W., & Fonseca, W. (2020). Early-Life Respiratory Syncytial Virus Infection, Trained Immunity and Subsequent Pulmonary Diseases. *Viruses*, 12(5), 505. <https://doi.org/10.3390/v12050505>
- Martínez, B. A., Hoyle, R. G., Yeudall, S., Granade, M. E., Harris, T. E., Castle, J. D., Leitinger, N., & Bland, M. L. (2020). Innate immune signaling in *Drosophila* shifts anabolic lipid metabolism from triglyceride storage to phospholipid synthesis to support immune function. *PLOS Genetics*, 16(11), e1009192. <https://doi.org/10.1371/journal.pgen.1009192>
- Masri, L., Branca, A., Sheppard, A. E., Papkou, A., Laehnemann, D., Guenther, P. S., Prah, S., Saebelfeld, M., Hollensteiner, J., Liesegang, H., Brzuszkiewicz, E., Daniel, R., Michiels, N. K., Schulte, R. D., Kurtz, J., Rosenstiel, P., Telschow, A., Bornberg-Bauer, E., & Schulenburg, H. (2015). Host–pathogen coevolution: The selective advantage of *Bacillus thuringiensis* virulence and its cry toxin genes. *PLoS Biology*, 13(6), 1–30. <https://doi.org/10.1371/journal.pbio.1002169>
- McDonald, M. J. (2019). Microbial Experimental Evolution - a proving ground for evolutionary theory and a tool for discovery. *EMBO Reports*, 20(8), e46992. <https://doi.org/10.15252/embr.201846992>
- Mellroth, P., Karlsson, J., Håkansson, J., Schultz, N., Goldman, W. E., & Steiner, H. (2005). Ligand-induced dimerization of *Drosophila* peptidoglycan recognition proteins in vitro. *Proceedings of the National Academy of Sciences of the United States of America*, 102(18), 6455–6460. <https://doi.org/10.1073/pnas.0407559102>
- Metcalf, C. J. E., Tate, A. T., & Graham, A. L. (2017). Demographically framing trade-offs between sensitivity and specificity illuminates selection on immunity. *Nature Ecology & Evolution*, 1(11), 1766–1772. <https://doi.org/10.1038/s41559-017-0315-3>
- Metcalf, C. J. E., Tepekule, B., Bruijning, M., & Koskella, B. (2022). Hosts, microbiomes, and the evolution of critical windows. *Evolution Letters*, 6(6), 412–425. <https://doi.org/10.1002/evl3.298>
- Miller, S. C., Miyata, K., Brown, S. J., & Tomoyasu, Y. (2012). Dissecting Systemic RNA Interference in the Red Flour Beetle *Tribolium castaneum*: Parameters Affecting the Efficiency of RNAi. *PLoS ONE*, 7(10), e47431. <https://doi.org/10.1371/journal.pone.0047431>
- Milutinović, B., Höfling, C., Futo, M., Scharsack, J. P., & Kurtz, J. (2015). Infection of *Tribolium castaneum* with *Bacillus thuringiensis*: Quantification of bacterial replication within cadavers, transmission via cannibalism, and inhibition of spore germination. *Applied and Environmental Microbiology*, 81(23), 8135–8144.

<https://doi.org/10.1128/AEM.02051-15>

- Mira, P., Barlow, M., Meza, J. C., & Hall, B. G. (2017). Statistical Package for Growth Rates Made Easy. *Molecular Biology and Evolution*, 34(12), 3303–3309. <https://doi.org/10.1093/molbev/msx255>
- Mitchell, S., Vargas, J., & Hoffmann, A. (2016). Signaling via the NFκB system. *Wiley Interdisciplinary Reviews: Systems Biology and Medicine*, 8(3), 227–241. <https://doi.org/10.1002/WSBM.1331>
- Moran, N. A. (1994). ADAPTATION AND CONSTRAINT IN THE COMPLEX LIFE CYCLES OF ANIMALS. *Annual Review of Ecology and Systematics*, 25(1), 573–600. <https://doi.org/10.1146/annurev.es.25.110194.003041>
- Navarro, L., Bari, R., Achard, P., Lisón, P., Nemri, A., Harberd, N. P., & Jones, J. D. G. (2008). DELLAs Control Plant Immune Responses by Modulating the Balance of Jasmonic Acid and Salicylic Acid Signaling. *Current Biology*, 18(9), 650–655. <https://doi.org/10.1016/j.cub.2008.03.060>
- Nicolas, E., Reichhart, J. M., Hoffmann, J. A., & Lemaitre, B. (1998). In Vivo Regulation of the IκB Homologue cactus during the Immune Response of Drosophila. *Journal of Biological Chemistry*, 273(17), 10463–10469. <https://doi.org/10.1074/JBC.273.17.10463>
- Nielsen-LeRoux, C., Gaudriault, S., Ramarao, N., Lereclus, D., & Givaudan, A. (2012). How the insect pathogen bacteria *Bacillus thuringiensis* and *Xenorhabdus/Photorhabdus* occupy their hosts. *Current Opinion in Microbiology*, 15(3), 220–231. <https://doi.org/10.1016/j.mib.2012.04.006>
- Nishide, Y., Kageyama, D., Yokoi, K., Jouraku, A., Tanaka, H., Futahashi, R., & Fukatsu, T. (2019). Functional crosstalk across IMD and Toll pathways: insight into the evolution of incomplete immune cascades. *Proceedings of the Royal Society B: Biological Sciences*, 286(1897), 20182207. <https://doi.org/10.1098/rspb.2018.2207>
- Ntwasa, M., Goto, A., & Kurata, S. (2012). Coleopteran antimicrobial peptides: prospects for clinical applications. *International Journal of Microbiology*, 2012, 101989. <https://doi.org/10.1155/2012/101989>
- Papkou, A., Guzella, T., Yang, W., Koepper, S., Pees, B., Schalkowski, R., Barg, M.-C., Rosenstiel, P. C., Teotónio, H., & Schulenburg, H. (2019). The genomic basis of Red Queen dynamics during rapid reciprocal host-pathogen coevolution. *Proceedings of the National Academy of Sciences of the United States of America*, 116(3), 923–928. <https://doi.org/10.1073/pnas.1810402116>
- Paredes, J. C., Welchman, D. P., Poidevin, M., & Lemaitre, B. (2011a). Negative Regulation by Amidase PGRPs Shapes the Drosophila Antibacterial Response and Protects the Fly from Innocuous Infection. *Immunity*, 35(5), 770–779. <https://doi.org/10.1016/j.immuni.2011.09.018>
- Paredes, J. C., Welchman, D. P., Poidevin, M., & Lemaitre, B. (2011b). Negative Regulation by Amidase PGRPs Shapes the Drosophila Antibacterial Response and Protects the Fly from Innocuous Infection. *Immunity*, 35(5), 770–779. <https://doi.org/10.1016/j.immuni.2011.09.018>
- Park, T. (1948). Interspecies Competition in Populations of *Trilobium confusum* Duval and *Trilobium castaneum* Herbst. *Ecological Monographs*, 18(2), 265–307. <https://doi.org/10.2307/1948641>
- Parthasarathy, R., & Palli, S. R. (2008). Proliferation and differentiation of intestinal stem cells during metamorphosis of the red flour beetle, *Tribolium castaneum*. *Developmental Dynamics*, 237(4), 893–908. <https://doi.org/10.1002/dvdy.21475>
- Pointer, M. D., Gage, M. J. G., & Spurgin, L. G. (2021). *Tribolium* beetles as a model system in evolution and ecology. *Heredity*, 126(6), 869–883. <https://doi.org/10.1038/s41437-021-00420-1>
- Pollock, T. Y., Vázquez Marrero, V. R., Brodsky, I. E., & Shin, S. (2023). TNF licenses macrophages to undergo rapid caspase-1, -11, and -8-mediated cell death that restricts *Legionella pneumophila* infection. *PLOS Pathogens*, 19(6), e1010767. <https://doi.org/10.1371/journal.ppat.1010767>
- Posnien, N., Schinko, J., Grossmann, D., Shippy, T. D., Konopova, B., & Bucher, G. (2009). RNAi in the red flour beetle (*Tribolium*). *Cold Spring Harbor Protocols*, 2009(8), pdb.prot5256. <https://doi.org/10.1101/pdb.prot5256>
- Prakash, A., Monteith, K. M., & Vale, P. F. (2021). Negative regulation of IMD contributes to disease tolerance during systemic bacterial infection in *Drosophila*. *BioRxiv*, 2021.09.23.461574. <https://doi.org/10.1101/2021.09.23.461574>
- Qiu, P., Pan, P. C., & Govind, S. (1998). A role for the *Drosophila* Toll/Cactus pathway in larval hematopoiesis. *Development*, 125(10), 1909–1920. <https://doi.org/10.1242/DEV.125.10.1909>

- Randall, J., Cable, J., Guschina, I. A., Harwood, J. L., & Lello, J. (2013). Endemic infection reduces transmission potential of an epidemic parasite during co-infection. *Proceedings of the Royal Society B: Biological Sciences*, 280(1769), 20131500. <https://doi.org/10.1098/rspb.2013.1500>
- Raymond, B., Ellis, R. J., & Bonsall, M. B. (2009). Moderation of pathogen-induced mortality: the role of density in *Bacillus thuringiensis* virulence. *Biology Letters*, 5(2), 218–220. <https://doi.org/10.1098/rsbl.2008.0610>
- Raymond, B., Johnston, P. R., Nielsen-LeRoux, C., Lereclus, D., & Crickmore, N. (2010). *Bacillus thuringiensis*: an impotent pathogen? *Trends in Microbiology*, 18(5), 189–194. <https://doi.org/10.1016/j.tim.2010.02.006>
- Read, A. F. (1994). The evolution of virulence. In *Trends in Microbiology* (Vol. 2, Issue 3, pp. 73–76). Elsevier Current Trends. [https://doi.org/10.1016/0966-842X\(94\)90537-1](https://doi.org/10.1016/0966-842X(94)90537-1)
- Reaney, L. T., & Knell, R. J. (2010). Immune activation but not male quality affects female current reproductive investment in a dung beetle. *Behavioral Ecology*, 21(6), 1367–1372. <https://doi.org/10.1093/beheco/arq139>
- Rera, M., Bahadorani, S., Cho, J., Koehler, C. L., Ulgherait, M., Hur, J. H., Ansari, W. S., Lo, T., Jones, D. L., & Walker, D. W. (2011). Modulation of longevity and tissue homeostasis by the *Drosophila* PGC-1 homolog. *Cell Metabolism*, 14(5), 623–634. <https://doi.org/10.1016/j.cmet.2011.09.013>
- Rera, M., Clark, R. I., & Walker, D. W. (2012). Intestinal barrier dysfunction links metabolic and inflammatory markers of aging to death in *Drosophila*. *Proceedings of the National Academy of Sciences*, 109(52), 21528–21533. <https://doi.org/10.1073/pnas.1215849110>
- Rhodes, V. L., Thomas, M. B., & Michel, K. (2018). The interplay between dose and immune system activation determines fungal infection outcome in the African malaria mosquito, *Anopheles gambiae*. *Developmental and Comparative Immunology*, 85, 125–133. <https://doi.org/10.1016/j.dci.2018.04.008>
- Richards, S., Gibbs, R. A., Weinstock, G. M., Brown, S. J., Denell, R., Beeman, R. W., Gibbs, R., Beeman, R. W., Brown, S. J., Bucher, G., Friedrich, M., Grimmelikhuijzen, C. J. P., Klingler, M., Lorenzen, M., Richards, S., Roth, S., Schröder, R., Tautz, D., Zdobnov, E. M., ... Bucher, G. (2008). The genome of the model beetle and pest *Tribolium castaneum*. *Nature*, 452(7190), 949–955. <https://doi.org/10.1038/nature06784>
- Ritchie, H., & Roser, M. (2018). Causes of Death, Our World in Data. In *Our World in Data*. <https://ourworldindata.org/causes-of-death>
- Roberts, A. W., Lee, B. L., Deguine, J., John, S., Shlomchik, M. J., & Barton, G. M. (2017). Tissue-Resident Macrophages Are Locally Programmed for Silent Clearance of Apoptotic Cells. *Immunity*, 47(5), 913–927.e6. <https://doi.org/10.1016/j.immuni.2017.10.006>
- Rodriguez, Y., Omoto, C. K., & Gomulkiewicz, R. (2007). Individual and Population Effects of *Eugregarina*, *Gregarina niphandrodes* (Eugregarinida: Gregarinidae), on *Tenebrio molitor* (Coleoptera: Tenebrionidae). *Environmental Entomology*, 36(4), 689–693. <https://doi.org/10.1093/ee/36.4.689>
- Roth, S., Hiromi, Y., Godt, D., & Nüsslein-Volhard, C. (1991). cactus, a maternal gene required for proper formation of the dorsoventral morphogen gradient in *Drosophila* embryos. *Development (Cambridge, England)*, 112(2), 371–388. <https://doi.org/10.1242/dev.112.2.371>
- Rovenolt, F. H., & Tate, A. T. (2022). The Impact of Coinfection Dynamics on Host Competition and Coexistence. *The American Naturalist*, 199(1), 91–107. <https://doi.org/10.1086/717180>
- Roy, B. A., & Kirchner, J. W. (2000). EVOLUTIONARY DYNAMICS OF PATHOGEN RESISTANCE AND TOLERANCE. *Evolution*, 54(1), 51–63. <https://doi.org/10.1111/j.0014-3820.2000.tb00007.x>
- Royet, J. (2011). Epithelial homeostasis and the underlying molecular mechanisms in the gut of the insect model *Drosophila melanogaster*. *Cellular and Molecular Life Sciences*, 68(22), 3651–3660. <https://doi.org/10.1007/s00018-011-0828-x>
- Rumbaugh, K. P., Diggle, S. P., Watters, C. M., Ross-Gillespie, A., Griffin, A. S., & West, S. A. (2009). Quorum Sensing and the Social Evolution of Bacterial Virulence. *Current Biology*, 19(4), 341–345. <https://doi.org/10.1016/j.cub.2009.01.050>
- Russell, V., & Dunn, P. E. (1996). Antibacterial proteins in the midgut of *Manduca sexta* during metamorphosis. *Journal of Insect Physiology*, 42(1), 65–71. [https://doi.org/10.1016/0022-1910\(95\)00083-6](https://doi.org/10.1016/0022-1910(95)00083-6)
- Ryu, J.-H., Kim, S.-H., Lee, H.-Y., Bai, J. Y., Nam, Y.-D., Bae, J.-W., Lee, D. G., Shin, S. C., Ha, E.-M., & Lee, W.-J. (2008). Innate immune homeostasis by the homeobox gene caudal and commensal-gut mutualism in *Drosophila*. *Science (New York, N.Y.)*, 319(5864), 777–782. <https://doi.org/10.1126/science.1149357>

- Sandín, D., Valle, J., Morata, J., Andreu, D., & Torrent, M. (2022). Antimicrobial Peptides Can Generate Tolerance by Lag and Interfere with Antimicrobial Therapy. *Pharmaceutics*, *14*(10). <https://doi.org/10.3390/pharmaceutics14102169>
- Schmid-Hempel, P. (2003). Variation in immune defence as a question of evolutionary ecology. *Proceedings. Biological Sciences*, *270*(1513), 357–366. <https://doi.org/10.1098/rspb.2002.2265>
- Schmitt-Engel, C., Schultheis, D., Schwirz, J., Ströhlein, N., Troelenberg, N., Majumdar, U., Dao, V. A., Grossmann, D., Richter, T., Tech, M., Dönitz, J., Gerischer, L., Theis, M., Schild, I., Trauner, J., Koniszewski, N. D. B., Küster, E., Kittelmann, S., Hu, Y., ... Bucher, G. (2015). The iBeetle large-scale RNAi screen reveals gene functions for insect development and physiology. *Nature Communications*, *6*(1), 7822. <https://doi.org/10.1038/ncomms8822>
- Schmittgen, T. D., & Livak, K. J. (2008a). Analyzing real-time PCR data by the comparative CT method. *Nature Protocols*, *3*(6), 1101–1108. <https://doi.org/10.1038/nprot.2008.73>
- Schmittgen, T. D., & Livak, K. J. (2008b). Analyzing real-time PCR data by the comparative C(T) method. *Nature Protocols*, *3*(6), 1101–1108. <https://doi.org/10.1038/nprot.2008.73>
- Schwenke, R. A., Lazzaro, B. P., & Wolfner, M. F. (2016). Reproduction–Immunity Trade-Offs in Insects. *Annual Review of Entomology*, *61*, 239. <https://doi.org/10.1146/ANNUREV-ENTO-010715-023924>
- Sears, B. F., Rohr, J. R., Allen, J. E., & Martin, L. B. (2011). The economy of inflammation: when is less more? *Trends in Parasitology*, *27*(9), 382–387. <https://doi.org/10.1016/J.PT.2011.05.004>
- Shapiro, S. S., & Wilk, M. B. (1965). An analysis of variance test for normality (complete samples). *Biometrika*, *52*(3–4), 591–611. <https://doi.org/10.1093/biomet/52.3-4.591>
- Sheldon, B. C., & Verhulst, S. (1996). Ecological immunology: costly parasite defences and trade-offs in evolutionary ecology. *Trends in Ecology & Evolution*, *11*(8), 317–321. [https://doi.org/10.1016/0169-5347\(96\)10039-2](https://doi.org/10.1016/0169-5347(96)10039-2)
- Shudo, E., & Iwasa, Y. (2001). Inducible defense against pathogens and parasites: optimal choice among multiple options. *Journal of Theoretical Biology*, *209*(2), 233–247. <https://doi.org/10.1006/jtbi.2000.2259>
- Silverman*, K. A. & N. (2008). Positive and negative regulation of the Drosophila immune response. *BMB Reports*, *41*(4), 267–277. <https://www.bmbreports.org/journal/view.html?spage=267&volume=41&number=4>
- Simon, A. K., Hollander, G. A., & McMichael, A. (2015). Evolution of the immune system in humans from infancy to old age. *Proceedings of the Royal Society B: Biological Sciences*, *282*(1821), 20143085. <https://doi.org/10.1098/rspb.2014.3085>
- Slamti, L., Perchat, S., Huillet, E., Lereclus, D., Slamti, L., Perchat, S., Huillet, E., & Lereclus, D. (2014). Quorum Sensing in *Bacillus thuringiensis* Is Required for Completion of a Full Infectious Cycle in the Insect. *Toxins*, *6*(8), 2239–2255. <https://doi.org/10.3390/toxins6082239>
- Sneed, S. D., Dwivedi, S. B., DiGate, C., Denecke, S., & Povelones, M. (2022). *Aedes aegypti* Malpighian tubules are immunologically activated following systemic Toll activation. *Parasites & Vectors*, *15*(1), 469. <https://doi.org/10.1186/s13071-022-05567-2>
- Sprouffs, K., Aguilar-Rodríguez, J., & Wagner, A. (2016). How Archiving by Freezing Affects the Genome-Scale Diversity of *Escherichia coli* Populations. *Genome Biology and Evolution*, *8*(5), 1290–1298. <https://doi.org/10.1093/gbe/evw054>
- Stenbak, C. R., Ryu, J.-H., Leulier, F., Pili-Floury, S., Parquet, C., Hervé, M., Chaput, C., Boneca, I. G., Lee, W.-J., Lemaitre, B., & Mengin-Lecreulx, D. (2004). Peptidoglycan molecular requirements allowing detection by the *Drosophila* immune deficiency pathway. *Journal of Immunology (Baltimore, Md. : 1950)*, *173*(12), 7339–7348. <https://doi.org/10.4049/jimmunol.173.12.7339>
- Sturm, A., Heinemann, M., Arnoldini, M., Benecke, A., Ackermann, M., Benz, M., Dormann, J., & Hardt, W. D. (2011). The cost of virulence: Retarded growth of salmonella typhimurium cells expressing type iii secretion system 1. *PLoS Pathogens*, *7*(7), e1002143. <https://doi.org/10.1371/journal.ppat.1002143>
- Suzawa, M., Muhammad, N. M., Joseph, B. S., & Bland, M. L. (2019). The Toll Signaling Pathway Targets the Insulin-like Peptide Dilp6 to Inhibit Growth in *Drosophila*. *Cell Reports*, *28*(6), 1439-1446.e5. <https://doi.org/10.1016/j.celrep.2019.07.015>
- Tabunoki, H., Dittmer, N. T., Gorman, M. J., & Kanost, M. R. (2019). Development of a new method for

- collecting hemolymph and measuring phenoloxidase activity in *Tribolium castaneum*. *BMC Research Notes*, 12(1), 7. <https://doi.org/10.1186/s13104-018-4041-y>
- Tanji, T., Hu, X., Weber, A. N. R., & Ip, Y. T. (2007). Toll and IMD Pathways Synergistically Activate an Innate Immune Response in *Drosophila melanogaster*. *Molecular and Cellular Biology*, 27(12), 4578–4588. <https://doi.org/10.1128/MCB.01814-06>
- Tardy, L., Giraudeau, M., Hill, G. E., McGraw, K. J., & Bonneaud, C. (2019). Contrasting evolution of virulence and replication rate in an emerging bacterial pathogen. *Proceedings of the National Academy of Sciences*, 116(34), 16927–16932. <https://doi.org/10.1073/pnas.1901556116>
- Tate, A. T., Andolfatto, P., Demuth, J. P., & Graham, A. L. (2017). The within-host dynamics of infection in trans-generationally primed flour beetles. *Molecular Ecology*, 26(14), 3794–3807. <https://doi.org/10.1111/mec.14088>
- Tate, A. T., & Graham, A. L. (2015a). Dynamic Patterns of Parasitism and Immunity across Host Development Influence Optimal Strategies of Resource Allocation. *The American Naturalist*, 186(4), 495–512. <https://doi.org/10.1086/682705>
- Tate, A. T., & Graham, A. L. (2015b). Dynamic Patterns of Parasitism and Immunity across Host Development Influence Optimal Strategies of Resource Allocation. *The American Naturalist*, 186(4), 495–512. <https://doi.org/10.1086/682705>
- Tate, A. T., & Graham, A. L. (2015c). Trans-generational priming of resistance in wild flour beetles reflects the primed phenotypes of laboratory populations and is inhibited by co-infection with a common parasite. *Functional Ecology*, 29(8), 1059–1069. <https://doi.org/10.1111/1365-2435.12411>
- Tate, A. T., & Graham, A. L. (2015d). Trans-generational priming of resistance in wild flour beetles reflects the primed phenotypes of laboratory populations and is inhibited by co-infection with a common parasite. *Functional Ecology*, 29(8), 1059–1069. <https://doi.org/10.1111/1365-2435.12411>
- Tate, A. T., & Graham, A. L. (2015e). Trans-generational priming of resistance in wild flour beetles reflects the primed phenotypes of laboratory populations and is inhibited by co-infection with a common parasite. *Functional Ecology*, 29(8), 1059–1069. <https://doi.org/10.1111/1365-2435.12411>
- Tate, A. T., & Graham, A. L. (2017a). Dissecting the contributions of time and microbe density to variation in immune gene expression. *Proceedings of the Royal Society B: Biological Sciences*, 284(1859), 20170727. <https://doi.org/10.1098/rspb.2017.0727>
- Tate, A. T., & Graham, A. L. (2017b). Dissecting the contributions of time and microbe density to variation in immune gene expression. *Proceedings of the Royal Society B: Biological Sciences*, 284(1859), 20170727. <https://doi.org/10.1098/rspb.2017.0727>
- The i5K Initiative: Advancing Arthropod Genomics for Knowledge, Human Health, Agriculture, and the Environment. (2013). *Journal of Heredity*, 104(5), 595–600. <https://doi.org/10.1093/jhered/est050>
- THOMAS, A. M., & RUDOLF, V. H. W. (2010). Challenges of metamorphosis in invertebrate hosts: maintaining parasite resistance across life-history stages. *Ecological Entomology*, 35(2), 200–205. <https://doi.org/10.1111/j.1365-2311.2009.01169.x>
- Tomoyasu, Y., Miller, S. C., Tomita, S., Schoppmeier, M., Grossmann, D., & Bucher, G. (2008). Exploring systemic RNA interference in insects: a genome-wide survey for RNAi genes in *Tribolium*. *Genome Biology*, 9(1), R10. <https://doi.org/10.1186/gb-2008-9-1-r10>
- Tukey, J. W. (1949). Comparing Individual Means in the Analysis of Variance. *Biometrics*, 5(2), 99. <https://doi.org/10.2307/3001913>
- Tzou, P., Ohresser, S., Ferrandon, D., Capovilla, M., Reichhart, J. M., Lemaitre, B., Hoffmann, J. A., & Imler, J. L. (2000). Tissue-specific inducible expression of antimicrobial peptide genes in *Drosophila* surface epithelia. *Immunity*, 13(5), 737–748. [https://doi.org/10.1016/s1074-7613\(00\)00072-8](https://doi.org/10.1016/s1074-7613(00)00072-8)
- Ulrich, J., Dao, V. A., Majumdar, U., Schmitt-Engel, C., Schwirz, J., Schultheis, D., Ströhlein, N., Troelenberg, N., Grossmann, D., Richter, T., Dönitz, J., Gerischer, L., Leboulle, G., Vilcinskas, A., Stanke, M., & Bucher, G. (2015). Large scale RNAi screen in *Tribolium* reveals novel target genes for pest control and the proteasome as prime target. *BMC Genomics*, 16(1), 674. <https://doi.org/10.1186/s12864-015-1880-y>
- Urban, M. C., Bürger, R., & Bolnick, D. I. (2013). Asymmetric selection and the evolution of extraordinary defences. *Nature Communications* 2013 4:1, 4(1), 1–8. <https://doi.org/10.1038/ncomms3085>

- Valanne, S., Vesala, L., Maasdorp, M. K., Salminen, T. S., & Rämet, M. (2022). The *Drosophila* Toll Pathway in Innate Immunity: from the Core Pathway toward Effector Functions. *The Journal of Immunology*, 209(10), 1817–1825. <https://doi.org/10.4049/JIMMUNOL.2200476>
- Van Allen, B. G., & Rudolf, V. H. W. (2013). Ghosts of Habitats Past: Environmental Carry-Over Effects Drive Population Dynamics in Novel Habitat. *The American Naturalist*, 181(5), 596–608. <https://doi.org/10.1086/670127>
- Verplaetse, E., Slamti, L., Gohar, M., & Lereclus, D. (2015). Cell Differentiation in a *Bacillus thuringiensis* Population during Planktonic Growth, Biofilm Formation, and Host Infection. *MBio*, 6(3), e00138-15. <https://doi.org/10.1128/mBio.00138-15>
- Vincent, C. M., & Dionne, M. S. (2021). Disparate regulation of IMD signaling drives sex differences in infection pathology in *Drosophila melanogaster*. *Proceedings of the National Academy of Sciences*, 118(32). <https://doi.org/10.1073/pnas.2026554118>
- Wang, F., & Xia, Q. (2018). Back to homeostasis: Negative regulation of NF- κ B immune signaling in insects. *Developmental and Comparative Immunology*, 87, 216–223. <https://doi.org/10.1016/j.dci.2018.06.007>
- Wang, M., Wang, Y., Chang, M., Wang, X., Shi, Z., Raikhel, A. S., & Zou, Z. (2022). Ecdysone signaling mediates the trade-off between immunity and reproduction via suppression of amyloids in the mosquito *Aedes aegypti*. *PLoS Pathogens*, 18(9), e1010837. <https://doi.org/10.1371/journal.ppat.1010837>
- Wang, P. H., Gu, Z. H., Wan, D. H., Zhu, W. bin, Qiu, W., Chen, Y. G., Weng, S. P., Yu, X. Q., & He, J. G. (2013). *Litopenaeus vannamei* Toll-interacting protein (LvTollip) is a potential negative regulator of the shrimp Toll pathway involved in the regulation of the shrimp antimicrobial peptide gene penaeidin-4 (PEN4). *Developmental & Comparative Immunology*, 40(3–4), 266–277. <https://doi.org/10.1016/J.DCI.2013.02.011>
- Werner, T., Borge-Renberg, K., Mellroth, P., Steiner, H., & Hultmark, D. (2003). Functional diversity of the *Drosophila* PGRP-LC gene cluster in the response to lipopolysaccharide and peptidoglycan. *The Journal of Biological Chemistry*, 278(29), 26319–26322. <https://doi.org/10.1074/jbc.C300184200>
- Westra, E. R., van Houte, S., Oyesiku-Blakemore, S., Makin, B., Broniewski, J. M., Best, A., Bondy-Denomy, J., Davidson, A., Boots, M., & Buckling, A. (2015). Parasite Exposure Drives Selective Evolution of Constitutive versus Inducible Defense. *Current Biology*, 25(8), 1043–1049. <https://doi.org/10.1016/j.cub.2015.01.065>
- Whalen, A. M., & Steward, R. (1993). Dissociation of the dorsal-cactus complex and phosphorylation of the dorsal protein correlate with the nuclear localization of dorsal. *The Journal of Cell Biology*, 123(3), 523. <https://doi.org/10.1083/JCB.123.3.523>
- WHITTEN, M. M. A., SHIAO, S. H., & LEVASHINA, E. A. (2006). Mosquito midguts and malaria: cell biology, compartmentalization and immunology. *Parasite Immunology*, 28(4), 121–130. <https://doi.org/10.1111/j.1365-3024.2006.00804.x>
- Williams, A. M., Ngo, T. M., Figueroa, V. E., & Tate, A. T. (2023). The Effect of Developmental Pleiotropy on the Evolution of Insect Immune Genes. *Genome Biology and Evolution*, 15(3). <https://doi.org/10.1093/GBE/EVAD044>
- Witzel, F., Maddison, L., & Blüthgen, N. (2012). How scaffolds shape MAPK signaling: what we know and opportunities for systems approaches. *Frontiers in Physiology*, 3, 475. <https://doi.org/10.3389/fphys.2012.00475>
- Wu, S., Zhang, X., He, Y., Shuai, J., Chen, X., & Ling, E. (2010). Expression of antimicrobial peptide genes in *Bombyx mori* gut modulated by oral bacterial infection and development. *Developmental & Comparative Immunology*, 34(11), 1191–1198. <https://doi.org/10.1016/j.dci.2010.06.013>
- Yassour, M., Vatanen, T., Siljander, H., Hämäläinen, A.-M., Härkönen, T., Ryhänen, S. J., Franzosa, E. A., Vlamakis, H., Huttenhower, C., Gevers, D., Lander, E. S., Knip, M., & Xavier, R. J. (2016). Natural history of the infant gut microbiome and impact of antibiotic treatment on bacterial strain diversity and stability. *Science Translational Medicine*, 8(343). <https://doi.org/10.1126/scitranslmed.aad0917>
- Ye, J., Coulouris, G., Zaretskaya, I., Cutcutache, I., Rozen, S., & Madden, T. L. (2012a). Primer-BLAST: a tool to design target-specific primers for polymerase chain reaction. *BMC Bioinformatics*, 13(1), 134. <https://doi.org/10.1186/1471-2105-13-134>

- Ye, J., Coulouris, G., Zaretskaya, I., Cutcutache, I., Rozen, S., & Madden, T. L. (2012b). Primer-BLAST: A tool to design target-specific primers for polymerase chain reaction. *BMC Bioinformatics*, *13*(1), 134. <https://doi.org/10.1186/1471-2105-13-134>
- Yokoi, K., Ito, W., Kato, D., & Miura, K. (2022). RNA interference-based characterization of Caspar, DREDD and FADD genes in immune signaling pathways of the red flour beetle, *Tribolium castaneum* (Coleoptera: Tenebrionidae). *European Journal of Entomology*, *119*, 23–35. <https://doi.org/10.14411/eje.2022.003>
- Yokoi, K., Koyama, H., Ito, W., Minakuchi, C., Tanaka, T., & Miura, K. (2012a). Involvement of NF- κ B transcription factors in antimicrobial peptide gene induction in the red flour beetle, *Tribolium castaneum*. *Developmental & Comparative Immunology*, *38*(2), 342–351. <https://doi.org/10.1016/j.dci.2012.06.008>
- Yokoi, K., Koyama, H., Ito, W., Minakuchi, C., Tanaka, T., & Miura, K. (2012b). Involvement of NF- κ B transcription factors in antimicrobial peptide gene induction in the red flour beetle, *Tribolium castaneum*. *Developmental & Comparative Immunology*, *38*(2), 342–351. <https://doi.org/10.1016/J.DCI.2012.06.008>
- Yokoi, K., Koyama, H., Ito, W., Minakuchi, C., Tanaka, T., & Miura, K. (2012c). Involvement of NF- κ B transcription factors in antimicrobial peptide gene induction in the red flour beetle, *Tribolium castaneum*. *Developmental & Comparative Immunology*, *38*(2), 342–351. <https://doi.org/10.1016/j.dci.2012.06.008>
- Yokoi, K., Koyama, H., Minakuchi, C., Tanaka, T., & Miura, K. (2012a). Antimicrobial peptide gene induction, involvement of Toll and IMD pathways and defense against bacteria in the red flour beetle, *Tribolium castaneum*. *Results in Immunology*, *2*, 72–82. <https://doi.org/10.1016/j.rinim.2012.03.002>
- Yokoi, K., Koyama, H., Minakuchi, C., Tanaka, T., & Miura, K. (2012b). Antimicrobial peptide gene induction, involvement of Toll and IMD pathways and defense against bacteria in the red flour beetle, *Tribolium castaneum*. *Results in Immunology*, *2*, 72–82. <https://doi.org/10.1016/j.rinim.2012.03.002>
- Zhai, Z., Huang, X., & Yin, Y. (2018). Beyond immunity: The Imd pathway as a coordinator of host defense, organismal physiology and behavior. *Developmental & Comparative Immunology*, *83*, 51–59. <https://doi.org/10.1016/J.DCI.2017.11.008>
- Zhang, G., & Ghosh, S. (2002a). Negative Regulation of Toll-like Receptor-mediated Signaling by Tollip. *Journal of Biological Chemistry*, *277*(9), 7059–7065. <https://doi.org/10.1074/jbc.M109537200>
- Zhang, G., & Ghosh, S. (2002b). Negative regulation of toll-like receptor-mediated signaling by Tollip. *The Journal of Biological Chemistry*, *277*(9), 7059–7065. <https://doi.org/10.1074/jbc.M109537200>
- Zhong, K., & Tate, A. T. (2023). Characterizing Negative Regulation of Immune Signaling Pathways in *Tribolium castaneum*. *Bachelor's Thesis, Vanderbilt University*.
- Zhou, B., Lindsay, S. A., & Wasserman, S. A. (2015). Alternative NF- κ B Isoforms in the *Drosophila* Neuromuscular Junction and Brain. *PLOS ONE*, *10*(7), e0132793. <https://doi.org/10.1371/journal.pone.0132793>
- Zhu, L., Peng, D., Wang, Y., Ye, W., Zheng, J., Zhao, C., Han, D., Geng, C., Ruan, L., He, J., Yu, Z., & Sun, M. (2015). Genomic and transcriptomic insights into the efficient entomopathogenicity of *Bacillus thuringiensis*. *Scientific Reports*, *5*(1), 14129. <https://doi.org/10.1038/srep14129>
- Zou, Z., Evans, J. D., Lu, Z., Zhao, P., Williams, M., Sumathipala, N., Hetru, C., Hultmark, D., & Jiang, H. (2007a). Comparative genomic analysis of the *Tribolium* immune system. *Genome Biology*, *8*(8), R177. <https://doi.org/10.1186/gb-2007-8-8-r177>
- Zou, Z., Evans, J. D., Lu, Z., Zhao, P., Williams, M., Sumathipala, N., Hetru, C., Hultmark, D., & Jiang, H. (2007b). Comparative genomic analysis of the *Tribolium* immune system. *Genome Biology*, *8*(8), R177. <https://doi.org/10.1186/gb-2007-8-8-r177>

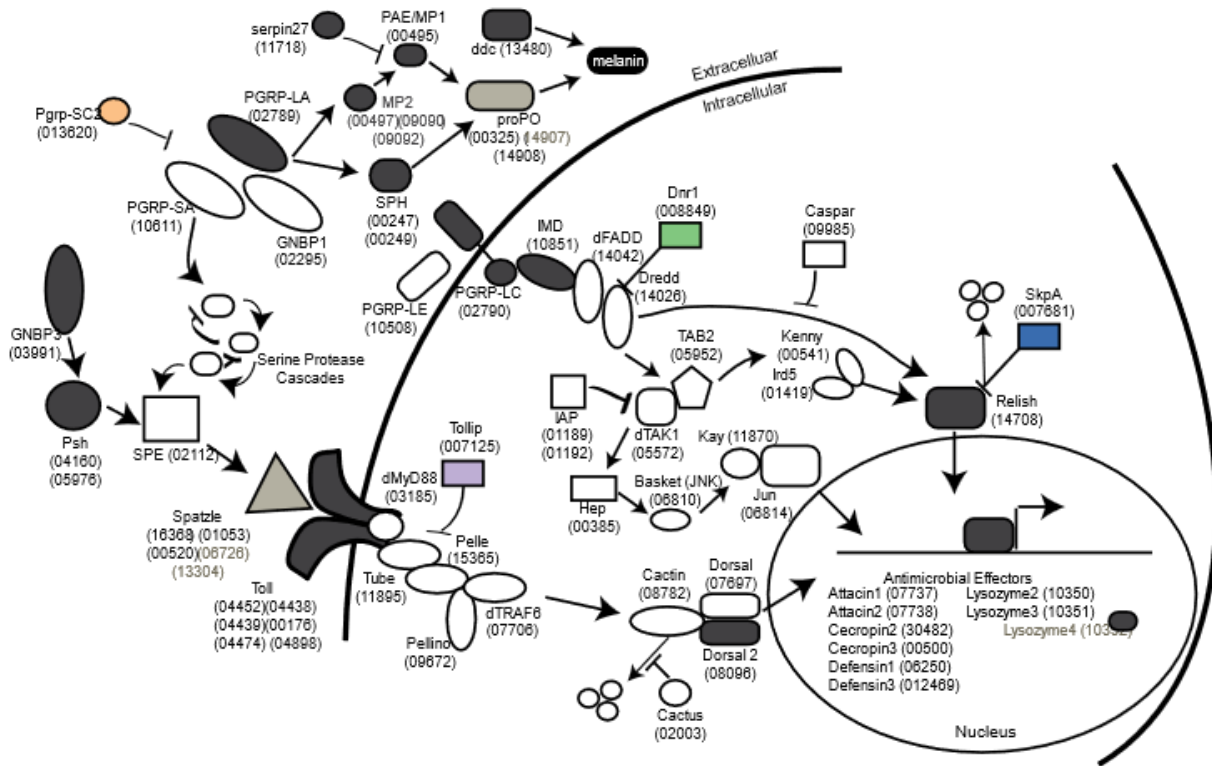
Appendix A

A. The impact of life stage parasite exposure and their interaction on gene expression in the gut and whole body. P values adjusted via Benjamini-Hochberg method to account for false discovery rate. Values in bold are significant after adjustment. Uninfected larvae serve as the level of comparison for all tests. Exposure refers to gregarine exposure.

		<i>Gut</i>					<i>Whole Body</i>				
		Estimate	Error	t val	Pval	Padj	Estimate	Error	t val	Pval	Padj
Defensin-1	Intercept	-19.0	1.08	-17.6	< 2e-16		-19.6	0.60	-32.6	< 2e-16	
	Pupa	7.52	1.53	4.93	3.1E-05	0.0007	4.90	0.81	6.08	1.7E-07	3.3E-06
	Adult	-1.38	1.45	-0.96	0.35	0.54	-0.12	0.81	-0.15	0.88	0.95
	Exposure	-3.67	1.39	-2.64	0.013	0.052	-0.76	0.85	-0.90	0.37	0.75
	Pupa*Exp.	1.89	1.94	0.97	0.34	0.54	1.48	1.14	1.30	0.20	0.50
	Adult*Exp.	4.24	1.84	2.30	0.029	0.082	-0.69	1.14	-0.60	0.55	0.84
Pgrp-LC	Intercept	-17.2	0.50	-34.3	< 2e-16		-19.9	0.27	-74.5	< 2e-16	
	Pupa	-0.39	0.71	-0.55	0.58	0.67	1.44	0.36	4.03	0.000192	0.00077
	Adult	2.25	0.67	3.35	0.002	0.015	1.85	0.36	5.19	3.9E-06	5.2E-05
	Exposure	-2.35	0.65	-3.64	0.001	0.0084	-0.19	0.38	-0.49	0.62	0.86
	Pupa*Exp.	1.60	0.90	1.78	0.086	0.19	0.26	0.51	0.51	0.61	0.86
	Adult*Exp.	1.05	0.85	1.23	0.23	0.40	0.31	0.51	0.61	0.55	0.84
pgrp-LA	Intercept	-19.8	1.12	-17.7	<2e-16		-20.8	0.38	-54.9	< 2e-16	
	Pupa	3.01	1.58	1.91	0.067	0.16	2.06	0.51	4.04	0.000182	0.00077
	Adult	0.94	1.50	0.63	0.53	0.65	2.38	0.51	4.67	2.3E-05	0.00018
	Exposure	-1.21	1.44	-0.84	0.41	0.56	0.03	0.54	0.06	0.96	0.98
	Pupa*Exp.	0.69	2.01	0.34	0.73	0.76	-0.21	0.72	-0.29	0.77	0.90
	Adult*Exp.	1.77	1.91	0.93	0.36	0.54	-0.07	0.72	-0.10	0.92	0.97
duox	Intercept	-19.3	0.62	-31.0	< 2e-16		-24.3	0.42	-57.9	< 2e-16	
	Pupa	-1.70	0.88	-1.93	0.063	0.16	2.43	0.56	4.32	7.4E-05	0.00049
	Adult	2.56	0.83	3.08	0.0045	0.026	2.27	0.56	4.04	0.000	0.00077
	Exposure	-3.91	0.80	-4.88	3.5E-05	0.0007	-0.87	0.59	-1.46	0.15	0.40
	Pupa*Exp.	5.28	1.12	4.73	5.4E-05	0.0007	0.79	0.80	1.00	0.32	0.75
	Adult*Exp.	2.98	1.06	2.81	0.0088	0.039	-0.24	0.80	-0.30	0.76	0.90
pgrp-SC2	Intercept	-18.82	0.87	21.59	<2e-16		-20.72	0.53	39.35	<2e-16	
	Pupa	-1.06	1.23	-0.86	0.40	0.56	0.01	0.71	0.02	0.99	0.99
	Adult	-1.16	1.17	-0.99	0.33	0.34	-0.63	0.71	-0.89	0.38	0.75
	Exposure	-2.92	1.13	-2.60	0.015	0.054	-0.34	0.74	-0.46	0.65	0.87
	Pupa*Exp.	1.21	1.57	0.77	0.45	0.57	0.51	1.00	0.51	0.61	0.86
	Adult*Exp.	3.07	1.49	2.06	0.048	0.078	-0.73	1.00	-0.73	0.47	0.84
tepB	Intercept	-18.9	0.81	-23.4	< 2e-16		-19.9	0.47	-41.9	< 2e-16	
	Pupa	-1.57	1.14	-1.38	0.18	0.34	1.88	0.64	2.95	0.0048	0.015

	Adult	5.04	1.08	4.66	6.6E-05	0.0007	4.26	0.64	6.69	1.8E-08	7.2E-07
	Exposure	-0.97	1.04	-0.93	0.36	0.54	0.28	0.67	0.41	0.68	0.88
	Pupa*Exp.	2.38	1.45	1.64	0.11	0.24	0.31	0.90	0.34	0.73	0.90
	Adult*Exp.	0.15	1.38	0.11	0.92	0.92	-0.57	0.90	-0.64	0.53	0.84
cec3	Intercept	-19.4	1.33	-14.6	6.4E-15		-25.8	0.65	-39.6	< 2e-16	
	Pupa	-0.82	1.87	-0.44	0.66	0.74	4.32	0.87	4.95	8.8E-06	8.8E-05
	Adult	4.38	1.78	2.46	0.020	0.067	3.68	0.87	4.21	0.000105	6.0E-04
	Exposure	-4.91	1.71	-2.87	0.0076	0.038	-0.22	0.92	-0.24	0.81	0.90
	Pupa*Exp.	4.79	2.38	2.01	0.054	0.14	1.11	1.23	0.90	0.37	0.75
	Adult*Exp.	3.56	2.26	1.58	0.13	0.25	-0.92	1.23	-0.75	0.46	0.84
ddc	Intercept	-19.8	1.31	-15.1	3.0E-15		-19.4	0.52	-37.0	< 2e-16	
	Pupa	-1.06	1.86	-0.57	0.57	0.67	2.56	0.70	3.64	0.000649	0.0024
	Adult	0.68	1.76	0.38	0.70	0.76	2.48	0.70	3.53	0.000898	0.0030
	Exposure	-1.38	1.69	-0.82	0.42	0.56	0.19	0.74	0.26	0.79	0.90
	Pupa*Exp.	0.80	2.36	0.34	0.74	0.76	0.68	0.99	0.68	0.50	0.84
	Adult*Exp.	1.50	2.24	0.67	0.51	0.64	-1.61	0.99	-1.62	0.11	0.32

Appendix B



B. A revised representation of the canonical *T. castaneum* Toll and IMD immunological pathways. The targeted potential immune regulating genes for this dissertation are highlighted in color. Figure is adapted from “Dissecting the contributions of time and microbe density to variation in immune gene expression”, Volume: 284, Issue: 1859, DOI: (10.1098/rspb.2017.0727).

Appendix C

C. Combinatorial RNAi efficiently silences target gene expression for all combinations. One-way ANOVA – aov(dct ~ treatment) and Tukey HSD was conducted in R for analysis.

Gene comparison	diff	lwr	upr	Pval adjusted
malE-dnr1	-2.11	-3.13	-1.10	2.03E-04
tollip+dnr1-dnr1	0.01	-1.00	1.03	1.00
tollip+dnr1-malE	2.13	1.11	3.14	1.90E-04
pgrp-sc2-malE	2.62	1.41	3.84	1.43E-04
tollip+pgrp-sc2-malE	2.94	1.73	4.16	4.18E-05
tollip+pgrp-sc2-pgrp-sc2	0.32	-0.90	1.54	0.78
tollip-malE	2.34	1.01	3.66	4.48E-04
tollip+dnr1-malE	2.75	1.42	4.08	6.41E-05
tollip+pgrp-sc2-malE	2.47	1.15	3.80	2.30E-04
tollip+dnr1-tollip	0.41	-0.92	1.74	0.82
tollip+pgrp-sc2-tollip	0.14	-1.19	1.47	0.99
tollip+pgrp-sc2-tollip+dnr1	-0.27	-1.60	1.06	0.94

Appendix D

D. Combinatorial RNAi does not significantly alter *defensin-2* or *cecropin-2* transcript abundance.

For *cec-2*, Δ ct values were non-parametrically distributed, thus a Kruskal-Wallis test was run to determine significance. For *def-2*, a parametric one-way ANOVA – aov(dct ~ treatment) was run in R with a post-hoc Tukey test for multiple comparisons.

	RNAi treatment	diff	lwr	upr	Pval adjusted
<i>def-2</i>	malE-dnr1	-1.11	-4.33	2.10	0.90
	pgrp-sc2-dnr1	-0.87	-4.08	2.35	0.96
	tollip-dnr1	-1.05	-4.26	2.16	0.92
	tollip+dnr1-dnr1	0.09	-3.12	3.31	1.00
	tollip+pgrp-sc2-dnr1	1.16	-2.06	4.37	0.88
	pgrp-sc2-malE	0.25	-2.97	3.46	1.00
	tollip-malE	0.06	-3.15	3.28	1.00
	tollip+dnr1-malE	1.21	-2.01	4.42	0.86
	tollip+pgrp-sc2-malE	2.27	-0.94	5.48	0.29
	tollip-pgrp-sc2	-0.18	-3.40	3.03	1.00
	tollip+dnr1-pgrp-sc2	0.96	-2.25	4.18	0.94
	tollip+pgrp-sc2-pgrp-sc2	2.02	-1.19	5.24	0.41
	tollip+dnr1-tollip	1.14	-2.07	4.36	0.88
	tollip+pgrp-sc2-tollip	2.21	-1.01	5.42	0.32
	tollip+pgrp-sc2-tollip+dnr1	1.06	-2.15	4.28	0.91
	<i>cec-2</i>	X²	df	Pval	
0.13		1	0.72		

Appendix E

E. Effect of *dnr1* RNAi (500 ng) on knockdown efficiency and AMP Gene expression to *Bacillus thuringiensis* Infection in Red Flour Beetles compared to MalE control. Linear models (expression ~ treatment*hour) conducted with "lm" function in R. Expression values are on a log scale. For AMP genes, P Values less than the significance threshold after correcting for multiple testing (Bonferroni method; $\alpha = 0.0167$) are in bold.

Gene	Factor	Estimate	Std. Error	t value	Pval
Induction (hours 0-12)					
<i>dnr1</i>	Intercept	-7.02	0.12	-57.01	< 2e-16
	treatment	2.01	0.17	11.54	< 2e-16
	hour	0.07	0.02	3.52	6.66E-04
	treatment*hour	-0.03	0.03	-1.07	0.29
<i>attacin-1</i>	Intercept	-7.33	0.51	-14.46	< 2e-16
	treatment	0.30	0.72	0.42	0.68
	hour	0.27	0.08	3.54	5.81E-04
	treatment*hour	0.03	0.11	0.30	0.76
<i>defensin-2</i>	Intercept	-4.98	0.46	-10.80	< 2e-16
	treatment	0.14	0.65	0.21	0.83
	hour	0.52	0.07	7.57	9.54E-12
	treatment*hour	-0.01	0.10	-0.07	0.94
<i>cecropin-2</i>	Intercept	-10.95	0.28	-39.08	< 2e-16
	treatment	0.84	0.40	2.11	0.04
	hour	0.24	0.04	5.71	8.69E-08
	treatment*hour	-0.01	0.06	-0.15	0.88
<hr/>					
Decay (hours 12-48)					
<i>dnr1</i>	Intercept	-6.35	0.17	-36.44	< 2e-16
	treatment	1.73	0.25	7.03	1.27E-09
	hour	-0.01	0.01	-1.21	0.23
	treatment*hour	0.01	0.01	0.66	0.51
<i>attacin-1</i>	Intercept	-6.85	0.79	-8.70	1.17E-12
	treatment	0.92	1.11	0.83	0.41
	hour	0.05	0.02	1.86	0.07
	treatment*hour	-0.03	0.04	-0.82	0.42
<i>defensin-2</i>	Intercept	1.23	0.60	2.04	0.05
	treatment	-0.88	0.85	-1.04	0.30
	hour	-0.14	0.02	-7.15	7.60E-10
	treatment*hour	0.04	0.03	1.60	0.11

<i>cecropin-2</i>	Intercept	-8.33	0.54	-15.40	< 2e-16
	treatment	0.47	0.77	0.61	0.54
	hour	-0.06	0.02	-3.30	1.52E-03
	treatment*hour	0.04	0.02	1.50	0.14
Constitutive (hour 0)					
<i>dnr1</i>	Intercept	-6.58	0.14	-47.50	< 2e-16
	treatment	2.05	0.20	10.46	5.31E-10
<i>defensin-2</i>	Intercept	-6.64	0.34	-19.72	1.80E-15
	treatment	0.48	0.48	1.01	0.33
<i>cecropin-2</i>	Intercept	-10.49	0.40	-25.92	<2e-16
	treatment	0.67	0.57	1.17	0.26
<i>attacin-1</i>	Intercept	-8.64	0.22	-38.47	<2e-16
	treatment	0.73	0.32	2.31	0.03
Resolution (hour 48)					
<i>dnr1</i>	Intercept	-6.52	0.09	-74.24	< 2e-16
	treatment	1.92	0.12	15.47	2.64E-13
<i>defensin-2</i>	Intercept	-5.07	0.32	-16.02	1.29E-13
	treatment	1.33	0.45	2.97	7.10E-03
<i>cecropin-2</i>	Intercept	-10.68	0.36	-29.42	< 2e-16
	treatment	2.12	0.51	4.14	4.30E-04
<i>attacin-1</i>	Intercept	-4.09	0.33	-12.42	2.04E-11
	treatment	-0.34	0.47	-0.74	0.47

Appendix F

F. Effect of pgrp-sc2 or tollip RNAi (500ng) on knockdown efficiency and AMP Gene expression to *Bacillus thuringiensis* Infection in Red Flour Beetle guts compared to MalE control. Linear models (expression ~ treatment*hour) conducted with "lm" function in R. Expression values are on a log scale. For AMP genes, P Values less than the significance threshold after correcting for multiple testing (Bonferroni method; $\alpha = 0.0167$) are in bold. * Induction for cecropin-2 ends at 8 hours post infection.

Gene	Factor	Estimate	Std. Error	t value	Pval
Induction (hours 0-12)					
<i>pgrp-sc2</i>	Intercept	-7.0623	0.54616	-12.931	1.42E-12
	treatment	-1.4848	0.77239	-1.922	0.07
	hour	0.91381	0.18697	4.888	4.99E-05
	treatment*hour	0.06095	0.26878	0.227	0.82
<i>tollip</i>	Intercept	-6.3653	0.32042	-19.866	< 2e-16
	treatment	-1.2469	0.43465	-2.869	7.13E-03
	hour	0.02101	0.05123	0.41	0.68
	treatment*hour	-0.0509	0.07076	-0.72	0.48
<i>defensin-2</i>	Intercept	-9.19	0.86	-10.67	1.74E-14
	treatment (pgrp)	-1.36	1.23	-1.11	0.27
	treatment (tollip)	-0.65	1.20	-0.54	0.59
	hour	0.34	0.14	2.42	0.02
	treatment(pgrp)*hour	0.20	0.20	1.01	0.32
<i>thaumatin-1</i>	treatment(tollip)*hour	0.2064	0.1978	1.044	0.30
	Intercept	-7.72	0.75	-10.28	6.27E-14
	treatment (pgrp)	-0.27	1.07	-0.25	0.80
	treatment (tollip)	0.62	1.04	0.60	0.55
	hour	0.48	0.12	3.91	2.76E-04
	treatment(pgrp)*hour	-0.14	0.17	-0.79	0.44
<i>cecropin-2</i>	treatment(tollip)*hour	-0.02	0.17	-0.14	0.89
	Intercept	-6.33	0.60	-10.470	2.63E-14
	treatment (pgrp)	-0.27	0.88	-0.304	0.76
	treatment (tollip)	-0.08	0.86	-0.09	0.93
	hour	0.11	0.10	1.07	0.29
	treatment(pgrp)*hour	0.10	0.15	0.66	0.51
	treatment(tollip)*hour	0.06	0.14	0.44	0.66
Decay (hours 8-48)					
<i>pgrp-sc2</i>	Intercept	-3.376	1.38131	-2.444	0.02
	treatment	-3.6351	1.99375	-1.823	0.08
	hour	-0.073	0.03715	-1.965	0.06
	treatment*hour	0.09687	0.05254	1.844	0.08
<i>tollip</i>	Intercept	-5.6347	0.634929	-8.875	1.75E-10
	treatment	-1.9206	0.892813	-2.151	0.04
	hour	-0.0213	0.018958	-1.124	0.27

	treatment*hour	0.00483	0.026326	0.184	0.86
<i>defensin-2</i>	Intercept	-3.85	1.48	-2.61	1.18E-02
	treatment (pgrp)	-1.73	2.11	-0.82	0.42
	treatment (tollip)	-0.95	2.07	-0.46	0.65
	hour	-0.15	0.04	-3.32	1.68E-03
	treatment(pgrp)*hour	0.08	0.06	1.35	0.18
	treatment(tollip)*hour	0.06229	0.06116	1.018	0.31
<i>thaumatin-1</i>	Intercept	-1.39	1.17	-1.19	0.24
	treatment (pgrp)	-3.14	1.67	-1.88	0.07
	treatment (tollip)	-0.43	1.64	-0.26	0.79
	hour	-0.10	0.03	-2.78	7.55E-03
	treatment(pgrp)*hour	0.11	0.05	2.14	0.04
	treatment(tollip)*hour	0.04	0.05	0.86	0.39
<i>cecropin-2</i>	Intercept	-2.53	0.93	-2.705	9.27E-03
	treatment (pgrp)	-0.26	1.33	-0.197	0.84
	treatment (tollip)	-0.88	1.31	-0.67	0.51
	hour	-0.09	0.03	-3.25	2.03E-03
	treatment(pgrp)*hour	0.02	0.04	0.51	0.61
	treatment(tollip)*hour	0.05	0.04	1.19	0.24
Constitutive					
(hour 0)					
<i>pgrp-sc2</i>	Intercept	-5.1129	0.6192	-8.257	7.28E-09
	treatment	-1.4848	0.8912	-1.666	0.11
<i>tollip</i>	Intercept	-6.2719	0.2207	-28.42	< 2e-16
	treatment	-1.46	0.308	-4.741	3.50E-05
<i>defensin-2</i>	Intercept	-7.75	0.79	-9.76	1.94E-13
	treatment(pgrp)	-0.50	1.14	-0.44	0.66
	treatment(tollip)	0.11	1.12	0.10	0.92
<i>thaumatin-1</i>	Intercept	-5.6893	0.6977	-8.155	6.34E-11
	treatment(pgrp)	-0.8427	1.0003	-0.842	0.40
	treatment(tollip)	0.429	0.9867	0.435	0.67
<i>cecropin-2</i>	Intercept	-5.89	0.47	-12.64	<2e-16
	treatment(pgrp)	0.16	0.68	0.24	0.81
	treatment(tollip)	0.1726	0.67	0.26	0.80
Resolution					
(hour 48)					
<i>pgrp-sc2</i>	Intercept	-6.881	0.816	-8.432	1.25E-06
	treatment	1.015	1.117	0.908	0.38
<i>tollip</i>	Intercept	-6.7471	0.3657	-18.452	1.05E-10
	treatment	-1.5251	0.5007	-3.046	9.37E-03
<i>defensin-2</i>	Intercept	-10.99	1.10	-10.02	5.10E-09
	treatment(pgrp)	2.55	1.55	1.64	0.12
	treatment(tollip)	2.57	1.50	1.71	0.10
<i>thaumatin-1</i>	Intercept	-6.3429	0.7453	-8.511	6.60E-08
	treatment(pgrp)	2.1168	1.054	2.008	0.06
	treatment(tollip)	2.0388	1.0205	1.998	0.06

<i>cecropin-2</i>	Intercept	-7.17	0.79	-9.05	2.56E-08
	treatment(pgrp)	0.96	1.12	0.86	0.40
	treatment(tollip)	1.5647	1.08	1.44	0.17

Appendix G

G. Effect of *pgrp-sc2*, *dnr1*, or *skpA* RNAi (500ng) on knockdown efficiency and AMP Gene expression to *Bacillus thuringiensis* Infection in Red Flour Beetles compared to MalE control after a 10-day incubation period. Linear models (expression ~ treatment*hour) conducted with "lm" function in R. Expression values are on a log scale. For AMP genes, P Values less than the significance threshold after correcting for multiple testing (Bonferroni method; $\alpha = 0.0167$) are in bold.

Gene Induction (hours 0- 12)	Factor	Estimate	Std. Error	t value	Pval
<i>pgrp-sc2</i>	Intercept	-6.507	0.5664	-11.488	1.06E-12
	treatment	-1.7708	0.7922	-2.235	0.03
	hour	0.2845	0.152	1.872	0.07
	treatment*hour	-0.1608	0.2148	-0.749	0.46
<i>skpA</i>	Intercept	-2.08408	0.18929	-11.01	3.07E-12
	treatment	-5.30403	0.26476	-20.033	< 2e-16
	hour	0.05051	0.0508	0.994	0.33
	treatment*hour	0.05764	0.07177	0.803	0.43
<i>dnr1</i>	Intercept	-4.58207	0.25518	-17.956	< 2e-16
	treatment	-1.55156	0.35692	-4.347	1.38E-04
	hour	-0.27953	0.06849	-4.081	2.91E-04
	treatment*hour	0.13185	0.09675	1.363	0.18
<i>defensin-2</i>	Intercept	-4.79	0.72	-6.69	6.79E-09
	treatment (<i>pgrp</i>)	1.52	1.00	1.51	0.14
	treatment (<i>dnr1</i>)	1.68	1.00	1.68	0.10
	treatment (<i>skpA</i>)	2.80	1.00	2.79	6.91E-03
	hour	0.52	0.19	2.70	8.84E-03
	treatment(<i>pgrp</i>)*hour	0.12	0.27	0.43	0.67
	treatment(<i>dnr1</i>)*hour	-0.2147	0.2715	-0.791	0.43
treatment(<i>skpA</i>)*hour	-0.4157	0.2715	-1.531	0.13	
<i>cecropin-2</i>	Intercept	-8.06	0.61	-13.301	< 2e-16
	treatment (<i>pgrp</i>)	-0.02	0.85	-0.026	0.98
	treatment (<i>dnr1</i>)	0.32	0.85	0.37	0.71
	treatment (<i>skpA</i>)	-3.66	0.85	-4.31	5.78E-05
	hour	0.06	0.16	0.37	0.72
	treatment(<i>pgrp</i>)*hour	0.18	0.23	0.78	0.44
	treatment(<i>dnr1</i>)*hour	0.02	0.23	0.09	0.93
treatment(<i>skpA</i>)*hour	0.01	0.23	0.06	0.95	
Decay (hours 8-48)					
<i>pgrp-sc2</i>	Intercept	-5.65696	0.48149	-11.749	3.69E-15
	treatment	-2.78793	0.68093	-4.094	1.78E-04
	hour	-0.03932	0.01741	-2.259	2.89E-02
	treatment*hour	-0.0037	0.02462	-0.15	0.88
<i>skpA</i>	Intercept	-1.89668	0.268785	-7.056	1.07E-08

	treatment	-4.6134	0.382437	-12.063	2.17E-15
	hour	-0.0048	0.009718	-0.494	0.62
	treatment*hour	-0.04407	0.014158	-3.112	3.30E-03
<i>dnr1</i>	Intercept	-5.82291	0.27984	-20.808	< 2e-16
	treatment	-1.29185	0.39817	-3.245	2.28E-03
	hour	0.02372	0.01012	2.345	2.37E-02
	treatment*hour	-0.03328	0.01474	-2.257	2.91E-02
<i>defensin-2</i>	Intercept	-2.22	0.63	-3.54	6.52E-04
	treatment (pgrp)	1.29	0.89	1.45	0.15
	treatment (dnr1)	0.96	0.89	1.08	0.29
	treatment (skpA)	1.19	0.89	1.33	0.19
	hour	-0.07	0.02	-3.26	1.62E-03
	treatment(pgrp)*hour	-0.03	0.03	-0.90	0.37
	treatment(dnr1)*hour	-0.00167	0.033016	-0.05	0.96
	treatment(skpA)*hour	0.019931	0.033016	0.604	0.55
<i>cecropin-2</i>	Intercept	-7.35	0.57	-12.937	< 2e-16
	treatment (pgrp)	1.10	0.80	1.369	0.18
	treatment (dnr1)	-0.08	0.81	-0.10	0.92
	treatment (skpA)	-4.09	0.81	-5.06	2.34E-06
	hour	-0.02	0.02	-1.09	0.28
	treatment(pgrp)*hour	-0.04	0.03	-1.46	0.15
	treatment(dnr1)*hour	-0.01	0.03	-0.25	0.80
	treatment(skpA)*hour	-0.02	0.03	-0.54	0.59

**Constitutive (hour
0)**

<i>pgrp-sc2</i>	Intercept	-7.3818	0.3794	-19.459	2.81E-09
	treatment	-1.481	0.5365	-2.761	0.02
<i>skpA</i>	Intercept	-2.1152	0.2176	-9.721	2.06E-06
	treatment	-5.1796	0.3077	-16.832	1.15E-08
<i>dnr1</i>	Intercept	-4.7962	0.2283	-21.012	1.32E-09
	treatment	-1.3595	0.3228	-4.212	1.80E-03
<i>defensin-2</i>	Intercept	-5.59	0.75	-7.42	3.68E-07
	treatment(pgrp)	1.71	1.07	1.61	0.12
	treatment(dnr1)	1.40	1.07	1.32	0.20
	treatment(skpA)	3.12	1.07	2.93	0.01
<i>cecropin-2</i>	Intercept	-7.65	0.78	-9.86	4.01E-09
	treatment(pgrp)	0.47	1.10	0.43	0.68
	treatment(dnr1)	0.1627	1.10	0.15	0.88
	treatment(skpA)	-3.6066	1.10	-3.29	0.00

**Resolution (hour
48)**

<i>pgrp-sc2</i>	Intercept	-7.5185	0.539	-13.949	7.01E-08
	treatment	-2.8404	0.7622	-3.726	0.00
<i>skpA</i>	Intercept	-2.0322	0.5698	-3.567	6.06E-03
	treatment	-6.8651	0.8451	-8.123	1.96E-05
<i>dnr1</i>	Intercept	-4.9006	0.1898	-25.817	9.46E-10

	treatment	-2.7257	0.2815	-9.681	4.68E-06
<i>defensin-2</i>	Intercept	-5.80	0.37	-15.85	5.10E-12
	treatment(pgrp)	0.24	0.52	0.46	0.65
	treatment(dnr1)	0.91	0.54	1.68	0.11
	treatment(skipA)	2.47	0.54	4.56	0.00
<i>cecropin-2</i>	Intercept	-8.24	0.69	-11.89	5.86E-10
	treatment(pgrp)	-1.21	0.98	-1.23	0.23
	treatment(dnr1)	-0.06952	1.03	-0.07	0.95
	treatment(skipA)	-4.85045	1.03	-4.72	0.00

Appendix H

H. Primer list for chapter III.

Type	Name	Forward primer sequence (5'-3')	Reverse primer sequence (5'-3')
dsRNA	<i>pgrp-sc2</i>	taatacgactcactatagggTCAAAATGTTCCGACTGGTG	taatacgactcactatagggCGTCCATCCACCAATTCAT
dsRNA	<i>tollip</i>	taatacgactcactatagggTGCGTTTACGAGACGCATAC	taatacgactcactatagggCGTCTTTATTGCCCCTGTTG
dsRNA	<i>dnr1</i>	taatacgactcactatagggTTCGGAGAGGAGACGTTTAC	taatacgactcactatagggTGCCGTTGTAGTCGAGATTG
dsRNA	<i>skpA</i>	taatacgactcactatagggACAAGGAGAAACGCACGGAT	taatacgactcactatagggCCAGGACGTGGCTGTACTTT
dsRNA	<i>malE</i> - (E. coli)	taatacgactcactatagggATTGCTGCTGACGGGGGTTAT	taatacgactcactatagggATGTTCCGGCATGATTCACCTTT
qPCR	<i>pgrp-sc2</i>	CAAGGGAGCAGGACCAGTTG	GCGTCAAAATGCGTCCATCC
qPCR	<i>tollip</i>	GAAAGGCCGAAGTCGGGTCC	GCAGTGCTATGGCTGTTTGG
qPCR	<i>dnr1</i>	GTCGTTTTTCGAAGTCCGGGT	TCACGAATTCGCACACCTTCT
qPCR	<i>skpA</i>	GGTGAAACGTTTCGAGGTGGA	GAGGCACCACTTCCTCTTCC
qPCR	<i>RPS18s</i> (ribosomal protein)	CGAAGAGGTCGAGAAAATCG	CGTGGTCTTGGTGTGTTGAC
qPCR	<i>defensin-2</i> (IMD AMP)	GCTTTTCTACAGATGGAGAACAC	AAAGAGGCAATGGGTGCAC
qPCR	<i>thaumatin-1</i> (Toll AMP)	TTGCAATCACTGCTTACCCAC	ACCCGGATATGTGCCACTTG
qPCR	<i>cecropin-2</i> (Toll AMP)	TAATGTGTTTTGTTCAAGTGATGGC	CAGCTCCTTCGGCCCACT
qPCR	<i>attacin-1</i> (IMD AMP)	GACTTTCTGGTCTGTAAGTACTGACA	ACTTCAGCACTAAAGGGCGGA

Appendix I

I. Effect of *cactus* RNAi (250ng) on knockdown efficiency and AMP gene expression to *Bacillus thuringiensis* infection in flour beetles compared to MalE control. Linear models (expression ~ RNAi treatment*time) conducted with "lm" function in R. Time denotes the hours passed post microbial challenge. Expression values are on a log scale. For AMP genes, P values less than the significance threshold after correcting for multiple testing (Bonferroni method; $\alpha = 0.0167$) are in bold. * Induction for cecropin-2 ends at 8 times post infection.

Gene	Factor	Estimate	Std. Error	Tval	Pval
<i>cactus</i>	Intercept	-12.53	0.16	-78.85	< 2e-16
	RNAi treatment	0.87	0.22	3.90	1.44E-04
	time	-0.06	0.01	-8.05	2.12E-13
	RNAi*time	0.00	0.01	-0.47	0.64
Induction (times 0-6)					
<i>defensin-2</i>	Intercept	-8.76	0.60	-14.72	< 2e-16
	RNAi treatment	-3.95	0.84	-4.73	1.43E-05
	time	-3.95	0.84	-4.73	1.43E-05
	RNAi*time	0.92	0.22	4.15	1.09E-04
<i>defensin-3</i>	Intercept	-13.64	0.50	-27.25	< 2e-16
	RNAi treatment	-2.65	0.70	-3.77	3.81E-04
	time	-0.14	0.13	-1.05	0.30
	RNAi*time	0.61	0.19	3.25	1.92E-03
<i>cecropin-2*</i>	Intercept	-18.27	0.54	-33.70	< 2e-16
	RNAi treatment	4.71	0.77	6.09	4.41E-08
	time	0.37	0.11	3.32	1.38E-03
	RNAi*time	-0.49	0.16	-3.09	2.78E-03
Decay (times 8-48)					
<i>defensin-2</i>	Intercept	-8.78	0.42	-21.13	< 2e-16
	RNAi treatment	0.37	0.59	0.63	0.53
	time	-0.11	0.02	-7.47	4.63E-11
	RNAi*time	-0.05	0.02	-2.19	0.031
<i>defensin-3</i>	Intercept	-14.38	0.40	-35.68	< 2e-16
	RNAi treatment	-0.11	0.57	-0.20	0.84
	time	-0.07	0.02	-4.41	2.49E-05
	RNAi*time	-0.08	0.02	-3.44	8.28E-04
<i>cecropin-2</i>	Intercept	-14.46	0.50	-28.79	< 2e-16
	RNAi treatment	-0.85	0.72	-1.19	0.24
	time	-0.02	0.02	-1.16	0.25
	RNAi*time	-0.09	0.03	-3.34	1.20E-03
Constitutive (time 0)					
<i>cactus</i>	Intercept	-12.02	0.41	-29.33	5.70E-14
	RNAi treatment	0.56	0.58	0.96	0.35
<i>defensin-2</i>	Intercept	-8.85	0.57	-15.59	3.06E-10
	treatment	-5.68	0.80	-7.08	5.54E-06
<i>defensin-3</i>	Intercept	-13.69	0.45	-30.27	3.69E-14

<i>cecropin-2</i>	RNAi treatment	-3.41	0.64	-5.33	1.06E-04
	Intercept	-15.79	0.57	-27.76	1.22E-13
	treatment	-4.32	0.80	-5.37	9.84E-05
Resolution (time 48)					
<i>cactus</i>	Intercept	-14.93	0.20	-73.51	< 2e-16
	RNAi treatment	0.76	0.29	2.65	1.92E-02
<i>defensin-2</i>	Intercept	-14.12	0.50	-28.25	9.54E-14
	RNAi treatment	-1.69	0.71	-2.39	0.03
<i>defensin-3</i>	Intercept	-17.60	0.51	-34.74	5.48E-15
	RNAi treatment	-3.50	0.72	-4.89	2.38E-04
<i>cecropin-2</i>	Intercept	-15.79	0.57	-27.76	1.22E-13
	RNAi treatment	-4.32	0.80	-5.37	9.84E-05

Appendix J

J. Effect of *cactus* RNAi (250ng) on knockdown efficiency and AMP gene expression to *Candida albicans* infection in flour beetles compared to MalE control. Linear models (expression ~ RNAi treatment*time) conducted with "lm" function in R. Time denotes the hours passed post microbial challenge. Expression values are on a log scale. For AMP genes, P values less than the significance threshold after correcting for multiple testing (Bonferroni method; $\alpha = 0.0167$) are in bold. * Induction for cecropin-2 ends at 8 times post infection.

Gene	Factor	Estimate	Std. Error	Tval	Pval
<i>cactus</i>	Intercept	-3.75	0.21	-18.23	< 2e-16
	RNAi				
	treatment	-3.88	0.29	-13.42	< 2e-16
	time	0.01	0.01	1.42	0.16
	RNAi*time	0.00	0.01	0.25	0.81
Induction (times 0-6)					
<i>defensin-2</i>	Intercept	-0.14	0.52	-0.26	0.79
	RNAi				
	treatment	-3.94	0.74	-5.36	1.43E-06
	time	0.10	0.14	0.72	0.47
	RNAi*time	0.67	0.20	3.42	1.14E-03
<i>defensin-3</i>	Intercept	-3.59	0.45	-7.90	8.24E-11
	RNAi				
	treatment	-2.43	0.64	-3.80	3.43E-04
	time	0.03	0.12	0.28	0.78
	RNAi*time	0.26	0.17	1.52	0.13
<i>cecropin-2*</i>	Intercept	-8.83	0.33	-26.65	< 2e-16
	RNAi				
	treatment	5.09	0.47	10.77	< 2e-16
	time	0.28	0.07	4.07	1.17E-04
	RNAi*time	-0.29	0.10	-2.99	3.80E-03
Decay (times 8-48)					
<i>defensin-2</i>	Intercept	0.83	0.38	2.20	0.03
	RNAi				
	treatment	-0.50	0.53	-0.93	0.35
	time	-0.03	0.01	-2.49	1.45E-02
	RNAi*time	-0.04	0.02	-2.11	0.04
<i>defensin-3</i>	Intercept	-3.16	0.38	-8.37	6.09E-13
	RNAi				
	treatment	-0.94	0.53	-1.76	0.08
	time	-0.02	0.01	-1.60	0.11
	RNAi*time	-0.07	0.02	-3.35	1.17E-03
<i>cecropin-2</i>	Intercept	-3.76	0.34	-10.96	< 2e-16
	RNAi				
	treatment	-2.96	0.48	-6.11	2.39E-08

	time	0.01	0.01	1.08	0.29
	RNAi*time	-0.03	0.02	-1.42	0.16
Constitutive (time 0)					
<i>cactus</i>	Intercept	-3.86	0.45	-8.62	5.69E-07
	RNAi				
	treatment	-4.70	0.63	-7.42	3.27E-06
<i>defensin-2</i>	Intercept	-0.37	0.54	-0.68	0.51
	RNAi				
	treatment	-4.90	0.76	-6.44	1.54E-05
<i>defensin-3</i>	Intercept	-3.87	0.44	-8.84	4.22E-07
	RNAi				
	treatment	-3.03	0.62	-4.89	2.37E-04
<i>cecropin-2</i>	Intercept	-3.86	0.45	-8.62	5.69E-07
	RNAi				
	treatment	-4.70	0.63	-7.42	3.27E-06
Resolution (time 48)					
<i>cactus</i>	Intercept	-3.52	0.57	-6.15	2.51E-05
	RNAi				
	treatment	-3.29	0.81	-4.06	1.16E-03
<i>defensin-2</i>	Intercept	-0.96	0.31	-3.10	7.80E-03
	RNAi				
	treatment	-1.69	0.44	-3.86	1.73E-03
<i>defensin-3</i>	Intercept	-4.15	0.52	-8.03	1.30E-06
	RNAi				
	treatment	-3.67	0.73	-5.02	1.87E-04
<i>cecropin-2</i>	Intercept	-3.52	0.57	-6.15	2.51E-05
	RNAi				
	treatment	-3.29	0.81	-4.06	1.16E-03

Appendix K

K. Effect of *cactus* RNAi dose on knockdown efficiency and AMP gene expression to *Bacillus thuringiensis* infection in flour beetles compared to Male control. Linear models (expression ~ dose*time) conducted with "lm" function in R. Time denotes the hours passed post microbial challenge while dose represents the effect of *cactus* dsRNA per ng. Expression values are on a log scale. P values less than the significance threshold after correcting for multiple testing (Bonferroni method; $\alpha = 0.0167$) are in bold.

Gene	Factor	Estimate	Std. Error	t value	Pval
<i>cactus</i>	Intercept	-2.64	0.06	-46.06	< 2e-16
	dose	0.00	0.00	-3.61	3.89E-04
	time	-0.01	0.00	-4.13	5.50E-05
	dose*time	0.00	0.00	0.27	0.79
Induction (times 0-6)					
<i>defensin-2</i>	Intercept	-2.70	0.36	-7.44	5.20E-11
	dose	0.01	0.00	3.60	5.23E-04
	time	0.48	0.10	4.78	6.51E-06
	dose*time	0.00	0.00	-1.85	0.07
<i>defensin-3</i>	Intercept	-6.24	0.24	-25.82	< 2e-16
	dose	0.01	0.00	3.90	1.85E-04
	time	0.22	0.07	3.30	1.38E-03
	dose*time	0.00	0.00	-1.27	0.21
<i>cecropin-2</i>	Intercept	-8.13	0.34	-23.69	< 2e-16
	dose	0.01	0.00	5.26	9.37E-07
	time	0.10	0.09	1.04	0.30
	dose*time	0.00	0.00	-0.92	0.36
Decay (times 12-48)					
<i>defensin-2</i>	Intercept	0.73	0.35	2.12	0.04
	dose	0.00	0.00	0.66	0.51
	time	-0.07	0.01	-6.71	1.71E-09
	dose*time	0.00	0.00	2.16	0.03
<i>defensin-3</i>	Intercept	-4.96	0.37	-13.55	<2e-16
	dose	0.01	0.00	1.84	0.07
	time	-0.06	0.01	-4.86	4.93E-06
	dose*time	0.00	0.00	1.33	0.19
<i>cecropin-2</i>	Intercept	-6.89	0.51	-13.53	<2e-16
	dose	0.01	0.00	1.27	0.21
	time	-0.01	0.02	-0.63	0.53
	dose*time	0.00	0.00	1.48	0.14
Constitutive (time 0)					
<i>cactus</i>	Intercept	-2.82	0.10	-28.85	<2e-16
	dose	0.00	0.00	-2.22	3.41E-02

<i>defensin-2</i>	Intercept	-3.87	0.43	-9.02	4.76E-10
	dose	0.01	0.00	4.39	1.30E-04
<i>defensin-3</i>	Intercept	-6.67	0.29	-22.98	<2e-16
	dose	0.01	0.00	3.84	5.99E-04
<i>cecropin-2</i>	Intercept	-8.19	0.34	-24.41	<2e-16
	dose	0.02	0.00	5.94	1.67E-06
Resolution (time 48)					
<i>cactus</i>	Intercept	-3.22	0.09	-34.65	<2e-16
	dose	0.00	0.00	-1.14	0.26
<i>defensin-2</i>	Intercept	-2.52	0.31	-8.23	3.47E-09
	dose	0.01	0.00	4.08	3.10E-04
<i>defensin-3</i>	Intercept	-7.41	0.33	-22.64	<2e-16
	dose	0.01	0.00	4.19	2.25E-04
<i>cecropin-2</i>	Intercept	-7.33	0.53	-13.83	1.49E-14
	dose	0.01	0.00	3.16	3.60E-03

Appendix L

L. Effect of cactus RNAi (250ng) on total circulating hemocytes. Full factorial Wilcoxon rank sum test on total circulating hemocyte counts. Conducted with "wilcox.test" function from the stats package in R. Post-hoc FDR correction for multiple comparisons using the p.adjust function in R. Significant P values are in bold ($\alpha = 0.05$). Time denotes the hours passed post-challenge, with 0 hours indicating the period before any challenge.

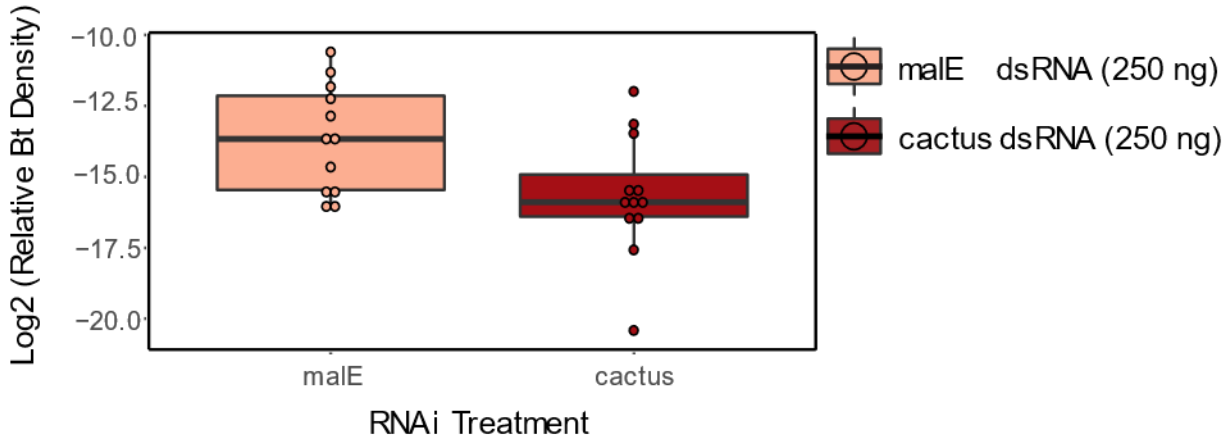
Treatment 1	Time 1	Infection 1	Treatment 2	Time 2	Infection 2	Pval	Pval.adjusted
Cactus	6	Bt	Cactus	12	Bt	1.19E-05	1.56E-04
Cactus	6	Bt	MalE	0	Naive	8.23E-05	2.21E-04
Cactus	6	Bt	Cactus	0	Naive	8.23E-05	2.21E-04
Cactus	6	Bt	Cactus	24	Bt	2.26E-04	3.72E-04
Cactus	6	Bt	MalE	12	Bt	1.45E-03	2.11E-03
Cactus	6	Bt	MalE	170	Bt	2.99E-03	4.16E-03
Cactus	6	Bt	MalE	24	Bt	0.14	0.16
Cactus	6	Bt	Cactus	170	Bt	0.50	0.53
Cactus	6	sham	Cactus	12	Bt	2.65E-05	1.56E-04
Cactus	6	sham	Cactus	24	Bt	2.65E-05	1.56E-04
Cactus	6	sham	Cactus	170	Bt	2.65E-05	1.56E-04
Cactus	6	sham	MalE	12	Bt	4.57E-05	1.84E-04
Cactus	6	sham	Cactus	6	Bt	8.23E-05	2.21E-04
Cactus	6	sham	MalE	24	Bt	8.23E-05	2.21E-04
Cactus	6	sham	MalE	12	sham	1.55E-04	2.58E-04
Cactus	6	sham	Cactus	12	sham	1.55E-04	2.58E-04
Cactus	6	sham	Cactus	24	sham	1.55E-04	2.58E-04
Cactus	6	sham	MalE	0	Naive	1.55E-04	2.58E-04
Cactus	6	sham	Cactus	0	Naive	1.55E-04	2.58E-04
Cactus	6	sham	MalE	24	sham	3.11E-04	5.06E-04
Cactus	6	sham	MalE	170	Bt	4.39E-03	5.99E-03
Cactus	6	sham	MalE	6	Bt	2.06E-02	2.59E-02
Cactus	6	sham	MalE	170	sham	0.19	0.22
Cactus	6	sham	Cactus	170	sham	0.19	0.22
Cactus	12	Bt	MalE	170	Bt	5.67E-06	1.56E-04
Cactus	12	Bt	Cactus	170	Bt	5.67E-06	1.56E-04
Cactus	12	Bt	MalE	0	Naive	2.65E-05	1.56E-04
Cactus	12	Bt	Cactus	0	Naive	2.65E-05	1.56E-04
Cactus	12	Bt	MalE	24	Bt	1.43E-04	2.58E-04
Cactus	12	Bt	Cactus	24	Bt	0.17	0.20
Cactus	12	sham	MalE	170	Bt	4.57E-05	1.84E-04
Cactus	12	sham	MalE	6	Bt	8.23E-05	2.21E-04
Cactus	12	sham	MalE	170	sham	1.55E-04	2.58E-04
Cactus	12	sham	Cactus	170	sham	1.55E-04	2.58E-04
Cactus	12	sham	MalE	0	Naive	1.55E-04	2.58E-04

Cactus	12	sham	Cactus	0	Naive	1.55E-04	2.58E-04
Cactus	12	sham	Cactus	6	Bt	5.76E-04	8.99E-04
Cactus	12	sham	Cactus	170	Bt	3.84E-03	5.29E-03
Cactus	12	sham	Cactus	12	Bt	4.97E-03	6.68E-03
Cactus	12	sham	MalE	24	sham	1.04E-02	1.34E-02
Cactus	12	sham	Cactus	24	sham	0.06	0.08
Cactus	12	sham	Cactus	24	Bt	0.11	0.13
Cactus	12	sham	MalE	24	Bt	0.17	0.19
Cactus	12	sham	MalE	12	Bt	0.90	0.90
Cactus	24	Bt	MalE	170	Bt	1.13E-05	1.56E-04
Cactus	24	Bt	MalE	0	Naive	2.65E-05	1.56E-04
Cactus	24	Bt	Cactus	0	Naive	2.65E-05	1.56E-04
Cactus	24	Bt	Cactus	170	Bt	1.28E-04	2.58E-04
Cactus	24	sham	MalE	170	sham	1.55E-04	2.58E-04
Cactus	24	sham	Cactus	170	sham	1.55E-04	2.58E-04
Cactus	24	sham	Cactus	12	Bt	1.06E-04	2.58E-04
Cactus	24	sham	MalE	0	Naive	1.55E-04	2.58E-04
Cactus	24	sham	Cactus	0	Naive	1.55E-04	2.58E-04
Cactus	24	sham	MalE	6	Bt	9.87E-04	1.50E-03
Cactus	24	sham	MalE	170	Bt	1.37E-03	2.02E-03
Cactus	24	sham	Cactus	24	Bt	2.54E-03	3.63E-03
Cactus	24	sham	MalE	12	Bt	0.07	0.08
Cactus	24	sham	Cactus	6	Bt	0.17	0.19
Cactus	24	sham	Cactus	170	Bt	0.44	0.47
Cactus	24	sham	MalE	24	Bt	0.74	0.76
Cactus	170	Bt	MalE	0	Naive	2.65E-05	1.56E-04
Cactus	170	Bt	Cactus	0	Naive	2.65E-05	1.56E-04
Cactus	170	sham	Cactus	12	Bt	2.65E-05	1.56E-04
Cactus	170	sham	Cactus	24	Bt	2.65E-05	1.56E-04
Cactus	170	sham	Cactus	170	Bt	2.65E-05	1.56E-04
Cactus	170	sham	MalE	12	Bt	4.57E-05	1.84E-04
Cactus	170	sham	Cactus	6	Bt	8.23E-05	2.21E-04
Cactus	170	sham	MalE	24	Bt	8.23E-05	2.21E-04
Cactus	170	sham	MalE	170	Bt	9.14E-05	2.41E-04
Cactus	170	sham	MalE	0	Naive	1.55E-04	2.58E-04
Cactus	170	sham	Cactus	0	Naive	1.55E-04	2.58E-04
Cactus	170	sham	MalE	6	Bt	9.87E-04	1.50E-03
MalE	0	Naive	Cactus	0	Naive	0.43	0.47
MalE	6	Bt	MalE	12	Bt	2.17E-05	1.56E-04
MalE	6	Bt	Cactus	12	Bt	1.19E-05	1.56E-04
MalE	6	Bt	Cactus	24	Bt	1.19E-05	1.56E-04
MalE	6	Bt	MalE	0	Naive	8.23E-05	2.21E-04
MalE	6	Bt	Cactus	0	Naive	8.23E-05	2.21E-04
MalE	6	Bt	Cactus	170	Bt	3.57E-04	5.63E-04
MalE	6	Bt	MalE	24	Bt	1.23E-03	1.83E-03

MalE	6	Bt	Cactus	6	Bt	2.76E-03	3.88E-03
MalE	6	Bt	MalE	170	Bt	0.28	0.31
MalE	6	sham	Cactus	12	Bt	2.65E-05	1.56E-04
MalE	6	sham	Cactus	24	Bt	2.65E-05	1.56E-04
MalE	6	sham	Cactus	170	Bt	2.65E-05	1.56E-04
MalE	6	sham	MalE	12	Bt	4.57E-05	1.84E-04
MalE	6	sham	MalE	170	Bt	4.57E-05	1.84E-04
MalE	6	sham	MalE	6	Bt	8.23E-05	2.21E-04
MalE	6	sham	Cactus	6	Bt	8.23E-05	2.21E-04
MalE	6	sham	MalE	24	Bt	8.23E-05	2.21E-04
MalE	6	sham	MalE	12	sham	1.55E-04	2.58E-04
MalE	6	sham	Cactus	12	sham	1.55E-04	2.58E-04
MalE	6	sham	MalE	24	sham	1.55E-04	2.58E-04
MalE	6	sham	Cactus	24	sham	1.55E-04	2.58E-04
MalE	6	sham	MalE	0	Naive	1.55E-04	2.58E-04
MalE	6	sham	Cactus	0	Naive	1.55E-04	2.58E-04
MalE	6	sham	Cactus	170	sham	0.34	0.38
MalE	6	sham	MalE	170	sham	0.46	0.49
MalE	6	sham	Cactus	6	sham	0.88	0.89
MalE	12	Bt	MalE	170	Bt	1.08E-05	1.56E-04
MalE	12	Bt	MalE	0	Naive	4.57E-05	1.84E-04
MalE	12	Bt	Cactus	0	Naive	4.57E-05	1.84E-04
MalE	12	Bt	Cactus	12	Bt	2.76E-03	3.88E-03
MalE	12	Bt	Cactus	170	Bt	4.79E-03	6.48E-03
MalE	12	Bt	Cactus	24	Bt	0.13	0.16
MalE	12	Bt	MalE	24	Bt	0.16	0.19
MalE	12	sham	MalE	170	Bt	4.57E-05	1.84E-04
MalE	12	sham	MalE	6	Bt	8.23E-05	2.21E-04
MalE	12	sham	MalE	170	sham	1.55E-04	2.58E-04
MalE	12	sham	Cactus	170	sham	1.55E-04	2.58E-04
MalE	12	sham	MalE	0	Naive	1.55E-04	2.58E-04
MalE	12	sham	Cactus	0	Naive	1.55E-04	2.58E-04
MalE	12	sham	Cactus	12	Bt	3.18E-04	5.06E-04
MalE	12	sham	Cactus	6	Bt	2.47E-03	3.56E-03
MalE	12	sham	Cactus	170	Bt	1.32E-02	1.68E-02
MalE	12	sham	Cactus	24	Bt	2.03E-02	2.57E-02
MalE	12	sham	MalE	24	sham	3.79E-02	4.72E-02
MalE	12	sham	Cactus	24	sham	0.19	0.22
MalE	12	sham	Cactus	12	sham	0.44	0.47
MalE	12	sham	MalE	24	Bt	0.48	0.51
MalE	12	sham	MalE	12	Bt	0.53	0.56
MalE	24	Bt	MalE	0	Naive	8.23E-05	2.21E-04
MalE	24	Bt	Cactus	0	Naive	8.23E-05	2.21E-04
MalE	24	Bt	MalE	170	Bt	6.50E-04	1.00E-03
MalE	24	Bt	Cactus	24	Bt	5.66E-03	7.53E-03

MalE	24	Bt	Cactus	170	Bt	0.29	0.33
MalE	24	sham	Cactus	12	Bt	5.29E-05	2.08E-04
MalE	24	sham	MalE	170	sham	1.55E-04	2.58E-04
MalE	24	sham	Cactus	170	sham	1.55E-04	2.58E-04
MalE	24	sham	MalE	0	Naive	1.55E-04	2.58E-04
MalE	24	sham	Cactus	0	Naive	1.55E-04	2.58E-04
MalE	24	sham	Cactus	24	Bt	3.18E-04	5.06E-04
MalE	24	sham	MalE	6	Bt	7.90E-03	1.04E-02
MalE	24	sham	MalE	12	Bt	8.55E-03	1.11E-02
MalE	24	sham	MalE	170	Bt	8.55E-03	1.11E-02
MalE	24	sham	MalE	24	Bt	0.17	0.19
MalE	24	sham	Cactus	24	sham	0.34	0.38
MalE	24	sham	Cactus	170	Bt	0.72	0.74
MalE	24	sham	Cactus	6	Bt	0.81	0.83
MalE	170	Bt	MalE	0	Naive	4.57E-05	1.84E-04
MalE	170	Bt	Cactus	0	Naive	4.57E-05	1.84E-04
MalE	170	Bt	Cactus	170	Bt	1.19E-03	1.79E-03
MalE	170	sham	Cactus	12	Bt	2.65E-05	1.56E-04
MalE	170	sham	Cactus	24	Bt	2.65E-05	1.56E-04
MalE	170	sham	Cactus	170	Bt	2.65E-05	1.56E-04
MalE	170	sham	MalE	12	Bt	4.57E-05	1.84E-04
MalE	170	sham	MalE	170	Bt	4.57E-05	1.84E-04
MalE	170	sham	MalE	6	Bt	8.23E-05	2.21E-04
MalE	170	sham	Cactus	6	Bt	8.23E-05	2.21E-04
MalE	170	sham	MalE	24	Bt	8.23E-05	2.21E-04
MalE	170	sham	MalE	0	Naive	1.55E-04	2.58E-04
MalE	170	sham	Cactus	0	Naive	1.55E-04	2.58E-04
MalE	170	sham	Cactus	170	sham	1.00	1.00

Appendix M



M. Unrestrained Toll signaling increases resistance to Bt infection. To measure shifts in host resistance to bacterial infection from *cactus* (250 ng) RNAi treatment, beetles were given an LD-50 dose of Bt and sacrificed six hours later. Relative bacterial density for each individual within each dsRNA treatment was quantified via RT-qPCR and calculated as the difference between Bt-specific and host reference gene expression (RP18s) on a log₂ scale.

Appendix N

N. Effect of cactus RNAi dose on flour beetle lifespan. Weighted multivariate cox regression (Survival ~ dose + sex) conducted with "coxphw" function from the coxphw package in R. Dose represents the effect of cactus dsRNA per ng. Significant P values are in bold ($\alpha = 0.05$).

Factor	Coef	Se(coef)	Exp(coef)	Lower 0.95	Upper 0.95	Z	Pval
dose	0.01	0.00	1.01	1.01	1.01	16.25	< 1.00E-03
sex	0.26	0.10	1.30	1.06	1.59	2.58	1.00E-02

Appendix O

O. Effect of cactus RNAi dose on female flour beetle reproductive output. Zero-Inflated Negative Binomial (ZINB) GLM (fecundity ~ dose + day + (1 | id) conducted with “zeroinfl” function from the glmmTMB package in R. Dose represents the effect of cactus dsRNA per ng. Significant P values are in bold ($\alpha = 0.05$).

Factor	Estimate	Std. Error	Tval	Pval
(Intercept)	1.81	0.12	14.95	<2e-16
dose	0.00	0.00	-2.50	1.23E-02
day	0.00	0.05	0.05	0.96

Appendix P

P. Effect of cactus RNAi dose on female flour beetle body mass. Linear models (mass ~ dose + day) conducted with "lm" function in R. Dose represents the effect of cactus dsRNA per ng. Significant P values are in bold ($\alpha = 0.05$).

Factor	Estimate	Std. Error	Tval	Pval
(Intercept)	8.04	0.42	19.22	< 2e-16
dose	0.00	0.00	-3.24	2.73E-03
day	-0.37	0.10	-3.63	9.42E-04

Appendix Q

Q. Effect of cactus RNAi dose on flour beetle gut integrity. Binomial GLM (smurfs ~ dose * day) conducted with "glm" function in R. Dose represents the effect of cactus dsRNA per ng. Significant P values are in bold ($\alpha = 0.05$).

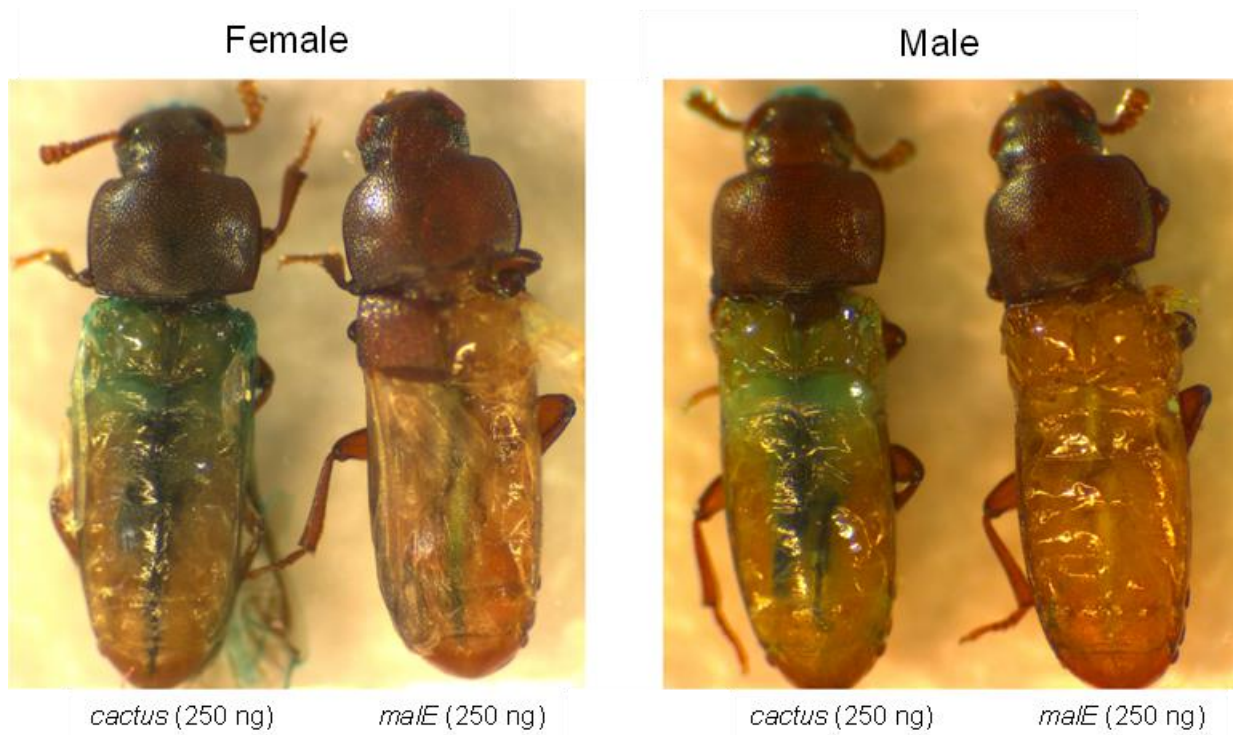
Factor	Estimate	Std. Error	Tval	Pval
(Intercept)	-1.24	0.43	-2.88	3.99E-03
dose	0.18	0.06	3.13	1.76E-03
day 5	0.39	0.59	0.67	0.51
day 8	-0.24	0.63	-0.38	0.70
dose*day 5	-0.08	0.06	-1.29	0.20
dose*day 8	-0.07	0.06	-1.09	0.27

Appendix R

R. Primer pair sequences for chapter IV. Primers used to assay immune gene expression in *T. castaneum*. RNAi primers begin with the T7 promoter sequence.


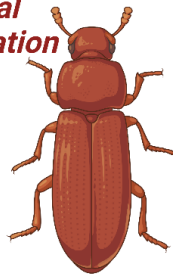
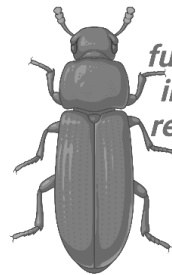

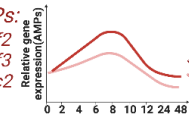





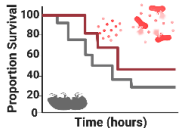


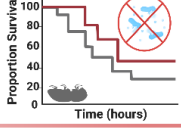


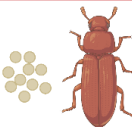






Type	Full name/function	Forward primer sequence (5'-3')	Reverse primer sequence (5'-3')
dsRNA	<i>cactus</i>	taatacgactcactatagggGAGAGTTTTTCC GGACTCCA	taatacgactcactatagggAGGGCTGTTTGG GGTAAGTT
dsRNA	<i>malE</i> - Maltose binding (<i>E. coli</i>)	taatacgactcactatagggATTGCTGCTGAC GGGGGTTAT	taatacgactcactatagggATGTTCGGCATG ATTCACCTTT
qPCR	<i>cactus</i>	TGGAACTACGAAGGTCAGACG	CTATGGAGTAGTGGAGGGCG
qPCR	<i>RPS18s</i> (ribosomal protein)	CGAAGAGGTCGAGAAAATCG	CGTGGTCTTGGTGTGTTGAC
qPCR	<i>defensin-2</i> (IMD AMP)	GCTTTTCCTACAGATGGAGAACA C	AAAGAGGCAATGGGTCGCAC
qPCR	<i>defensin-3</i> (Toll/IMD AMP)	TTGCAATCACTGCTTACCCAC	ACCCGGATATGTGCCACTTG
qPCR	<i>cecropin-2</i> (Toll AMP)	TAATGTGTTTTGTTCAAGTGATGG C	CAGCTCCTTCGGCCCACT
qPCR	Bt 16s rRNA	GACTTTCTGGTCTGTAAGTACTGACA	ACTTCAGCACTAAAGGGCGGA

Appendix S



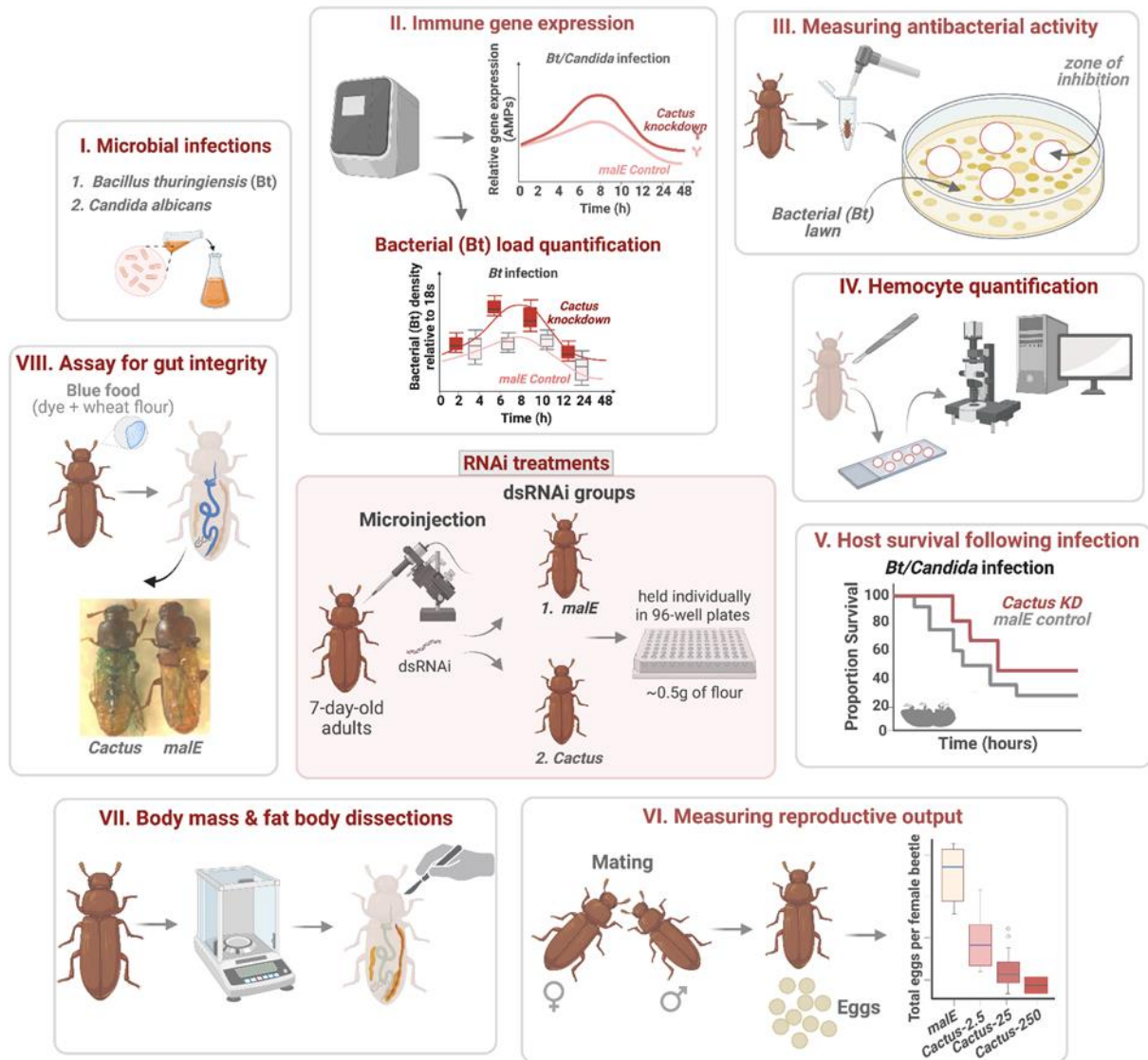
S. Unchecked Toll signaling disrupts intestinal integrity. Beetle gut integrity was measured by feeding adults flour stained blue and observing whether the blue dye entered the beetle hemolymph. Beetles with blue food dye in their hemolymph are counted as “smurfs”.

Appendix T

	RNAi - (<i>knockdown</i>) <i>cactus</i> dose			<i>maleE</i> (control)	
	250ng	25	2.5	250ng	
	<p><i>dysfunctional negative regulation</i></p>   <p>250ng <i>Cactus</i></p>			<p><i>fully functional immune regulation</i></p>  <p>250ng <i>maleE</i></p>	
I. AMPs transcription & translation	<p>AMPs: <i>Def2</i>, <i>Def3</i>, <i>Cec2</i></p>  			 Increased induction, delays decay	 Delayed induction, faster decay
II. Hemocyte numbers & antibacterial activity				 Enhanced antibacterial activity	 reduced antibacterial activity
III. Survival & resistance to microbial infection				 Increased survival to bacterial infection	 Susceptible to infections
IV. Lifespan without infection				 Increased risk of mortality	 low risk
V. Reproductive output				 Extremely low	 optimal fecundity (no. of eggs)
VI. Body mass				 Reduced	no change
VII. Gut integrity				 Severe leakage in gut/intestine barrier	no change

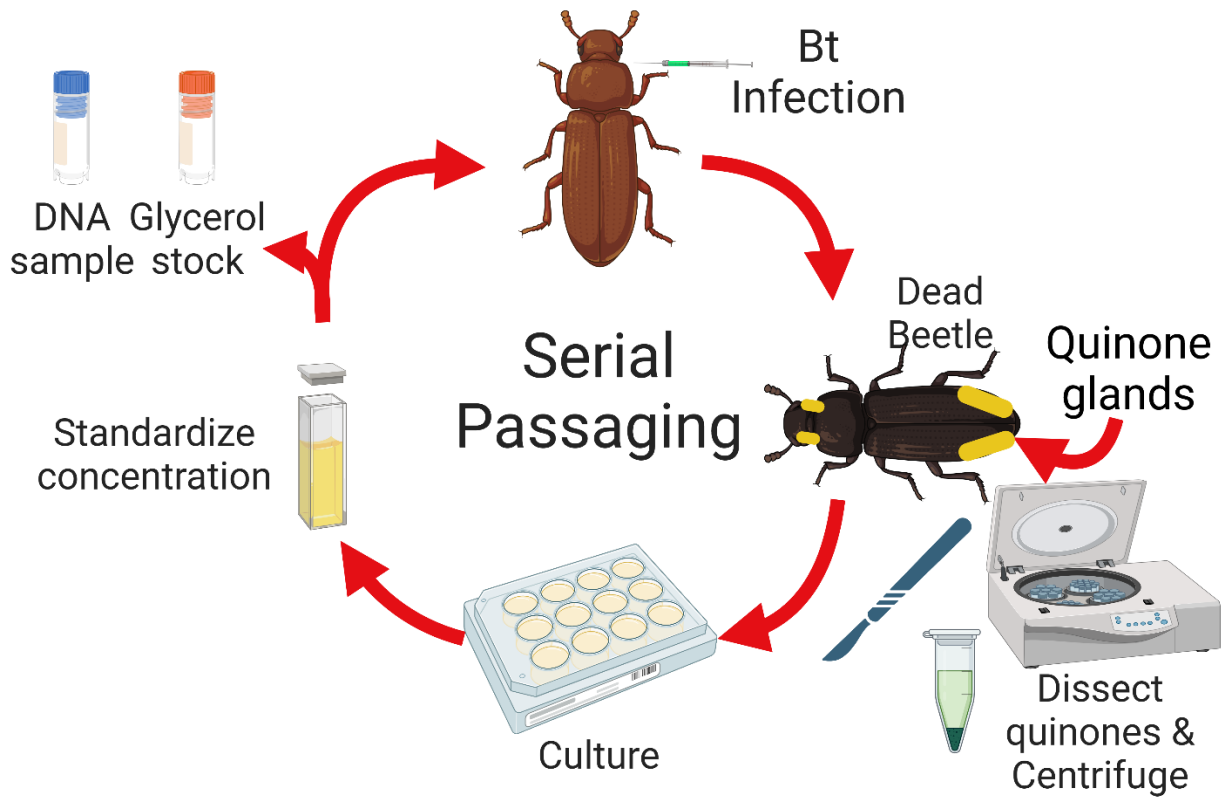
T. Summary of results when assessing the benefits and costs of increased Toll signaling.

Appendix U



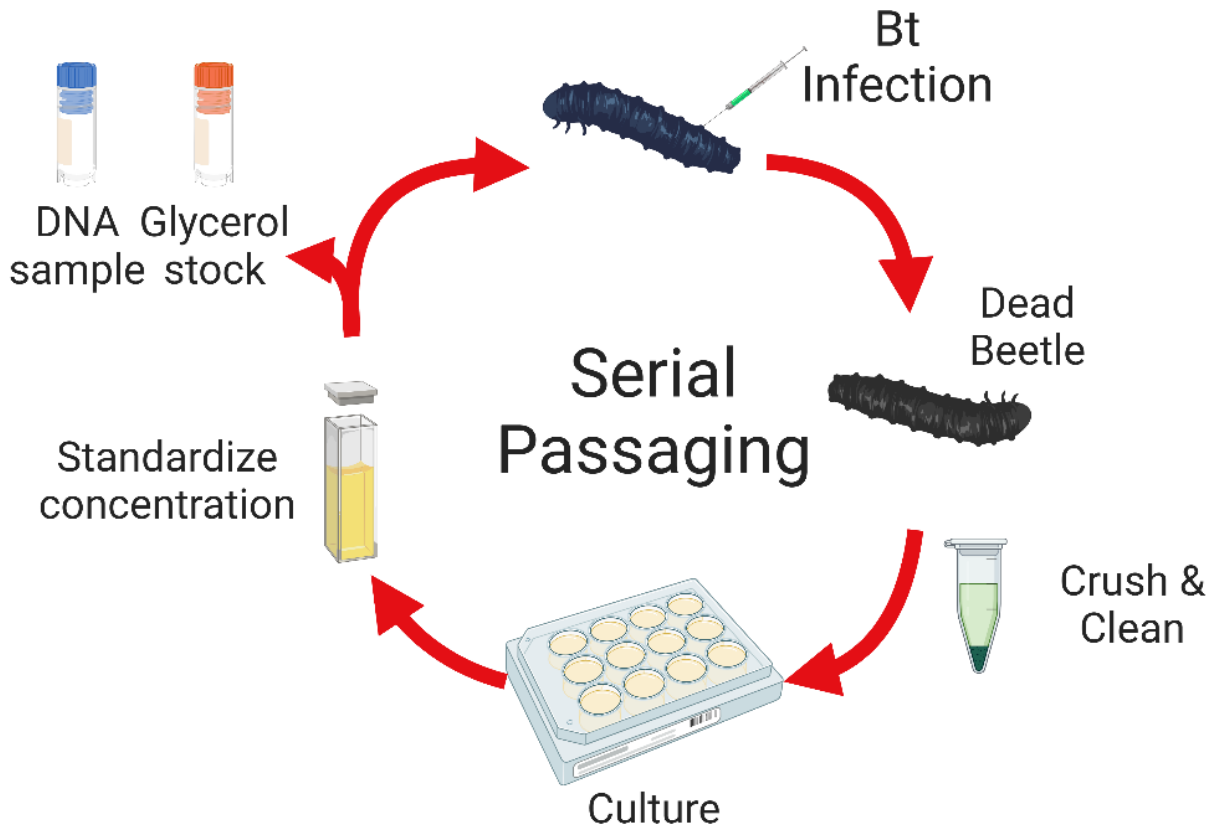
U. Experimental design for chapter IV. Our study investigated the benefits and costs of enhanced Toll signaling utilizing RNAi with four increasing concentrations of *cactus* dsRNA. **I)** Microbes *Bacillus thuringiensis* and *Candida albicans* were used to elicit immune activation. **II)** Immune gene expression and Bt load quantification were measured using RT-qPCR. **III)** Antibacterial activity was assessed by observing the inhibition of bacterial growth on a lawn of Bt. **IV)** Changes in total circulating hemocytes was examined by perfusing the hemolymph in adult beetles, staining, and counting the adhered hemocytes. **V)** Survival to pathogen infection was determined by monitoring RNAi treated beetles post-infection with an LD50 dose of Bt. **VI)** Female reproductive output was evaluated by pairing treated female beetles with male beetles for 24 hours and counting the number of eggs laid over three days. **VII)** Body mass and fat condition were assessed by cleaning and weighing beetles on the 3rd, 4th, and 5th day post-RNAi treatment. Additionally, on the 5th day, beetles were dissected and captured in images for fat body depletion. **VIII)** Gut integrity was examined by feeding the beetles media mixed with blue food dye and observing whether the dye entered the hemolymph.

Appendix V



V. Serial passaging Bt in flour beetle adults requires transitioning through infection, recovery, growth, and infection standardization stages. Created with BioRender.com.

Appendix W



W. Serial passaging Bt in flour beetle larva requires transitioning through infection, recovery, growth, and infection standardization stages. Created with BioRender.com.

Appendix X

S. Methods for serially passaging Bt in genetically modified red flour beetles.

For use cases of these methods see the following papers:

Critchlow, J. T., Prakash, A., Zhong, K. Y., & Tate, A. T. (2023). Mapping the functional form of the trade-off between infection resistance and reproductive fitness under dysregulated immune signaling. *BioRxiv : The Preprint Server for Biology*.
<https://doi.org/10.1101/2023.08.10.552815>

Jent, D., Perry, A., Critchlow, J., & Tate, A. T. (2019). Natural variation in the contribution of microbial density to inducible immune dynamics. *Molecular Ecology*, 28(24), 5360–5372.
<https://doi.org/10.1111/mec.15293>

1 Beetle Rearing (*Protocol 1*):

- 1.1 Select your population of *Tribolium castaneum* and note your choice due to potential impacts on RNAi outcomes.
- 1.2 Prepare beetle media by mixing brewer's yeast (5%) with organic whole-wheat flour (95%) and autoclave for sterilization.
- 1.3 Fill mason jars with 80 grams of sterile beetle media
- 1.4 Start beetle cultures with about 20 male and 20 female beetles and store at 30°C and 70% humidity.
- 1.5 After 24 hours, move adults to a fresh culture.
- 1.6 After egg laying, larva will be ready for RNAi in two weeks, pupa will be ready for sexing and splitting in three weeks, and adults will be ready for RNAi in five weeks.

2 RNAi protocol (*Protocol 2*): RNAi is a gene expression manipulation tool used to knockdown the expression levels of a gene of interest in order to assess gene function. This protocol outlines the steps from dsRNA design and synthesis through gene expression analysis after experiments.

2.1 dsRNA primer design

- 2.1.1 Before designing new primers, check <https://ibeetle-base.uni-goettingen.de/> to see if RNAi primers are designed for your target gene.
- 2.1.2 If so, scroll down to RNAi phenotypes for the left (forward) and right (reverse) sequences and only design your own qPCR primers.
- 2.1.3 Go to NCBI gene: <https://www.ncbi.nlm.nih.gov/gene/>.
- 2.1.4 Type in the name of your gene and “*Tribolium castaneum*” (gene identifiers will also work)
 - 2.1.4.1 e.g. “cactus *Tribolium castaneum*”.
- 2.1.5 Click on your gene.
- 2.1.6 If there are multiple paralogs of your gene be sure to select the correct one
 - 2.1.6.1 e.g. defensin- 1, 2, or 3
- 2.1.7 Your gene may have multiple isoforms, look at “genomic regions, transcripts, and products” to see the exons for each isoform.

- 2.1.8 Scroll down to RefSeq: mRNA and Protein(s) and click the NM link for the isoform you wish to design primers for.
 - 2.1.8.1 If your goal is to target all isoforms, be sure to select the isoform with only the conserved regions.
- 2.1.9 On the right, right click “Pick Primers” and open in new tab (do twice).
- 2.1.10 You need to design both RNAi and qPCR primers. These primers will need to not overlap and be of different lengths.
- 2.1.11 RNAi primers
 - 2.1.11.1 Change PCR product size to 250 Min and 700 Max.
 - 2.1.11.2 At bottom, click “Allow primer to amplify mRNA splice variants (requires refseq mRNA sequence as PCR template input).”
 - 2.1.11.3 Click “get primers.”
- 2.1.12 qPCR
 - 2.1.12.1 change PCR product size to 70 Min and 150 Max.
 - 2.1.12.2 select “Exon junction span.”
 - 2.1.12.2.1 primer MUST span exon junction.
 - This makes the qPCR primers specific to cDNA.
 - 2.1.12.3 It is possible NCBI cannot design any primers that span an exon junction. If so, select “no preference” and remember to remove DNA during or after RNA extraction.
 - 2.1.12.4 At bottom of page, click “Allow primer to amplify mRNA splice variants (requires refseq mRNA sequence as PCR template input).”
 - 2.1.12.5 Click “get primers.”
- 2.1.13 You now have 2 tabs. One for RNAi primers and one for qPCR. To differentiate, the RNAi products will be much longer than your qPCR products.
 - 2.1.13.1 Remember to choose RNAi-qPCR primer pairs where their binding sequences do not overlap.
- 2.1.14 For *cactus*, we will choose primer pairs 1 (RNAi) and 4 (qPCR).
 - 2.1.14.1 RNAi
 - 2.1.14.1.1 Forward primer CAAGTGTCTCACGGCTGTCT
 - 2.1.14.1.2 Reverse primer CAGAGGTCGTCTTTGGCAGT
 - 2.1.14.2 Qpcr
 - 2.1.14.2.1 Forward primer CAGAGCCATCACCGATCCAG
 - 2.1.14.2.2 Reverse primer CGCACGTCTGACCTTCGTA
- 2.1.15 Make sure to write down the expected size of the PCR products to compare to the size of your bands after gel electrophoresis.
- 2.2 **Ordering primers**
 - 2.2.1 For our synthesis we use the Megascript T7 kit (Invitrogen). If you are doing the same, then you must add the T7 sequence before your RNAi primer sequence. (Not qPCR)
 - 2.2.2 T7 sequence : taatacgaactcactataggg
 - 2.2.3 *Cactus* RNAi Forward primer
taatacgaactcactatagggCAAGTGTCTCACGGCTGTCT

- 2.2.4 *Cactus* RNAi Reverse primer
taatacgactcactatagggCAGAGGTCGTCTTTGGCAGT
- 2.2.5 Be sure to label your primers appropriately where you know the following: forward or reverse, RNAi or qPCR, gene name, your initials, and if you are ordering multiple primer pairs for the same target gene, which pair.
- 2.2.6 For example:
- 2.2.6.1 F_RNAi_cactus_JTC_X1
- 2.2.6.2 R_RNAi_cactus_JTC_X1
- 2.2.6.3 F_qPCR_cactus_JTC_X1
- 2.2.6.4 R_qPCR_cactus_JTC_X1
- 2.2.7 To control for off-target effects from the induction of the RNAi machinery, you will need to synthesize dsRNA for a control gene that does not exist in *T. castaneum*.
- 2.2.7.1 We use the *malE* gene (Maltose binding) from *E. coli* (Yokoi, Koyama, Minakuchi, et al., 2012b).
- 2.2.7.1.1 F: taatacgactcactatagggATTGCTGCTGACGGGGGTTAT R:
taatacgactcactatagggATGTTTCGGCATGATTTACCTTT
- 2.2.8
- 2.3 **PCR validation**
- 2.3.1 Before synthesizing dsRNA, you need to make sure your RNAi primers efficiently amplify cDNA.
- 2.3.2 Run your standard PCR protocol with any non-infected and wild type cDNA.
- 2.3.3 Run your gel and record positive and negative bands at the correct base pair size.
- 2.3.3.1 If you do not see bands, then test at multiple annealing temperatures.
- 2.3.3.2 If you still have no bands, then order new primer pairs and try again.
- 2.4 **DsRNA synthesis**
- Day 1**
- PCR amplification and purification**
- 2.4.1 Run the same PCR reaction in step 2.3.2
- 2.4.1.1 You want to run at least 8 reactions to get a high enough concentration of PCR product after DNA purification.
- 2.4.2 Pool your 8 PCR products together, mix, and run just 5 μ L on a gel to ensure the correct product was made by checking the band size.
- 2.4.3 Purify the remaining PCR product using a PCR product purification kit.
- 2.4.3.1 We use QIAquick PCR Purification Kit (Qiagen)
- 2.4.3.2 If you have multiple bands but still want to use these primers, then cut the bands you want from the gel and do a gel extraction/purification.
- 2.4.4 Use a nanodrop to ensure efficient DNA extraction and purification.
- Synthesis using the Megascript T7 kit**
- 2.4.5 For a detailed protocol of the kit see (https://assets.thermofisher.com/TFS-Assets/LSG/manuals/1330M_G.pdf).
- 2.4.6 Remove the nucleotides and reaction buffer from the kit stored at -20°C.
- 2.4.7 Thaw the nucleotides by laying them flat on top of ice for 15-20 minutes.
- 2.4.8 Thaw reaction buffer at room temperature.

- 2.4.9 Once thawed, use the following master mix for each sample into a single 1.5 mL tube:
 - 2.4.9.1 2 μ L for each nucleotide
 - 2.4.9.2 2 μ L reaction buffer
 - 2.4.9.3 2 μ L enzyme
 - 2.4.9.4 2 μ L nuclease free water
- 2.4.10 Mix by vortexing.
- 2.4.11 Pipette 14 μ L of MM into individual thermocycler wells (8-well strip).
- 2.4.12 Add 6 μ L DNA (RNAi PCR purified product from 2.4.4) to the proper well.
 - 2.4.12.1 You can use up to 8 μ L of DNA (up to 1 μ g of total DNA in each reaction).
 - 2.4.12.1.1 Make sure to subtract an equal volume of water for the master mix so each reaction always has a total volume of 20 μ L.
- 2.4.13 Incubate at 37°C for up to 16 hours.

Day 2

- 2.4.14 Remove the 8-well strip(s) from the thermocycler.
 - 2.4.15 Pipette mix each sample and add each to a sterile 1.5 mL microcentrifuge tube.
 - 2.4.16 Label this tube very well. It is your long-term storage tube.
 - 2.4.16.1 Gene, date, and eventually concentration.
 - 2.4.17 Add 30 μ L of LiCl from Megascript T7 kit.
 - 2.4.18 Mix the samples gently by flicking, then short centrifuge spin them, and finally incubate at -20°C for AT LEAST 2 hours.
 - 2.4.19 Just before your incubation is done, cool your centrifuge to 4°C.
 - 2.4.19.1 This temperature must be used to not heat your dsRNA during purification.
 - 2.4.20 Spin at max speed (14,000 rpm) for 15 minutes.
 - 2.4.21 Immediately make 70% ETOH using molecular grade ethanol.
 - 2.4.21.1 You will need 500 μ L of 70% ETOH per sample.
 - 2.4.22 Immediately submerge the 70% ETOH in ice.
 - 2.4.23 Once spinning is done, carefully remove the supernatant.
 - 2.4.24 You should be able to see an opaque pellet after removing supernatant.
 - 2.4.24.1 That is your dsRNA!
 - 2.4.25 Add 500 μ L of ice-cold 70% ETOH.
 - 2.4.26 Mix VERY GENTLY by flicking.
 - 2.4.27 Spin again at 4°C for 15 minutes at max speed (14,000 rpm).
 - 2.4.28 Sterilize your fume hood with 70% ETOH and an RNase decontamination solution
 - 2.4.29 After spinning, remove the supernatant.
 - 2.4.30 Move tubes into fume hood, open lids, and let dry for 5 minutes.
 - 2.4.31 All ETOH must evaporate off or else you may kill your beetles.
 - 2.4.32 Add 25 μ L of nuclease free water.
 - 2.4.33 Pipette mix thoroughly until pellet is mixed completely.
- 2.5 **Measure the dsRNA concentration**
- 2.5.1 You need to measure your dsRNA concentration to accurately dilute your dsRNA for injections.
 - 2.5.2 Do not use a nanodrop. It does not accurately measure dsRNA, but it will still give you an incorrect reading.

- 2.5.3 We use the Qubit™ microRNA Assay Kit to determine the concentration.
 - 2.5.3.1 If using this kit, make sure you have the right Qubit equipment.
- 2.5.4 Follow kit instructions to make standards and master mix for Qubit.
- 2.5.5 Use 1µL of your dsRNA product and dilute it in 99 µL of nuclease free water.
 - 2.5.5.1 If you do not dilute, the sample will be too concentrated for measurement.
- 2.5.6 If your sample is too high or low of a concentration when tested
 - 2.5.6.1 If too, high dilute the sample by 1:10 again.
 - 2.5.6.2 If too low, use up to 10 µL of the diluted dsRNA sample for measurement instead of 1 µL.
- 2.5.7 Convert the tube concentration output to µg/µL.
- 2.5.8 Record your dsRNA concentration as ug/µL on your tube and in your lab notebook.
- 2.5.9 Store samples long-term at -20°C
- 2.6 **Injections**
 - 2.6.1 Using the concentrations from section 2.5.8, dilute your dsRNA to the correct concentration (1 µg per µL for your first KD test).
 - 2.6.1.1 E.g. If your concentration is 3.76 ug/µL and you want 20 µL at 1 ug/uL, use the equation: $20/3.76 = 5.32$ µL dsRNA.
 - 2.6.1.2 Then add sterile insect saline or PBS to make the final volume 20 µL total.
 - 2.6.2 Make sure to use the same concentration for your RNAi control (MalE) injections.
 - 2.6.3 Ensure you have enough individuals for downstream analysis.
 - 2.6.3.1 You need to plan for around 30% of your injected individuals to die from injections.
 - 2.6.4 For detailed *T. castaneum* injection methods, see (Posnien et al., 2009).
 - 2.6.5 Wait for dsRNA to take effect.
 - 2.6.5.1 The incubation time will depend on your gene target, but typically 3 days is sufficient for effective knockdowns.
 - 2.6.6 For collections, flash freeze your samples on dry ice or add directly to -80°C.
- 2.7 **Testing Knockdown efficiency**
 - 2.7.1 Extract RNA from individuals using your preferred method and synthesize cDNA.
 - 2.7.1.1 Our methods use the RNeasy kits (Qiagen) for RNA extraction and the SuperScript™ VILO™ cDNA Synthesis Kit (Thermo Fisher).
 - 2.7.1.2 For the most accurate qPCR results, measure the RNA concentration (Nanodrop) for each sample, and use the same amount of RNA for each cDNA synthesis reaction.
 - 2.7.2 Run qPCR with the annealing temperature you determined following your qPCR guidelines.
 - 2.7.3 To determine the efficiency of your RNAi, use the delta-delta Ct method for calculating relative gene expression (Livak & Schmittgen, 2001) comparing average expression of gene of interest in KD group compared to the malE dsRNA treatment control

3 Bt serial passaging protocols (*protocol 3*)

Materials

1. Beetle media (5% brewer's yeast and whole wheat flour)

2. 12-well cell culture plate(s) with lid
3. 96-well cell culture plate(s) with lid
4. Temperature controlled spectrophotometer
5. Refrigerated centrifuge
6. Ultra-thin needle (0.10×12mm)
7. 50% glycerol
8. Stereo microscope
9. Razor blades
10. Fine and blunt tip tweezers
11. 15 mL culture tubes
12. Temperature controlled test tube shaker
13. 15 mL tube rack at a 30° angle
14. 1.5 mL microcentrifuge tubes
15. 0.5 mL microcentrifuge tubes
16. Cryogenic storage vials

Reagents

Sterilize reagents via autoclave

1. Luria-Bertani broth (LB) – 1 L H₂O, 10 g Tryptone, 10 g NaCl and 5 g Yeast extract
2. Insect saline (IS) - 1 L H₂O, 7.5g NaCl, 2.38g Na₂HPO₄, 2.72g KH₂PO₄

Adult serial passaging (Appendix V)

- 3.1 Select your population of flour beetle adults.

Bt infection

3.2 **Overnight Bt culture**

- 3.2.1 Choose your strain(s) of *Bacillus thuringiensis* (Bt).
- 3.2.2 On the day before infections, culture 4 biological replicates overnight.
 - 3.2.2.1 Add 5 mL of LB to a 15 mL falcon tube (x 5).
 - 3.2.2.2 Add Bt by dipping a 200 µL filtered pipet tip in a still frozen glycerol stock and flushing the contents into a 15 mL tube.
 - 3.2.2.3 Add Bt to 4 of the 5 tubes. The 5th tube acts as a culturing negative control for LB contamination.
 - 3.2.2.4 Incubate the 15 mL tubes for 12-15 hours at 30°C, 200 rpm and a 30° angle.
 - 3.2.2.4.1 If Bt is cultured for over 16 hours it will begin to form a biofilm, complicating infections by increasing variation in mortality (El-Khoury et al., 2016).

3.3 **Morning log culture**

- 3.3.1 Set up your subcultures by adding 3 mL of LB to a 15 mL tube (x 4).
- 3.3.2 Remove 15 mL tubes from shaker and vortex.
- 3.3.3 Aliquot 200 µL of an overnight culture into your corresponding subculture tube (x 4).
 - 3.3.3.1 You should have one subculture for every overnight culture.
- 3.3.4 Incubate for 1.25-2 hours (depending on Bt strain) at 30°C, 200 rpm and a 30° angle.

Note: Leave overnight culture tubes on bench at room temperature or on ice to halt growth.

3.4 **Infectious dose preparation**

- 3.4.1 Vortex each log and overnight culture and pipet 200 μL into an individual flat-bottom well from a 96-well plate (including the blank LB control).
- 3.4.2 Measure the OD_{600} at 600 nm.
- 3.4.3 Record the OD_{600} for each tube culture and subtract the blank OD_{600} value.
- 3.4.4 For the overnight cultures, you need an OD_{600} of 1.
 - 3.4.4.1 If your cultures are > 1.1 after subtracting the blank, dilute by adding fresh LB until the OD_{600} is in the range of 0.9-1.1.
- 3.4.5 For the log cultures you need to measure an OD_{600} of 0.5 after subtracting the blank.
 - 3.4.5.1 Since these cultures should be in log phase, you do not need to dilute.
- 3.4.6 Use the OD_{600} measurements to mix your overnight and corresponding log cultures into a 1.5 mL centrifuge tube.
 - 3.4.6.1 500 μL overnight (1.0 OD_{600}) and 500 μL log (0.5 OD_{600})
 - 3.4.6.2 Since your cultures will not be at exactly 1 or 0.5, you can adjust the volume of the culture you add to your mixture.
 - 3.4.6.2.1 For example, an overnight OD_{600} of 0.9 is adjusted to a volume of 555.6 μL ($500/0.9$) and a log culture of 0.39 is adjusted to a volume of 641 ($250/0.39$).
 - 3.4.6.2.2 This will ensure that each time you prepare your mixture your infectious dose remains consistent between experiments.
- 3.4.7 Centrifuge your 4 mixtures for 5 minutes at 4°C and 5000 rpm.
- 3.4.8 Remove the supernatant and wash the pellet by resuspending in 1 mL of ice cold IS.
- 3.4.9 Repeat the centrifugation and washing steps.
- 3.4.10 Remove the supernatant and resuspend the pellet in 150 μL of IS.
- 3.4.11 Vortex and add the 4 replicate mixtures together for a total of 600 μL of a Bt mixture.
- 3.4.12 Dilute the Bt mixture for the desired mortality rate.
 - 3.4.12.1 Typically, 1:20 for our flour beetles.
- 3.4.13 Store Bt mixture on ice and use within 4 hours of preparation.

3.5 **Septic infections**

- 3.5.1 Add 40 μL of your Bt mixture to the cap of an 8-well PCR strip.
- 3.5.2 Swirl the fine-tipped needle in your Bt mixture and insert between the head and thorax of the adult.
 - 3.5.2.1 Keep the needle parallel to the beetle as much as possible to reduce the chances of rupturing the beetle heart and gut.
- 3.5.3 Store beetles in individual wells from a 96-well plate, add beetle media, and store at 30°C .

3.6 **Passaging Bt for a new infection**

- 3.6.1 The next morning, collect the dead beetles.
 - 3.6.1.1 Since Bt begins its necrotrophic phase 18-24 hours after infection, and sporulation at 40 hours post infection (Verplaetse et al., 2015), collecting individuals the next morning should still limit extraneous selection pressures.

- 3.6.2 Since *T. castaneum* adults contain microbicidal quinone glands that will kill Bt during passaging, they must be removed from the cadavers (Appendix V).
- 3.6.3 Remove the head with a razor blade.
- 3.6.4 Carefully squeeze the abdomen with tweezers to expose the anterior odoriferous glands and cut them off using scissors or a razor blade.
- 3.6.5 Place the remaining beetle carcass in a 0.5 mL tube with 3 holes punctured at the bottom (Tabunoki et al., 2019).
- 3.6.6 Place this 0.5 mL tube into a 1.5 mL centrifuge tube containing 50 μ L of IS and put it on ice.
- 3.6.7 Complete the remaining dissections of deceased beetles.
- 3.6.8 Centrifuge your “double” tubes for 10 minutes at 4°C and 12,000 rpm.
- 3.6.9 Check the bottom of the tube to ensure the hemolymph collected into the IS at the bottom.
- 3.6.10 Remove the supernatant and clean the pellet with 1 mL of IS.
- 3.6.11 Centrifuge just the 1.5 mL tubes for 5 minutes at 4°C and 5,000 rpm.
- 3.6.12 Remove the supernatant (leave a small amount of IS since your pellet will be difficult to see at this stage).
- 3.6.13 Add 200 μ L of LB to your pellet and transfer to an individual well in a 12-well plate.
- 3.6.14 Add an additional 2 mL of LB to each well containing Bt.
- 3.6.15 Insert the 12-well plate into a spectrophotometer.
 - 3.6.15.1 Set the temperature at 30°C.
 - 3.6.15.2 Shake the plate using a “linear” pattern at the maximum speed.
 - 3.6.15.3 Continue shaking until all cultures reach your minimum desired OD₆₀₀ (3-5 hours).
 - 3.6.15.3.1 Do not allow any cultures to reach early stationary phase or else you may introduce competition during culturing and risk adaptation to *in vitro* conditions.
- 3.6.16 Remove the plate and transfer cultures to a new 1.5 mL tube.
- 3.6.17 Centrifuge the tubes for 5 minutes at 4°C and 5,000 rpm.
- 3.6.18 Resuspend pellets with 200 μ L of IS.
- 3.6.19 Measure the OD₆₀₀ for each tube.
- 3.6.20 Using C1V1 = C2V2, adjust the volume for your desired OD₆₀₀ to match your first infection concentration.
- 3.6.21 Transfer sub samples of your infection mixture for a micro glycerol stock (25-20% glycerol) and DNA sample and freeze at -80°C.
 - 3.6.21.1 A separate Bt DNA sample is taken since freezing in glycerol can eliminate rare alleles (Sprouffs et al., 2016).
- 3.6.22 Using your new Bt mixtures, infect the next batch of adult beetles with the methods detailed at section 3.5.

Larva serial passaging (Appendix W)

- 3.7 Select your larva and follow the steps detailed in sections 3.2-3.4 for Bt culturing and infection mixture preparation.
- 3.8 **Septic infections**

- 3.8.1 Add 40 μ L of your Bt mixture to the cap of an 8-well PCR strip.
- 3.8.2 Swirl the fine-tipped needle in your Bt mixture and insert between the second and third sclerites from the posterior end.
- 3.8.3 Store beetles in individual well from a 96-well plate, and minimal beetle media, and store at 30°C.

3.9 **Passaging Bt for a new infection**

- 3.9.1 The next morning (less than 18 hours post infection), collect the dead beetles and put each individual into a 1.5 mL microcentrifuge tube containing 50 μ L of IS.
- 3.9.2 Crush the larva with a pestle on ice and short centrifuge all samples.
- 3.9.3 To separate the hemolymph and Bt from the exoskeleton, transfer 50 μ L of supernatant into a new 1.5 mL microcentrifuge tube.
- 3.9.4 Follow the steps detailed between sections 3.6.8-3.8.3 for cleaning the pellet, growing the Bt, creating the infection mixture, saving glycerol and DNA samples, and infecting the next batch of larva.

3.10 **Alternate larval passaging protocol**

- 3.10.1 Instead of standardizing the dose of Bt, you can alternatively infect the next batch of larva using the infection mixture from section 3.9.2 and no culturing.
 - 3.10.1.1 This alternative method allows for the changing of infectious dose from final Bt loads in cadavers.
- 3.10.2 After infections save glycerol and DNA samples from the Bt mixtures.

Serial passaging control

- 3.11 To control for the effect of serial passaging without immunity, which is known to increase virulence (Duangurai et al., 2020), culture Bt in test tubes only.
 - 3.11.1 Culture while conducting your *in vivo* passaging.
- 3.12 Follow the steps for Bt morning log culture, and infectious dose preparation.
 - 3.12.1 Make the infection mixture OD₆₀₀ match the OD₆₀₀ of your *in vivo* passaging.
- 3.13 Instead of infecting a beetle, swirl a needle in the infection mixture and drop it into a 15 mL culture tube with 5 mL of LB.
- 3.14 Incubate the 15 mL tubes for 12-15 hours at 30°C, 200 rpm and a 30° angle.
 - 3.14.1 Ensure the Bt is not cultured for over 16 hours or else it will begin to form a biofilm, influencing Bt evolution (El-Khoury et al., 2016).
- 3.15 Repeat the steps for Bt morning log culture, and infectious dose preparation.

4 Bt growth curve protocol (*Protocol 4*):

Materials

1. 96-well cell culture plate(s) with lid
2. Temperature controlled spectrophotometer
3. Refrigerated centrifuge
4. 15 mL culture tubes
5. Temperature controlled test tube shaker
6. 15 mL tube rack at a 30° angle

Reagents

1. Lauria broth (LB) – 1 L H₂O, 10 g Tryptone, 10 g NaCl, 5 g Yeast extract, and 7.5 g agar (if making plates)

Day 1

- 4.1 Using a sterile loop, streak Bt from the glycerol stock on an LB agar plate.
 - 4.1.1 Ensure that you spread enough to have single colonies the next morning.
- 4.2 Incubate the plate at 30 °C for up to 16 hours.
 - 4.2.1 You must not incubate longer than 16 hours or else some cells will begin to sporulate, which will introduce variation into your growth curves (Laut et al., 2022).

Day 2

- 4.3 Remove the Bt agar plate from the incubator and store on a lab bench at room temperature until the evening.
- 4.4 Fill 15 mL culture tubes with 5 mL of LB.
- 4.5 Using a sterile loop or pipette tip, take a small amount of a single Bt colony, and add it to one of your 15 mL culture tubes with LB.
 - 4.5.1 Try to add the same amount of Bt to each culture tube, since differences can affect downstream growth curves.
- 4.6 Repeat step 4.5 at minimum 2 more times with new single colonies from the same agar plate.
 - 4.6.1 You now have 3 culture tubes representing 3 biological replicates for this Bt isolate.
 - 4.6.2 Repeat steps 4.5-4.6 for each isolate.
- 4.7 Make sure your 15 mL tube rack is at a 30° angle and culture for 16 hours at 30 °C.
 - 4.7.1 Do not culture longer than 16 hours.

Day 3

- 4.8 Take your tubes out of the shaker and check their OD₆₀₀.
 - 4.8.1 Vortex your tubes and pipette 200 µL into a well in a 96-well plate
 - 4.8.1.1 Make sure all cultures have an OD₆₀₀ of ~1.
 - 4.8.1.1.1 Any cultures above 1.2 need to be diluted with LB to ~1.
- 4.9 Back dilute your overnight cultures.
 - 4.9.1 Add 30 µL of your ~1 OD₆₀₀ overnight culture into 2.7 mL LB.
 - 4.9.2 Culture at a 30° angle in 30°C for ~ 3 hours and 30 minutes for a log phase OD₆₀₀ of ~ 0.4.
- 4.10 Making your growth curve plates.
 - 4.10.1 Open a brand new 96-well flat bottom cell culture plate with plastic lid.
 - 4.10.2 Add 200 µL of LB to each well you plan to use.
 - 4.10.3 Add 1 µL from your morning log culture tube to a well.
 - 4.10.3.1 Repeat these steps 2 more times for a total of 3 technical replicates per biological replicate.
 - 4.10.3.1.1 This means, for each Bt isolate, you will have 9 wells occupied.
 - 4.10.4 All log cultures will not be at a perfect 0.4 OD₆₀₀, so you need to adjust the volume of morning culture you add to each well.

- 4.10.4.1 Example: If your morning culture reads an OD₆₀₀ of 0.296, you find the volume you need to add by taking the desired OD₆₀₀ (0.4) and dividing by 0.296 = 1.35 μL.
- 4.10.5 Remember to have AT LEAST one well where you add 200 μL of LB without Bt.
 - 4.10.5.1 This will serve as your blank control for the entire growth curve process.
- 4.10.6 Add your 96-well plate to your spectrophotometer.
- 4.10.7 Immediately record the OD₆₀₀ as time 0 for all samples.
- 4.11 Run your automated program that should last for at least 17 hours.
- 4.12 Your settings should be:
 - 4.12.1 Temperature 30°C.
 - 4.12.2 17 hours.
 - 4.12.3 Read Interval 30 minutes.
 - 4.12.4 Linear shake at max speed (1096 cpm).
 - 4.12.5 Wavelength 600 nm.
- 4.13 Label your plate on the software.
 - 4.13.1 Give each isolate, biological replicate, and technical replicate a unique name for analysis.
 - 4.13.2 Remember to label your blank control (just 200 μL of LB)
 - 4.13.2.1 The software will automatically subtract your OD₆₀₀ readings for you.
- 4.14 Export your data into excel for analysis in R or another statistical program.
- 4.15 For analysis using the Growthcurver in R follow the paper:
<https://www.ncbi.nlm.nih.gov/pmc/articles/PMC4837600/>
- 4.15.1 Directions on how to use the package are located at: <https://cran.r-project.org/web/packages/growthcurver/vignettes/Growthcurver-vignette.html>